UNIVERSITÀ DEGLI STUDI DI TRIESTE

UNIVERSITÀ DEGLI STUDI DI TRIESTE

XXXIV CICLO DEL DOTTORATO DI RICERCA IN BIOMEDICINA MOLECOLARE

Implication of p27 ^{kip1} in Luminal breast cancer onset and progression

Settore scientifico-disciplinare: BIO/11 BIOLOGIA MOLECOLARE

DOTTORANDA

FRANCESCA RUSSO

COORDINATORE

PROF.SSA GERMANA MERONI

SUPERVISORE DI TESI

DOTT.SSA BARBARA BELLETTI

CO-SUPERVISORE DI TESI

DOTT. GUSTAVO BALDASSARRE

ANNO ACCADEMICO 2020/2021

Alla nostra battaglia silenziosa.
A quella che ero.
A quello che siamo.

Part of the results included in this PhD thesis has been published on “CDKN1B mutation and copy number variation are associated with tumor aggressiveness in Luminal breast cancer” Viotto D., Russo F. et al.; Journal of Pathology (2021).

ABSTRACT

p27^{kip1} is a cyclin-dependent kinase (CDK) inhibitor (CKI) and mainly acts as a negative regulator of cell proliferation. Through distinct domains, p27^{kip1} has also been involved in the control of other cellular processes, including migration, differentiation and cytoskeleton dynamics. p27^{kip1} protein is frequently inactivated in human cancer and its subcellular localization (cytoplasmic versus nuclear) can be prognostic in some tumors, such as breast, colon, prostate, lung, esophageal, and gastric cancers (Ananthanarayanan et al. 2011; Wen et al. 2012).

With the advent of next generation sequencing approaches, p27^{kip1} has been identified as one of the 18 most significantly mutated genes in Luminal breast cancer (Stephens et al. 2012; Ellis et al. 2012; Belletti, Baldassarre et al. 2012). Furthermore, the analysis of copy number variation showed that a fraction of Luminal breast cancer also displayed loss or gain of *CDKN1B* gene, encoding for p27^{kip1} (Viotto, Russo et al. 2021), reinforcing the idea that p27^{kip1} may be critical for Luminal breast cancer onset and/or progression. Interestingly, many of the identified somatic mutations are located in the C-terminal domain, leading to protein loss or truncated protein formation.

Therefore, to further elucidate the role of p27^{kip1} in Luminal breast cancer, we used a gene-editing approach in MCF7 Luminal cell line. First, we abrogated p27^{kip1} expression and second, we expressed two different p27^{kip1} C-terminal truncated mutants (K134fs and T171*) to investigate the impact of p27^{kip1} loss and to clarify the role of p27^{kip1} C-terminal domain.

Our results clearly showed that p27^{kip1} K134fs and T171* mutants, failed to rescue most of the phenotypes induced by *CDKN1B* gene knock-out, indicating that the functions retained by this portion are critical for its role as an oncosuppressor, both *in vitro* (Viotto, Russo et al. 2021) and *in vivo.* Moreover, we observed that lack of p27^{kip1} or expression of its mutant forms increased the resistance to the treatment with Palbociclib, currently one of the most common therapeutic strategies for Luminal breast cancer patients.

Finally, to evaluate whether p27^{kip1} could also represent a driver genetic lesion during the process of transformation, we have also shown the involvement of p27^{kip1} in the process of cell transformation and tumor initiation. Generating p27^{kip1} knock-out clones in normal human mammary Luminal epithelial cell line, we have noticed its ability to significantly increase the proliferation cell rate of these normal cells. Interestingly, the only deficiency of p27^{kip1} seems to lead the cells toward a stem phenotype and also therapy resistance, highlight the important role of p27^{kip1} also in the early steps of mammary cancer formation.

1 INTRODUCTION

1.1 Breast Cancer (BC)

Breast cancer (BC) is the most diagnosed tumor in women. According to the World Health Organization (WHO), 2.3 million women were diagnosed with BC in 2020 and 685,000 died of BC, globally. As of the end of 2020, there were 7.8 million women alive who were diagnosed with breast cancer in the past 5 years, making it the world's most prevalent cancer. Improvements in breast cancer detection and therapy have led to >85% 5-year survival, yet, half of affected women die from their disease, reflecting an incomplete understanding of the molecular alterations and heterogeneity of this type of tumor (Marcotte et al. 2016).

Genetic factors, including a family history of breast or ovarian cancer and inherited mutations (such as BRCA1, BRCA2) account for only 5% to 10% of breast cancer cases (Nielsen et al, 2016).The reproductive profile and the exposure to sex hormones also explain part of the excess in risk. BC risk is increased by nulliparity and late first full-term pregnancy (Tavani et al. 1997), by endogenous sex hormones intake (i.e., oral contraceptives and use of hormone replacement therapy) (Corrao et al. 2008) and by early age at menarche and late menopause, while it is reduced by breastfeeding (Victora et al. 2016). Active and passive smoking (Dossus et al. 2014), as well as alcohol consumption (Bagnardi et al. 2015) and obesity (Picon-Ruiz et al. 2017) explain, at least in part, the excess in risk of BC.

Moreover, incidence rate is higher in developed countries, and varies greatly with race and ethnicity: increasing trends in BC incidence in high-income countries over the past several decades are thought to reflect increases in the prevalence of known risk factors and increased detection through mammography. Mortality and survival rates vary considerably among different parts of the world, due in part to health care quality and access disparities (Rojas et al, 2016).

Classification

BC is not a single disease, but the collection of breast pathologies heterogeneous in terms of histologic, genetic and genomic variations, therapeutic response and patient outcomes. Several classification schemes have been created to stratify breast tumors, attempting to comprehend the intricate biological mechanisms driving these tumors and to allow more effective clinical trials and treatments (Taherian-Fard et al, 2015).

I) Histological Classification:

- *Non-invasive carcinoma (in situ)* refers to an early carcinoma, which does not invade and therefore has no metastatic potential. This characteristic is also due to restriction of neoplastic proliferation by the presence of a natural barrier, the myoepithelial cell layer. There are two types of in-situ carcinoma: *Ductal carcinoma in situ (DCIS)* starts inside the milk ducts and remains in its original place. However, even if it is not a lethal type of cancer, it represents the intermediate precursor of invasive breast cancer (Allred 2010). *Lobular carcinoma in situ (LCIS)* starts by distortion of the terminal duct-lobular unit, which may then undergo expansion due to abnormal proliferation of cells present within this structure. LCIS, as DCIS, is considered a pre-cancerous lesion and an indicator for increased risk of developing invasive BC (Wen et al 2018).

- *Invasive carcinomas* are characterized by cells with the capacity to pass through the basal membrane and invade the surrounding tissues. They can be divided in different types, based on where they are located: the most frequent type is the *invasive ductal carcinoma (IDC)*, which originates from ductal cells (70-80% of cases). The second most common type of invasive breast cancer after IDC is *invasive lobular carcinoma (ILC)*, which originates from lobules of the breast (10-15 % of cases). There are also less frequent invasive ductal carcinomas such as, tubular, papillary, mucinous, and medullary, which have a better prognosis respect to more common types of IDCs (Cserni 2020).

II) Molecular Classification

Another type of classification is the molecular classification (**figure 1**), which comprises molecular subtypes defined by gene expression and genetic profiles, and it is used to predicts prognosis and drug response:

- *Luminal A* (40% of cases), is estrogen-receptor (ER) and/or progesterone-receptor (PR) positive, human epidermal growth factor receptor 2 (HER2) negative. These cancers tend to be slow in growth, with a Ki-67 (indicator of actively dividing cells) level <20%. For this reason, Luminal A BC is less aggressive than other subtypes and is associated with more favorable prognosis (particularly in short term). This type of cancer can be successfully treated with hormone therapy and benefit, to a lesser extent, from chemotherapy (Eisen et al. 1998).

- *Luminal B* (20-30% of cases), is hormone-receptor (ER and PR) positive and either HER2 positive or negative. Furthermore, they are highly proliferative, with Ki67>20%. Luminal B breast cancers tend to be higher in grade and more aggressive than Luminal A. This type of cancer can benefit from chemotherapy, hormone therapy and, if HER2 positive, from targeted therapy against HER2 (Arpino et al. 2002).

- *HER2-enriched* (10-15% of cases), is hormone-receptor negative and HER2 positive.
These cancers tend to grow and spread more aggressively than other breast cancers and are associated with poorer short-term prognosis compared to ER+ breast cancers (Iwanaga et al. 2012). However, the recent widespread use of targeted therapies for HER2+ cancers, in association with chemotherapy, has reversed the major part of the adverse prognostic impact of HER2 overexpression (American Cancer Society. Breast Cancer Facts& Figure 2017-2018).

-*Triple-negative* (15-20% of cases), is hormone-receptor negative and HER2 negative. It is more likely to be diagnosed in people younger than 50-years, in Black and Hispanic women, and in people with BRCA1 mutation. Triple negative breast cancers have poorer short-term prognosis than other BC types, because there are no current targeted therapies for these tumors and is typically treated with a combination of surgery, radiotherapy and chemotherapy (Eliyatkın et al. 2015).

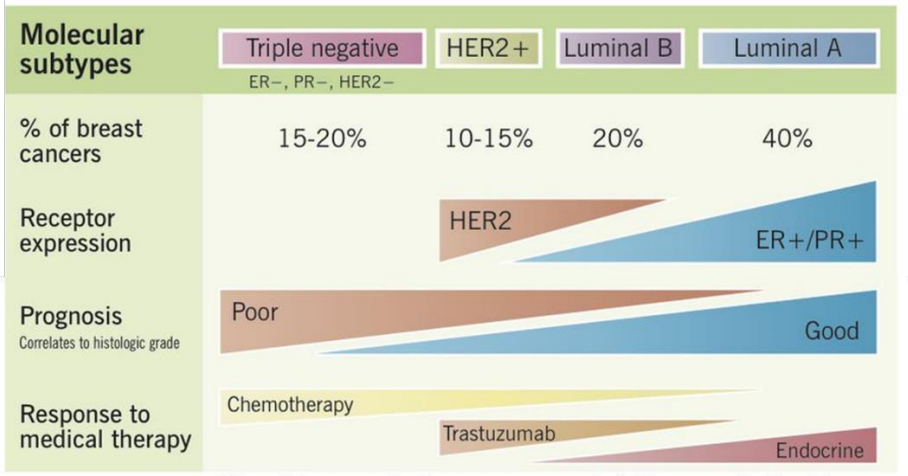

Figure 1. Molecular subtype of BC. *The table shows the percentage of different subtypes incidence, the receptor expression, prognosis and medical therapy. Image adapted from "McMaster Pathophysiology review - www.pathophys.org", Eric Wong, Jenna Rebelo and Sultan Chaudry.*

1.2 Luminal Breast Cancer (LBC)

1.2.1 Molecular characterization of LBC

Luminal BC presents a characteristic genetic profile: copy number alterations (CNAs), DNA methylation, and somatic point mutations, DNA amplifications and chromosomal aberrations. The Cancer Genome Atlas (TCGA) Network has characterized a high number of primary BC using a wide variety of platforms. They show that Luminal B BC often lacks of ATM (Ataxia-Telangiectasia Mutated) and MDM2 (Mouse Double Minute 2 homolog) gene expression amplification occurred frequently. Moreover, compared to Luminal A, Luminal B has lower frequency of PIK3CA (Phosphatidyl Inositol 4,5-bisphosphate 3-Kinase Catalytic subunit Alpha) mutations and higher frequency of TP53 mutations (Ades et al. 2014; Koboldt et al. 2012). Despite this decreased frequency of PIK3CA mutations, only Luminal B cancers have higher PI3K pathway activation (Loi et al. 2010). Literature data indicate that in LBC, PI3K activation is implicated also in *de novo* and acquired anti-estrogen therapy resistance (Miller et al, 2011).

Different sequencing studies have shown that the MLL3 (Mixed-Lineage Leukemia 3) gene was mutated in about 8% of Luminal tumors (Stephens et al. 2012). Even the genomic locus of FGFR1, 8p11–12, has been identified in about 15% of patients with ER+ breast cancers (Reis-Filho et al. 2006). FGFR1 gene amplification is associated with resistance to estrogen suppression in a cohort of patients with ER+ breast cancer treated with the aromatase inhibitor letrozole (Giltnane et al. 2017).

Through whole genome analysis, other significant mutated genes were considered related to anti-estrogen therapy sensitivity, such as GATA3 (transcriptional activator which binds to the enhancer of the T-cell receptor alpha and delta genes), RUNX1 (Runt-related transcription factor), CBFB (Core-Binding Factor Beta) and CDKN1B (Cyclin Dependent Kinase Inhibitor 1B). GATA3 was found to be mutated with significant degree in both Luminal A and B subtype with a similar frequency but in different ways: Luminal A displayed hotspot mutations associated with intron 4 deletions, while exon 5 frame shifts were mostly ascribed to Luminal B cancers (Ades et al. 2014). Mutations in GATA3 has been proved to be a positive predictive marker for anti-estrogen treatment response (Jiang et al. 2014; Yoon et al. 2010). RUNX1 loss-of-function mutations, affecting its expression and dimerization with its partner CBFB, have been associated with the Luminal B subtype and anti-estrogen resistance (Ellis et al. 2012). Expression and functional studies have demonstrated that high CDKN1B expression predicts sensitivity to endocrine and chemotherapy in LBC patients (Pohl et al. 2003; Stendahl et al. 2010), whereas

CDKN1B downregulation predicts resistance to radiotherapy (Payne et al. 2008; Berton et al. 2017) and anti-HER2 therapies (Nahta et al. 2004; Zhao et al. 2014).

1.2.2 Therapeutic treatments for LBC patients

Many different treatment strategies are currently available to treat LBC patients. Both the histological/molecular characteristics and the stage of the tumor are crucial factors to identify the optimal surgical and treatment strategy.

- **Surgery**

In the past, all breast cancers were treated surgically by *mastectomy* (complete removal of the breast). Nowadays, radical mastectomy is recommended only in selected cases, such as when the breast cancer has spread to the chest muscles. In most cases, a smaller procedure called a "lumpectomy" or "quadrantectomy" or partial mastectomy is preferred. This breast-conserving surgery has been proven to be equally effective, especially when coupled with radiation therapy to minimize recurrence, and much less disfiguring than mastectomy. In case of invasive cancers, also lymph nodes may be removed at the time of surgery. However, while in the past a complete axillary dissection was thought to be necessary to prevent the spread of cancer, currently a limited lymph node procedure, called "sentinel node biopsy", is preferred, using dye or radioactive tracers to find the closer lymph node to which cancer cells would spread from the breast (Ustun et al. 2019).

- **Radiotherapy**

Surgery aims to remove any disease that has been detected in the breast and regional lymph nodes, however, it does not remove undetected occult cancer cells that may remain within the breast, scar, chest wall or remaining lymph nodes. These microscopical tumor residues may lead to local recurrence and also to distant metastasis. Administration of radiotherapy after surgery has been shown to minimize these events, and it is thus used as standard adjuvant treatment of early BC (Langlands et al. 2013). Radiation is a cancer treatment that uses high doses of radiation to kill cancer cells by damaging their DNA beyond the possibility to repair. Radiation can be used in combination with other cancer treatments, surgery, chemotherapy and immunotherapy. It has been observed that recurrent tumors often localize close to the surgical scar; for this reason, radiotherapy can be used, in selected cases, as an intraoperative treatment (IntraOperative RadioTherapy, IORT) to "sterilize" the tumor bed. Furthermore, IORT is able to modify the post-surgical microenvironment by altering the wound fluid composition, reducing the production of growth factors and inflammatory cytokines, eventually diminishing the survival of residual cancer cells left behind by surgery in the tumor bed (Belletti et al. 2008).

- **Chemotherapy**:

Most chemotherapeutic agents act on dividing cells, thus making cancer cells a better target. In contrast to cancer cells, over time normal cells will mostly recover from chemotherapy effects.

Most used chemotherapeutic agents in BC are:

- Anthracyclines (*Epirubicin, Doxorubicin, Daunorubicin*): anti-tumor antibiotics that interfere with Topoisomerase II during DNA replication, by binding to DNA. Moreover, they cause formation of free radicals, increasing cell oxidative stress.
- Taxanes (*Paclitaxel, Docetaxel*): mitotic inhibitors, derived from plants. They work by blocking microtubules and mitotic spindle disassemble.
- Platinum derivatives (*Cis-platin, Carboplatin*): classified as alkylating agents, they bind to DNA, inhibiting its replication and transcription. Therefore, there is the block of protein synthesis, resulting in cell death.
- Fluorine derivatives (*5-fluorouracil*, *Capecitabine*): inhibit DNA synthesis and slow tumor growth (Fisusi et al., 2019)

- **Endocrine therapy**:

Administration of the endocrine therapy is based on the concept that changing the hormonal balance of the patient with hormone receptor positive (HR+) breast cancer will lead to changes in tumor growth and regression of metastatic disease (Goldhirsch et al. 2011). Both Luminal A and B tumors show benefit from endocrine treatment. There are three main categories of endocrine therapy agents: aromatase inhibitors (AIs), selective ER modulators (SERMs) and selective ER degrader or downregulators (SERDs). AIs, such as *Exemestane, Anastrazole* and *Letrozole*, inhibit an enzyme called 'aromatase' that converts testosterone to estradiol, and androstenedione to estrone, by aromatization. AIs are currently used in the standard treatment for postmenopausal breast cancer when the primary source of estrogen (ovaries) is terminated or in presence of ovarian activity suppression (Ratre et al. 2020).

Selective ER Modulators, such as *Tamoxifen, Raloxifen,* and *Toremifene*, competitively bind to ER to inhibit its pro-proliferative stimuli (Miller et al. 2014). Adjuvant Tamoxifen is currently considered standard of care for premenopausal women with endocrine-responsive disease. Selective ER degrader or downregulator, such as Fulvestrant, binds ER inducing a structural change that leads to increased surface hydrophobicity and subsequent receptor degradation. Fulvestrant-induced degradation affects the ligand-independent functions of ER that are not addressed by tamoxifen. Fulvestrant is currently approved for treatment of ER-positive metastatic breast carcinoma patients that have progressed after tamoxifen therapy (Lai et al., 2017).

In metastatic Luminal breast cancer, *de novo* or acquired resistance to endocrine therapy eventually develops; for this reason, clinical trials have considered to target alternative pathways (Ades et al. 2014; Creighton 2012), such as PI3K/AKT/mTOR axis, CDK4/6, p53-MDM2 interaction, FGFR1(Fibroblast Growth Factor 1 Receptor) and HDAC (Histone DeACetylases) (**figure 2**).

Once activated, in presence of growth factors, nutrients, energy signals through the AMP-activated kinase, and various stress signals, PI3K activates AKT (or PKB: Protein Kinase B) and downstream effector mTOR, to promote cell growth and division, by increasing mRNA translation and inhibiting autophagy (Zoncu et al., 2011). As describe above, Luminal B BC have higher PI3K pathway activation, for this reason there are numerous types of agents targeting the PI3K/AKT/mTOR pathway: *pan-PI3K inhibitors; isoform-specific PI3K inhibitors*; and the *PI3Kδ inhibitor*; dual *PI3K–mTOR inhibitors*; *AKT inhibitors*; and the most common mTOR inhibitors (including allosteric inhibitors such as the *Rapalogues Sirolimus, Temsirolimus, Ridaforolimus* and *Everolimus* or *mTOR catalytic inhibitors*). The FDA (Food and Drug Administration) and the EMA (European Medicine Agency) approved *Everolimus* in combination with *Exemestane* for the treatment of women with ER-positive/HER2-negative breast cancer with recurrence or progression after receiving *Letrozole* or *Anastrozole* (Rodon et al. 2013; Zardavas et al., 2013).

The cyclin D1 complex (cyclin D1 bound to CDK4 or CDK6) and the cyclin E–CDK2 complex phosphorylate the retinoblastoma (Rb) protein, preventing it from inactivating the E2F (E2 Factor) transcription factor, thus leading to cell cycle progression from G1 to S phase (Weinberg 1995; Harbour et al. 1999). In Luminal tumors, inhibition of the Rb protein is mediated through CCND1 (the gene coding for cyclin D1) or CDK4 amplification or overexpression, or loss of the endogenous CDK inhibitors (CDKN1B, CDKN2A, CDKN2B). *Palbociclib*, a highly selective oral inhibitor of CDK4 and CDK6, was active in Luminal-like breast cancer cell lines (Desmedt et al. 2008). FDA approved *Palbociclib* in combination with *Letrozole* for the treatment ER-positive/HER2-negative advanced BC as initial endocrine based therapy in postmenopausal women. Moreover, the FDA also granted *Palbociclib* in combination with *Fulvestrant* for the treatment of HR-positive/ HER2-negative advanced or metastatic breast cancer in women with disease progression following endocrine therapy.

The p53 tumor suppressor is a key transcription factor regulating cellular pathways such as DNA repair, cell cycle, apoptosis, angiogenesis, and senescence. It acts as an important defense mechanism against cancer onset and progression, and is negatively regulated by interaction with the oncoprotein MDM2 (Nag et al. 2013). In LBC, as described above, MDM2 gene expression is frequently amplified and TP53 is frequently mutated (Ades et al. 2014; Koboldt et al. 2012) leading to downregulation of tumor

suppressive p53 pathways. Preclinical studies show that targeting the MDM2–p53 interaction using *MDM2 inhibitors* increases apoptosis in cancer cells and might be a potentially powerful approach to reverse endocrine resistance in tumors with MDM2 amplification (Ellis et al., 2013).

FGFR1 belongs to the family of Fibroblast Growth Factor Receptors FGFRs, they are activated upon binding of ligands (fibroblast growth factors, FGFs) to their extracellular domain followed by receptor dimerization and phosphorylation of C-terminal tyrosines. These phosphorylated residues dock several adaptor proteins that induce activation of downstream signaling pathways, including RAS/RAF/MEK/ERK and PI3K/AKT (Turner et al., 2010). FGFR1 amplification is associated high proliferative tumors and with poor prognosis in ER-positive breast cancer (Elbauomy Elsheikh et al. 2007). Moreover, preclinical data suggest that *FGFR1* amplification drives anchorage-independent proliferation and resistance to endocrine therapy (Turner et al. 2010). Approaches to targeting FGFR in various tumor types include *tyrosine kinase inhibitors (TKIs)*, *monoclonal anti-FGFR antibodies*, *and FGF-trapping molecules*. Selective FGFR TKIs are at an earlier phase of development.

The MLL3 gene belongs to a family that encodes histone methyltransferases and, as described above, MLL3 gene is mutated in about 8% of Luminal mammary tumors. Furthermore, the TCGA has shown that a subset of Luminal B tumors exhibits a hypermethylation phenotype and a low frequency of PIK3CA, MAP3K1 and MAP2K4 mutations. Therefore, several evidences have suggested that *HDAC inhibitors*, combined with endocrine treatment, might be a promising approach to reverse endocrine resistance in a subset of Luminal tumor (Stephens et al. 2012; Koboldt et al. 2012). However, the *HDAC inhibitors* are still in a preclinical study phase.

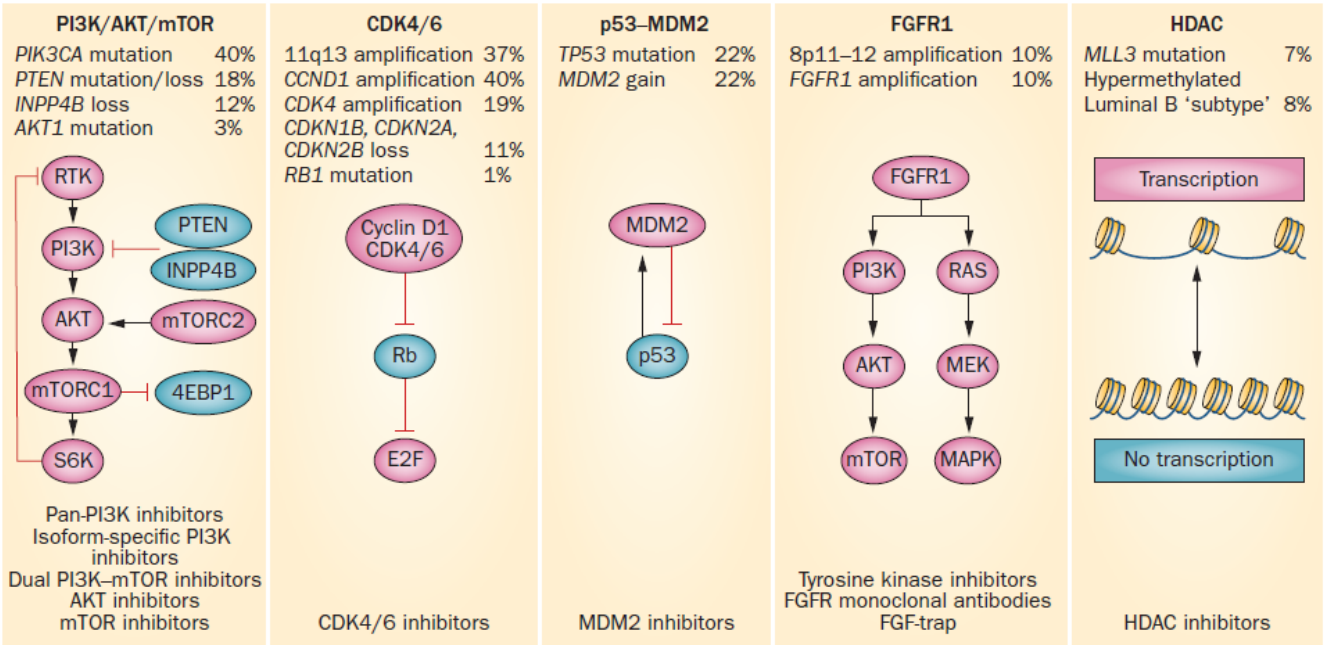

Figure 2. Genomic and epigenomic landscape, pathways and drugs to reverse endocrine resistance in estrogen receptor-positive breast cancer*. Data on genomic and epigenomic landscape are derived from next-generation sequencing studies and from a study combining gene-expression profiling and copy number aberration data. Each column shows the different pathways, mutations percentage and the specific inhibitor to block them. Pink denotes gene or protein activation and blue denotes gene or protein suppression in breast cancer. Figure has been adapted from "Luminal breast cancer: from biology to treatment" Ignatiadis, Sotiriou et al. 2013.*

1.3 CDKN1B ($p27^{kip1}$ gene)

CDKN1B gene, encoding for the cell cycle inhibitor $p27^{kip1}$ (here after p27), is an intrinsically unstructured, multifunctional protein that influences several biological functions, from cell cycle to migration and transcriptional regulation. p27 protein belongs to the Cip/Kip family of CDK (Cyclin Dependent Kinase) inhibitors, that includes also $p21^{cip1}$ and $p57^{kip2}$, all characterized by the presence of a conserved amino-terminal region containing the cyclin and CDK binding domains. **Figure 3** depicts the crucial roles played by p27 during the cell cycle. During the G1, p27 regulates cyclin E-CDK2 and cyclin A-CDK2 complex activities, binding both cyclin and CDK subunits, resulting in a block of the cell cycle progression (Polyak et al. 1994; Toyoshima et al., 1994; Coats et al. 1996). In early G1 phase, p27 promotes the assembly and the nuclear importation of cyclin D-CDK4/6 complex, supporting the stabilization of cyclin D. Mitogen stimulation determines the cell cycle progression, by both the activation of CDK4 and by impounding p27, that is maintained, in this way, displaced from its principal target, cyclin E-CDK2. Cyclin E-CDK2 complex then targets p27 to ubiquitin-dependent degradation through its nuclear phosphorylation in threonine 187 (Sherr et al., 1999), thus reinforcing CDK4 activity

to complete Rb phosphorylation. Large body of literature studying the regulation of p27 during cell cycle, highlighted a regulatory role for p27 also in G2-M transition. p27 was historically known as universal CDKs inhibitor, able to down-regulate *in vitro* not only cyclin E/A-CDK2 activity but also CDK1 (Toyoshima et al., 1994). Nakayama and colleagues showed *in vivo* how p27 accumulation at G2/M transition induces a strong decrease in CDK1-associated kinase activity. The prolonged G2 arrest induced by p27, through the suppression of CDK1 activity, was shown to be responsible for the centrosome duplication, cell endoreplication and polyploidy (Nakayama et al. 2004). Later, others proposed a different explanation to the mitotic defect, suggesting that p27 could be involved in the prevention of CDK1 expression instead of directly inhibit the activity (Serres et al. 2012; Sharma et al. 2012).

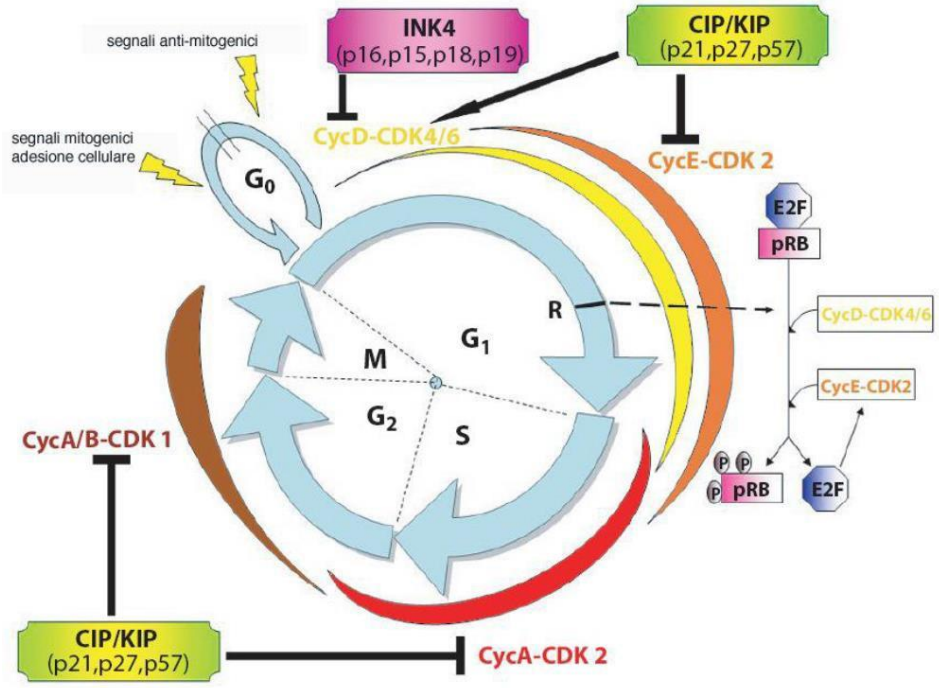

Figure 3. Schematic representation of the cell cycle regulation. *Mitogenic stimuli induce cell cycle progression from G0 to G1 inducing the expression of D type cyclins and lowering the expression of p27. Sequential activation of cyclin E-CDK2, cyclin A-CDK2, cyclin A-CDK1 and cyclin B1-CDK1 allows the cells to pass through the restriction point (R) at the G1-S transition and to complete the mitotic division. The passage through the R point is due to the inactivation of the pRb protein by CDKs-dependent phosphorylation. Figure has been adapted from "p27^{kip1} Functional Regulation in Human Cancer: A Potential Target for Therapeutic Designs" Belletti et al. 2005.*

The abundance of p27 within the cell is controlled by multiple mechanisms that operate at level of its synthesis (transcription/translation) and, particularly, its stability, degradation and localization. p27 levels increase in response to various stimuli that inhibit cell proliferation, such as cell-cell contact, loss of adhesion to extracellular matrix, cell differentiating stimuli and TGFβ (Transforming growth factor β), IFN-γ (Interferon-γ), c-AMP (Cyclic adenosine monophosphate), rapamycin and lovastatin treatments (Belletti et al. 2005). High level of p27 induces a G1 cell cycle arrest and accumulation in G0. As depicted in **Figure 4**, the most important cellular mechanisms that regulate p27 levels are:

• *sequestering* into higher order complexes with cyclin D-CDK4 after activation of the MAPK (Mitogen-Activated Protein Kinase) pathway, that promotes cyclin D transcription (Susaki et al., 2007). Also, the proto-oncogene c-Myc is responsible for p27 sequestration, by increasing the expression of cyclin D and cyclin E. This molecular event appears essential for Myc-induced cell cycle progression (Vlach et al. 1996),

• *translocation* to the cytoplasm, with consequent progression of the cell cycle, after phosphorylation by KIS (Kinase Interacting with Stathmin) or by MAPK and/or phosphorylation by AKT or RSK (Ribosomal S6 Kinase) (Belletti et al., 2005; Philipp-Staheli et al., 2001). The nuclear export of p27 by CRM1 (Chromosomal Maintenance 1) is necessary for mediated proteolysis (Boehm et al. 2002; Kamura et al. 2004).

• *degradation,* p27 can be translocated from the nucleus to the cytoplasm and degraded by the ubiquitin-proteasome pathway, *via* the KPC complex (Kip1 ubiquitination-promoting complex). This complex consists of KPC1 and KPC2 proteins, that interact with and ubiquitinate p27 in the cytoplasm (Kamura et al. 2004; Kotoshiba et al. 2005). The nuclear export of p27 by CRM1 is necessary for KPC-mediated proteolysis (Boehm et al. 2002; Kotoshiba et al. 2005).

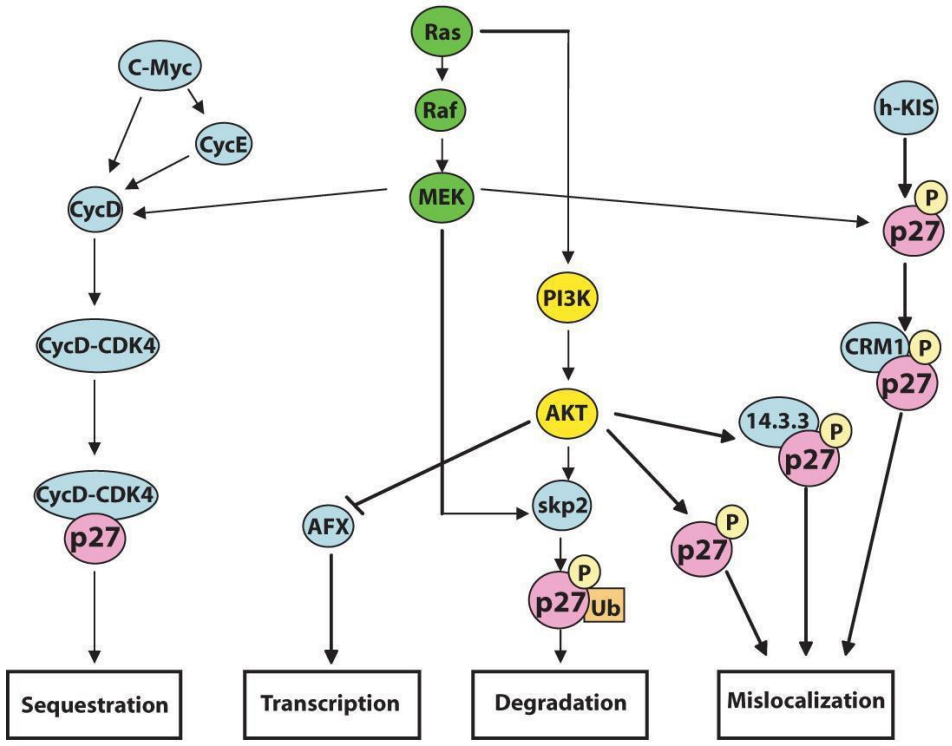

Figure 4. p27 regulation. *Representation of the different intracellular pathways to regulate p27 expression and function. Figure has been adapted from "p27^{kip1} Functional Regulation in Human Cancer: A Potential Target for Therapeutic Designs" Belletti et al. 2005.*

p27 coding sequence contains several functional domains and phosphorylation sites (**figure 5**). The phosphorylation at Serine *S10* plays a critical role in decreasing p27 nuclear abundance, thereby allowing for the initial activation of cyclin-CDKs complexes (Besson et al. 2006; Ishida et al. 2000; Rodier et al. 2001). This serine is a substrate for KIS, MAPK, AKT and Mirk/Dirk1B (Minibrain-related kinase/dual-specificity tyrosine-regulated kinase) (Boehm et al. 2002; Vervoorts et al. 2008; Besson et al. 2006).
The region containing the cyclin and CDK binding domains is highly conserved and is located in the amino-terminal region.
The tyrosines *Y74, Y88* and *Y89*, located in the CDK-binding domain, are preferentially phosphorylated in active proliferating cells and convert p27 to a non-inhibitory state (James et al. 2008). The residue *Y88* can be phosphorylated by the Src-family kinase and by the oncogene product BCR-ABL. Once phosphorylated on *Y88*, CDK2 efficiently phosphorylates p27 on threonine *T187*, promoting in turn its SCF-Skp2-dependent degradation, suggesting an explanation for premature p27 elimination in cells transformed by these activated tyrosine kinases (Grimmler et al. 2007). The oncogenic kinase Src regulates p27 stability through its phosphorylation not only at *Y88* but also at *Y74* and, to a less degree, at *Y89*, facilitating p27 proteolysis and impeding the efficient action of CDK4/6 inhibitors on their targets (Chu et al. 2007).
The p27 protein could be phosphorylated at serine *S83* by CK2 (Casein Kinase 2)(Tapia et al. 2004) in cardiomyocites stimulated by angiotensin II, a major cardiac growth factor, inducing its proteasomal degradation (Hauck et al. 2008).
Recently, it has been shown that serine in position *S140* can be phosphorylated by ATM kinase after DNA damage induced by ionizing γ-radiation, stabilizing p27 for G1/S cell cycle checkpoint activation (Cassimere et al. 2016). The *T187* of p27 is phosphorylated by the cyclin E-CDK2 and cyclin B-CDK1 (Sheaff et al. 1997; Vlach et al 1997) and leads to its degradation *via* the cytosolic ubiquitin-proteasome system (Grimmler et al. 2007; Hara et al. 2001). Other phosphorylation sites of p27 are the *T157* and the *T198*, both regulated by AKT. The *T157* residue, mapping within the NLS (Nuclear Localization Signal) of p27, is phosphorylated by AKT and causes retention of p27 in the cytoplasm, precluding p27- induced G1 arrest (Liang et al. 2002; Shin et al. 2002; Viglietto et al. 2002). AKT phosphorylates p27 also at *T198*, making p27 recognizable by the 14-3-3 family of proteins and, thereby, retained in the cytoplasm (Fujita et al. 2002). Moreover, it has been demonstrated that phosphorylation at *T198* is able to regulate p27 stability, localization and interaction with stathmin, interfering with p27 ubiquitination and with p27 role in cell motility (Schiappacassi et al. 2011).

In addition to phosphorylation and ubiquitination, other post-translational modifications regulate p27 activity. Evidence demonstrates that, in response to TGFβ treatment, p27 is SUMOylated on K134, increasing protein stability and nuclear localization (Lovisa et al. 2016) (Jun e Lau 2010). SUMOylation also regulates p27 binding to CDK2, thereby governing its nuclear proteasomal degradation.

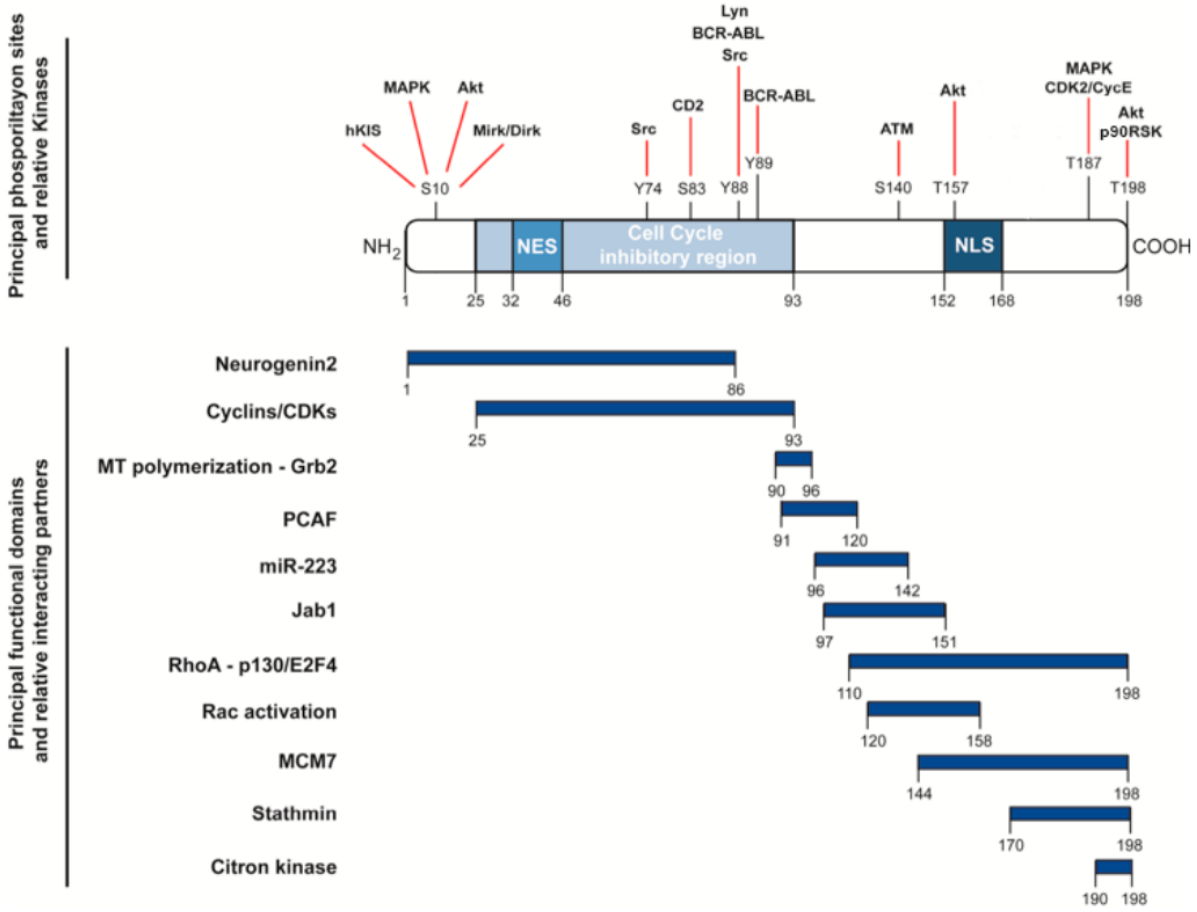

Figure 5. Schematic representation of the main functional domains and phosphorylation sites of p27*. p27 protein is composed by 198 amino acids and contains a nuclear exportation signal (NES) at the N-terminus and a nuclear localization signal (NLS) at the C-terminus. Key phosphorylation sites and corresponding kinases are depicted in the upper part of the figure and linked with red lines. The cell cycle inhibitory region is comprised between amino acids 25 and 93 and is necessary for the binding to cyclin/CDK complexes. Known functional domains and relative interacting protein/microRNA are reported below and highlighted by blue rectangles. Figure has been adapted from "Landscape of CDKN1B Mutations in Luminal Breast Cancer and Other Hormone-Driven Human Tumors" Cusan et al. 2018.*

1.3.1 $p27^{kip1}$ in tumors

The importance of p27 in the regulation of exit from and entry into the cell cycle and its impact in tumorigenesis was firstly revealed by the generation of p27-deficient mice. The p27 KO mice show an increase body size of about 20-30% compared to WT (wild type) mice (Fero et al. 1998; Nakayama et

al. 1996) that demonstrates a key role of p27 in controlling cell growth also *in vivo*. Loss of p27 in mice cooperates strongly to the neoplastic phenotype, increasing the frequency and severity of the tumors, decreasing latency, and in certain contexts, increasing the number of metastases.

Furthermore, the lack of this gene in conjunction with specific oncogenic stimuli increases malignancy and frequency of tumors, emphasizing that the presence of p27 is an important limiting factor for tumor progression (Belletti et al. 2005). However, p27 has been found to be mutated in only a few types of tumors, such as prostate cancer (Barbieri et al. 2012), small intestine neuroendocrine tumors (SI-NETs), a rare malignant neoplasm arising from neuroendocrine precursor cells, in which CDKN1B represents the most frequently mutated gene (Francis et al. 2013) and Luminal breast cancer (Stephens et al. 2012; Viotto, Russo et al. 2021).

CDKN1B germline mutations have been proposed to be the cause of multiple endocrine neoplasia type 4 (MEN4), an autosomal dominant disorder, characterized by the occurrence of tumors in endocrine glands (Lee et al. 2013). CDKN1B is rarely mutated (<1%) in epithelial ovarian cancer and HNSCC (head and neck squamous cell carcinomas) (Viotto, Russo et al. 2021).

Unlike prototypic tumor suppressor genes (e.g., TP53 and Rb), p27 does not appear to follow the Knudson's "two-hit" theory, behaving as haplo-insufficient tumor suppressor gene (Fero et al. 1998). Complete loss of p27 expression is not uncommon in human malignancies but silencing or mutations of both alleles are very rare, which is consistent with the notion that p27 loss in tumors is mainly due to an accelerated proteolysis. Accordingly, a plethora of studies shows the involvement of p27 protein reduction or loss in many tumors, such as carcinomas of the colon, breast, lung and ovary as well as brain tumors, lymphomas and soft tissue sarcomas (Belletti et al. 2005). Multivariate analysis showed that reduced levels of p27 are of independent prognostic significance for many of these tumors. Yet, apparently in contrast with these data, some tumors may contain high levels of p27, suggesting that mechanisms other than protein degradation allow transformed cells to circumvent p27 growth inhibition. A retrospective analysis of p27 expression in 2,031 breast cancer samples from a randomized clinical trial, demonstrated that reduced p27 was an independent prognostic factor for reduced overall survival (Porter et al. 2006). In another work including 500 patients with premenopausal ER+ BC, low p27 strongly correlated with poor survival, showing the predictive potential of p27 in a prospective trial (Pohl et al. 2003). Through meta-analysis of 20 studies, Guan *et al.* correlated p27 expression and clinical outcome of BC including overall survival (OS), disease-free survival (DFS) and relapse-free survival (RFS). A total of 60% of the studies showed a significant association between p27 high expression and OS, whereas 25% and 60% studies demonstrated a correlation between p27 high expression and DFS

and RFS, respectively (Guan et al. 2010). Together, these data indicate that reduced p27 is an independent prognostic factor for shorter OS and DFS.

Moreover, reduced p27 levels correlate with lower level of cyclin D1(Barnes et al. 2003) and with *ERBB2* (HER2 encoding gene) amplification (Newman et al. 2001; Spataro et al. 2003).

1.3.2 CDKN1B mutation and Copy Number Variation (CNV)

The advent of massive parallel sequencing allowed to analyze the cancer genome at very high sensitivity. In our recently published article (Viotto, Russo et al. 2021), we assessed the frequency of CDKN1B mutations in a large cohort of cancer patients (i.e., breast cancer, HNSCC and epithelial ovarian cancer). From our analyses, we confirm literature data indicating that CDKN1B is mutated predominantly in LBC (3.1%) than in other BC subtypes. As p27 is an haploinsufficient oncosuppressor, its allelic loss could be another mechanism exploited for gene inactivation. The results showed that 11.8% of the analyzed BC patients displayed a CDKN1B CNV with a loss in 7.5% and a gain in 4.3% of them. Interestingly, when only LBC were considered, the percentage of CNV raised to 13.7%, again indicating that CDKN1B is mainly altered in the Luminal subtype. These findings support the possibility that loss of p27, via either protein mutation, truncation or allelic CNV, could represent a significant event in the onset and progression of LBC. To verify whether CDKN1B could be related to progression more than to the onset of LBC, we next evaluated the presence of CDKN1B mutations in ccfDNA (circulating cell-free DNA). These patients displayed a substantially higher mutation frequency (8.5%), suggesting that CDKN1B alterations may more frequently occur later during the disease progression.

Of the 13 somatic mutations that we identified, four generated a stop codon and resulted in the loss of p27 C-terminus (**figure 6**). As already described, the binding of cyclin/CDK complexes is located in N-terminal portion of p27 protein, while the C-terminal region is a more disordered region and contains sites important for protein stability and localization. The fact that more than 50% of mutations observed in sporadic breast cancer are truncating/frame shift mutations (Stephens et al. 2012; Ellis et al. 2012; Viotto, Russo et al. 2021) supports the possibility that C-terminus loss may directly contribute to onset and/or progression of breast cancer (Cusan et al. 2018; Berton et al. 2017; Rampioni Vinciguerra et al. 2019; Huh et al. 2016; Ding et al. 2019).

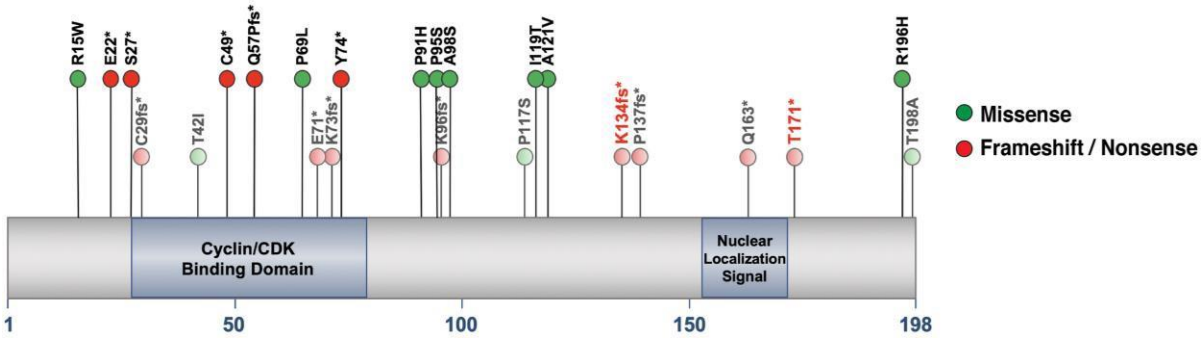

Figure 6. Lollipop plot of CDKN1B gene mutations. *Lollipop plot represents mutations identified in our cohort of solid biopsies (long lines, bright colors) or by others (Ellis et al. 2012; Stephens et al. 2012) (short lines, faded colors). Green dots indicate missense mutations and red dots indicate frameshift/nonsense mutations. The two mutations chosen for the functional studies in MCF-7 cells (K134fs* and T171*), identified by Ellis et al (Ellis et al. 2012), are written in red. Figure has been adapted from " CDKN1B mutation and copy number variation are associated with tumor aggressiveness in Luminal breast cancer" Viotto, Russo et al. 2021.*

1.4 CDK4/6 inhibitors

As described above, the cyclin D/CDK4/6/Rb pathway is frequently dysregulated in cancer (O'Leary et al. 2016). Moreover, increased levels of cyclin D and CDK4 are commonly observed (Fumagalli et al. 2016; Finn et al. 2020), which makes inhibitors targeting the cyclin D/CDK4/6/Rb pathway ideal candidates for cancer therapeutics (Y. Yang et al. 2020). Palbociclib, Ribociclib, and Abemaciclib have been approved by the Food and Drug Administration for advanced hormone receptor-positive (HR+) breast cancer patients when combined with Letrozole or Fulvestrant (O'Leary et al. 2016; Lynce et al. 2018). The combinatorial strategy presented a substantial improvement in progression-free survival with a well-tolerated toxicity profile in multiple clinical trials (Tripathy et al. 2018; Finn et al. 2016). The combination of CDK4/6 inhibitors and other targeted drugs also shows promising prospects (Rampioni Vinciguerra et al. 2022). All three CDK4/6 inhibitors bind to the ATP domain of CDK4/6 blocking their kinase activity (**figure 7**) (Finn et al. 2009).

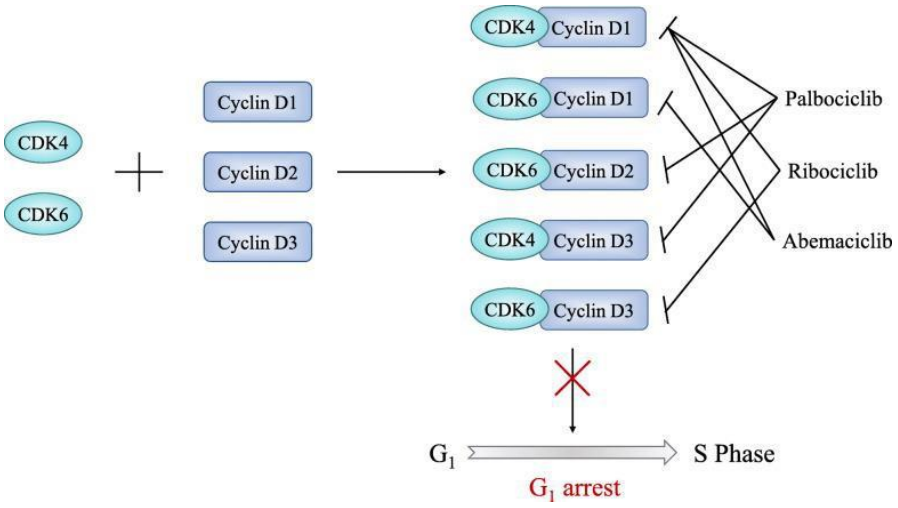

Figure 7. Specific targets of CDK4/6 inhibitors. *CDK4/6 inhibitors specifically bind to CDK4/6, thus inducing G1 phase arrest. Although these inhibitors perform the same function in cell cycle progression, their targets are slightly different. Palbociclib inhibits cyclin D1-CDK4, cyclin D2- CDK6, and cyclin D3-CDK4. Ribociclib targets cyclin D1-CDK4 and cyclin D3-CDK6. Abemaciclib targets cyclin D1-CDK4/6. Figure has been adapted from "CDK4/6 inhibitors: a novel strategy for tumor radiosensitization" Yang et al. 2020.*

1.4.1 Palbociclib

Palbociclib (PD-0332991) is the first CDK4/6 inhibitor received FDA approval. It is a highly selective reversible inhibitor of CDK4/6, with a limited inhibitory effect on the other cyclin-dependent kinases. The Palbociclib therapeutic potential was tested in a preclinical study in a large panel of BC cell lines, showing that the most sensitive cells were the Luminal breast cancer cell lines. Furthermore, the same study showed a synergistic effect of Palbociclib in combination with selective ER modulator, Tamoxifen. Clinical studies (i.e., Paloma-1, Paloma-2 and Paloma-3) were designed to test the efficacy and safety of Palbociclib and, following the positive results, Palbociclib has been approved for the first line treatment of advanced ER+ HER2- cancer, in combination with aromatase inhibitors and also in patients with disease progression, in combination with Fulvestrant (Finn et al. 2009).

1.4.2 CDK4/6 inhibitors resistance

Despite promising clinical outcomes, intrinsic or acquired resistance to CDK4/6 inhibitors has limited the success of these treatments. Some patients show a primary resistance, instead others show a acquired resistance after 24-48 months (AIOM, AIRTUR, Cancer number 2020; Rampioni Vinciguerra et al. 2022). There are various mechanisms that are directly or indirectly responsible for resistance to CDK4/6 inhibitors, categorizable into two broad main groups (Pandey et al. 2019):

I) Cell cycle-specific mechanisms. Loss of Rb with concurrent p16 overexpression resulted in failure to respond to CDK4/6 inhibitors because of the absence of Rb function. CDK6 overexpression was reported to promote resistance to CDK4/6 inhibitors in preclinical models (Yang et al. 2017)**.** Overexpression of

CCNE1, which encodes cyclin E, is a well-known mechanism for resistance to CDK4/6 inhibitors, as demonstrated by several studies (Konecny et al. 2011; Herrera-Abreu et al. 2016; Taylor-Harding et al. 2015). The overexpression of E2F causes the cell to circumvent CDK4/6 inhibition and rely upon signaling pathways other than the cyclin D-CDK4/6 axis for cell cycle progression (Dean et al. 2010). Also, overexpression of *CDK4*, which has been described in several cancers, may limit the efficacy of CDK4/6 inhibitors (Cen et al. 2012; Olanich et al. 2015; Wu et al. 2011).

II) Cell cycle-nonspecific mechanisms. Activation of the FGFR pathway appear to be associated with resistance to CDK4/6 inhibitors, as well as with endocrine resistance (Brooks et al. 2012). Also, activation of the PI3K/AKT/mTOR pathway is known to be a crucial event in driving the resistance to endocrine therapy and, as recently reported, to CDK4/6 inhibitors (Herrera-Abreu et al. 2016; Jansen et al. 2017).

1.5 Senescence

Cellular senescence is a mechanism whereby a dividing cell enters a stable cell cycle arrest upon stress stimuli and generally exerts a complex secretion of factors, known as Senescence-Associated Secretory Phenotype (SASP) that impacts on the nearby tissue, while the cell remains metabolically active and unresponsive to mitogenic and apoptotic signals (Kumari et al.2021).

The stress may include telomere shortening, oxidative stress, DNA damage, onco-gene activation or treatment with chemotherapeutics (González-Gualda et al. 2021). Senescence contributes to tumor suppression, wound healing and tissue homeostasis, primarily due to the arrested cell cycle and the secretion of specific factors and cytokines via the SASP. This secretion informs the immune system to initiate the clearance of senescent cells and stimulates the damaged tissue to heal (Muñoz-Espín et al. 2013; Storer et al. 2013). However, upon consistent and chronic damage, the process of immune surveillance is dysregulated and senescent cells accumulate, contributing to tissue dysfunction, chronic inflammation and a variety of age-associated disorders, including cancer, cardiovascular diseases, fibrosis, diabetes, neurological disorders and osteoarthritis (González-Gualda et al. 2021).

1.5.1 Senescence hallmarks

The arrest of cell cycle and SASP are not the only senescence traits, as depicted in **Figure 8** and described here below:

- **DNA Damage Response (DDR)**. DSB (Double-Strand DNA Break) and SSB (Single-Strand DNA Break) can lead to cellular senescence when are unresolved. H3K9 methylation is required for ATM-mediated DNA damage signaling (Ayrapetov et al. 2014). The ATM recruitment drives phosphorylation of the histone H2AX, which facilitates the assembly of specific DNA repair complex (Celeste et al. 2002). The persistence of DDR induces the phosphorylation of p53 at multiple serine residues, which enhances the ability of p53 to induce the transcription of many genes to induce senescence (Turenne et al. 2001). Inductions of ɣ-H2AX nuclear foci or phosphorylated p53 are commonly used as markers of senescence (Hernandez-Segura, Nehme, e Demaria 2018).

- **Cell cycle arrest**. The protein p16 directly inhibits the cyclin D-CDK4 complex, which allows for the dephosphorylation and stabilization of the Rb-E2F complex, and thus the inhibition of the cell cycle (Ben-Porath et al 2005). p53 is activated via phosphorylation after a DNA-damaging stimulus and then upregulates the transient expression of p21 that inhibits cyclin E-CDK2 which allows the dephosphorylation of Rb leading to the sequestering of E2F to arrest the cell cycle (González-Gualda et al. 2021). Additionally, the p15 and p27 and the mitogen-activated protein kinase p38 can also be used as markers although their involvement in the senescent program is not completely defined (Muñoz-Espín et al. 2013).

- **Chromatin reorganization**. To silence proliferation-promoting genes, the chromatin rearranges and forms dense structures know as Senescence-Associated Heterochromatin Foci (SAHFs). There are nuclear structures containing a collection of proteins associated with DDR, such as ATM, ATR, CHK2 and ɣ-H2AX that are formally considered a type of DNA-SCARS that reinforce senescence (Herbig et al. 2006).

- **Increased lysosomal content**. SA-βgal (senescence-associated β-galactosidase) is the most common marker of lysosomal activity and one of the first tests used to assess senescence. SA-βgal is a hydrolase enzyme that catalyzes the hydrolysis of β-galactosides into monosaccharides (Dimri et al. 1995).

- **Metabolic adaptation**. Mitochondrial dysfunction plays an important role in maintaining pro-inflammatory senescent phenotypes. The reduction of mitochondrial degradation (mitophagy) during

senescence program, lead to an increase of mitochondria number and size. Structural changes in the mitochondria also lead to alterations such as the increase in ROS (Reactive oxygen species), which is considered another senescence hallmark (Victorelli et al. 2019). An additional hallmark of senescence related to mitochondria is the resistance to apoptosis, resulting from the upregulation of pro-survival pathways. This event is mediated by the increased expression of antiapoptotic Bcl-2 family members, located on the membranes of mitochondria as well as the endoplasmic reticulum (Yosef et al. 2016).

- **Morphological changes**. Abnormally large and flat morphology defines senescent cells. Interestingly, the increase in size, which translates into an increased cytoplasm to DNA ratio, can contribute to the growth arrest observed in senescent cells. Granularity also changes in senescent cells, possibly due to the increase in size and number of lysosomes (Neurohr et al. 2019).

- **Cells surface marker**. Despite a universal or more specific membrane markers of cellular senescence remains to be defined, recent studies have provided significant insights into the so-called surfaceome of senescent cells. However, some of these reported surface receptors, namely ICAM-1, NOTCH1, NOTCH3, DEP1, B2M, DPP4, STX4, NTAL and, more recently, uPAR, have proven to serve as reliable markers of senescence (Althubiti et al. 2014).

- **Secretory phenotype**. The SASP comprises a number of factors, such as cytokines, chemokines, growth factors, metalloproteases and extracellular vehicles, that are secreted from senescent cells. The SASP is thought to be a major reason senescent cells contribute to either tissue homeostasis or dysfunction, as these factors play many roles in immune signaling, cell-to-cell communication and in the creation of pro-tumorigenic environments. Some of the factors most commonly found upregulated in senescent cells include the interleukins IL-1a, IL-6 and IL-15, the chemokine L-8, GRO-a and MIP-1a, and other factors, such as IFN-c,VEGF, ICAM-1 and GM-CSE (Coppé et al. 2010).

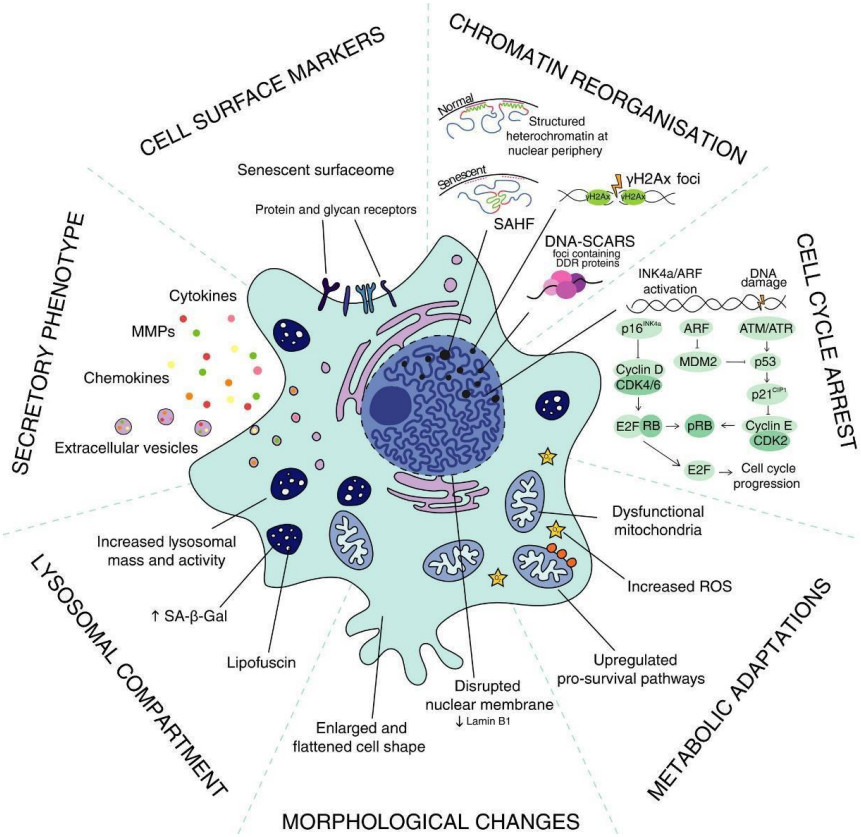

Figure 8. General hallmarks of cellular senescence*. These include a stable cell cycle arrest, driven by the action and cooperation of several proteins implicated, depending; chromatin alteration and reorganization, which includes SAHFs and DNA-SCARS marks; macromolecular damage and metabolic changes, including increased ROS levels and dysfunctional mitochondria; resistance to apoptosis, resulting from the upregulation of pro-survival pathways; increased lysosomal compartment, which is characterized by the well-known overexpression of SA-b-gal, and the implementation of a strong paracrine secretion termed SASP; morphology change, senescent cells generally present a characteristic enlarged and flattened morphology and particular senescence surfaceome. Figure has been adapted from "A guide to assessing cellular senescence in vitro and in vivo" González-Gualda et al. 2021.*

1.5.2 Senescence and Palbociclib

Palbociclib, as previously described, specifically bind CDK4/6 inducing G1 phase arrest. Depending on the cell type and the transforming event, some Rb-positive cells undergo quiescence and others undergo senescence, when treated with CDK4/6 inhibitors (Baughn et al. 2006). The senescent cells will not return to the cell cycle following removal of the inducing signal and are generally refractory to other proliferation-inducing signals (Rodier et al. 2011). However, the consequences of driving a cell into senescence after growth arrest are particularly interesting. Senescent cells express a cell type and signal specific program of gene expression and cytokine secretion (SASP), which can sculpt the immune response and the tumor microenvironment (Ohtani et al. 2012). On one hand, the SASP can induce the recruitment of immune cells that will mediate tumor clearance (Xue et al. 2007) or promote paracrine senescence (Acosta et al. 2013; Acosta et al. 2008). On the other hand, the SASP can create a pro-tumorigenic environment (Coppé et al. 2010). Furthermore, the SASP can induce cellular plasticity (Ritschka et al. 2017), and cancer cells that manage to escape senescence have a more aggressive

phenotype together with similarities to the stem cell state (Milanovic et al. 2018). Consequently, the SASP is often referred to as a "double-edged sword" and a better understanding of this biology will be paramount for its clinical manipulation.

Milanovic et al., studying lymphoma cells, revealed the unexpected twist that chemotherapy-induced senescence might generate into tumor cell phenotype, displaying an enhanced potential to drive tumor progression if they exit senescence. By investigating whether there might be a stem cell connection to senescence induced by chemotherapy, it was observed that cellular signaling pathways activated during chemotherapy-induced senescence are similar to the gene-expression patterns observed in stem cells.

2 AIM OF THE STUDY

Several clinical studies have highlighted that p27 downregulation may have prognostic and predictive potentia in various types of human tumors, particularly in breast cancer. In the Luminal subtype of BC, p27 displays an overall low, but higher rate of mutation compared to the other subtypes. The identified somatic mutations often resulted in p27 protein truncation, leading to loss of its C-terminal domain.

The overall aim of this PhD project is to understand the actual implications of p27 loss and C-terminal mutations during tumor transformation, growth and progression and, finally, dissect the role of p27 in response to therapies.

To achieve these aims, we have, first, explored *in vitro* and *in vivo,* the behavior of MCF-7 Luminal breast cancer cell line following knock-out of CDKN1B gene and the knock-in of CDKN1B mutants K134 frameshift (fs) and T171*.

Then, to better evaluate the possible involvement of p27 during the process of cell transformation and tumor initiation, we have also generated, characterized and tested the effect of p27 loss in normal human mammary epithelial cells with luminal phenotype (Breast Primary Epithelial Cells, BPEC), to better recapitulate the early steps of mammary cancer formation.

Finally, in order to test the implication of p27 in drug response, we have analyzed the response of MCF-7 and BPEC p27-modified clones to Palbociclib, an anti-tumor agent recently approved for the treatment of Luminal breast cancer in combination with endocrine therapy.

3 MATERIALS AND METHODS

3.1 *In vitro* experimentation

3.1.1 Cell culture and generation of cell lines modified for $p27^{kip1}$

Human breast adenocarcinoma MCF-7 cell line (ER+/PR+) were obtained from ATCC (LGC Standards) and maintained in DMEM (Gibco) supplemented with 10% fetal bovine serum (FBS, Gibco) and 1% Penicillin-Streptomycin (PS, Merck Life Science).

Human immortalized normal mammary epithelial cells of the Luminal subtype BPE-3 cells (hereafter BPEC) were purchased from LTCC (Live Tissue Culture Service Center-LTCC@med.miami.edu) and grown in BMI-P medium (LTCC), supplemented with cholera toxin 100 ng/ml (Merck Life Science), and strictly following all manufacturer's instructions.

All cell lines were grown in standard conditions at 37ºC and 5% CO_2.

MCF-7 p27 KO cell clones and MCF-7 KI clones (GFP-p27 WT, GFP-p27 T171* and GFP-p27 K134fs) were previously generated in our laboratory as previously described (Berton et al. 2017). Briefly, p27 KO cell clones were obtained by Nucleofection of custom Zinc Finger Nucleases (ZFNs) pair for p27 genomic sequence (Merck Life Science) using the AMAXA V kit for nucleofection (Lonza Biosciences), following the manufacturer instruction. Following electroporation, cells were maintained at 30°C for 2–3 days, then at 37°C before being single-cell seeded into 96-well plates. p27 KI clones were generated by co-transfection of the donor vector (pZDonor-AAVS1vector cloned with the coding DNA sequence of GFP-p27 WT, GFP-p27 K134fs and GFP-p27 T171*) by electroporation into p27 KO MCF-7 clone #17, along with the mRNA coding for the ZFN specific for AAVS1 locus (Merck Life Science).

BPEC p27 KO and KI cell clones were obtained using the CRISPR-Cas9 technology. Using the GenomeCRISPR online tool, different RNA guides (gRNA) were designed to target CDKN1B, the gene encoding for p27, in order to generate KO cells and the K134fs and T171* p27 mutants overexpressing cells (**figure 1**). To obtain the KO of p27, two different guides were positioned within the initial 100 nucleotides from the ATG codon of CDKN1B sequence (gRNA 18: 5'-GTCCCGGGTTAACTCTTCG-3'; gRNA 20: 5'- AGGAACCTCTTCGGCCCGG- 3', named KO 18 and KO 20). To generate the stop codon T171*, we designed a guide targeting 6 nucleotides close to the position T170 (gRNA sequence: 5'-TCCCCAAATGCCGGTTCTG-3') and for the K134fs mutation, a guide to target 10-20 nucleotides around the position K134 was drawn (gRNA sequence 5'- CTCTGAGGACACGCATTTGG- 3').

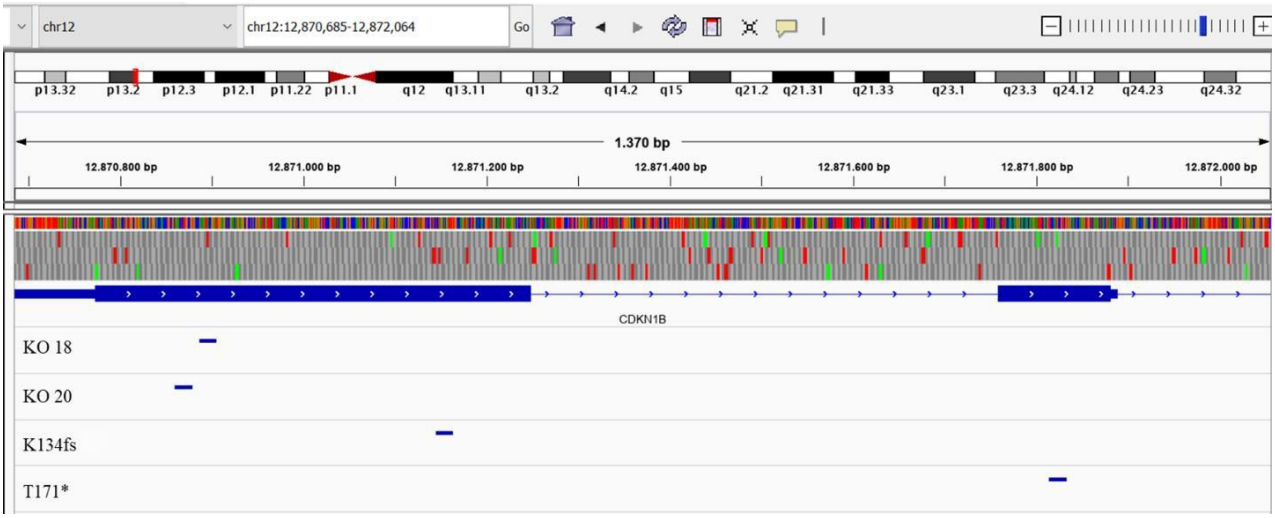

Figure 1. Guide RNA to generate BPEC p27 modified clones. *The image, taken from IGV software, reports the gRNA positions on CDKN1B sequence.*

BPEC cells were transduced with commercial *LentiCas9-Blast* lentiviral particles (pLv5-Cas9-Blast, Merck Life Science, **figure 2A**), in presence of Polybrene (8µg/mL) to induce Cas9 expression. After 72 hours from the transduction, cells were selected with 0.8 µM Blasticidin (Merck Millipore) to obtain a stable pool overexpressing Cas9.

BPEC Cas9 pool was then transduced in presence of Polybrene with the commercial *phU6-gRNA* lentiviral particles (LV04 phU6-gRNA:hPGK-puro-2A-tBFP, Merck Life Science, **figure 2B**) containing the guides described before, for the generation of the KO and T171* expressing cells. After 72 hours, cells were incubated with Puromycin (1µ/ml, Merck Life Science) to select the BPEC Cas9 cells expressing the phU6-gRNA vector. To generate cells overexpressing the p27 mutant K134fs, BPEC Cas9 pool were electroporated with the vector phU6 gRNA (Addgene, **figure 2C**). To evaluate the Cas9 cutting efficiency, genomic DNA was isolated from pools and analyzed using NGS (Next Generation Sequencing, MiSeq V2 Kit, Illumina) analysis. Then, cells were seeded as single cells into 96-well plates and obtained clones were analyzed through NGS and western blot to verify the loss of p27 protein or the expression of the mutants. In all experiments, multiple cell clones were tested, in duplicates or triplicates as appropriate.

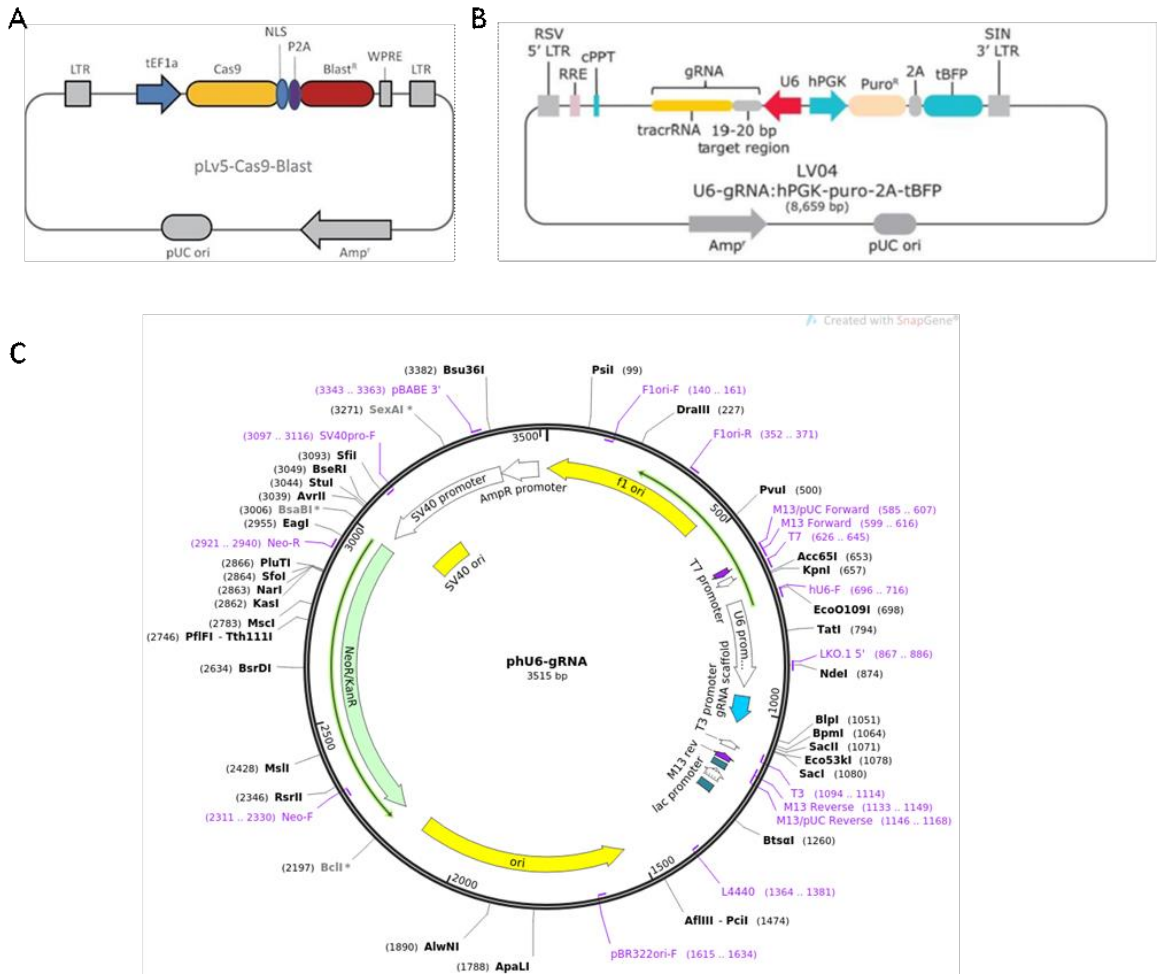

Figure 2. Lentiviral vectors employed for the generation of BPEC p27 modified clones, using CRISPR-CAS9 technology. ***A)*** *Scheme representing pLv5-Cas9-Blast vector used for the expression of Cas9 endonuclease.* ***B)*** *Scheme represents LV04 phU6-gRNA:hPGK-puro-2A-tBFP vector containing the specific gRNAs used for the generation of p27 KO and p27 T171* overexpressing cells. Figures were modified from Merck Life Science website.* ***C)*** *phU6-gRNA vector containing gRNA for p27 K134fs expression. Figure was taken from Addgene.*

3.1.2 Growth curve analysis

MCF-7 and BPEC p27 modified clones were plated in 6-well plate in duplicate ($5x10^4$ cells/well) in complete medium (DMEM 10% FBS, 1% PS for MCF-7 or BMI-P cholera toxin 100 ng/mL for BPEC cells). Where indicated, Palbociclib (PD0332991, Selleckchem, 2.5 μM) were added to the culture medium. At the indicated times, cells were detached with Trypsin-EDTA and counted using Trypan blue to exclude dead cells.

3.1.3 Cell viability assay

MCF-7 and BPEC clones were plated in 96-well plate ($3x10^3$ cells/well) and after 24 hours of incubation at 37°C, cells were treated with increasing doses of Palbociclib (PD0332991, Selleckchem). After 72 hours from the treatment, cell viability was determined using the CellTiter 96 AQueous Cell Proliferation Assay Kit (Promega) and absorbance was detected at 490-500 nm through Tecan Infinite M1000 PRO instrument.

3.1.4 SA-β-Gal activity assay

Evaluation of SA-β-Gal activity is commonly used to detect senescent cells. SA-β-Gal activity was analyzed in MCF-7 clones at different time points. Cells were plated in duplicate in 24-well plates ($15x10^4$ cells/well), the day after, clones were treated with Palbociclib (0.1μM) for 24 hours and SA-β-Gal activity was detected as described below.

In another set of experiments, MCF-7 clones were plated in 150 cm^2 flasks dishes ($5x10^6$ cells) and treated with Palbociclib (2.5 μM) for 72 hours, then cells were detached with Trypsin-EDTA and seeded in duplicate in 24-well plates without drug for 1, 10 or 20 days ($15x10^3$, $2.5x10^3$ e 500 cells/well, respectively). The cells were fixed with 2% formaldehyde and 0.2% glutaraldehyde solution for 20 min at 4°C and, after 3 washes in PBS, they were incubated overnight at 37°C in X-gal solution (2 mM MgCl2, 5mM potassium ferrocyanide, 5mM potassium ferricyanide, 1 mg/ml 5-bromo-4-chloro-3-indolyl-β-D-galactoside). The X-gal is the substrate for the activity of SA-β-Gal (β-Galactosidase associated with senescence), a lysosomal hydrolase enzyme that catalyzes the hydrolysis of β-galactoids into monosaccharides. X-Gal is catalyzed by SA-β-Gal in galactose and 5-bromo-4-chloro-3-hydroxyindole-1 which dimerizes and forms the blue precipitate. Using X-Gal as a chromogen substrate, this enzyme test evaluates the increased expression and activity of this lysosomal protein in senescent cells. Blue positive cells were counted in at least 5 randomly selected fields/well in duplicate.

3.1.5 Protein extraction and western blot analysis

Total protein extract was obtained scraping cells on ice using an appropriate volume of cold RIPA lysis buffer (NaCl 150 mM, Tris HCl pH 8 50 mM, Igepal 1%, Sodium-deoxycholate 0.5%, SDS 0.1% in deionized water), implemented with a protease inhibitor cocktail (cOmplete™ Protease Inhibitor Cocktail, Merck Life Science), dithiothreitol (Merck Life Science, 1 mM), sodium fluoride (Merck Life Science, 50 mM) and sodium orthovanadate (Merck Life Science, 1 mM) as phosphatase inhibitors.

After an incubation of 30 minutes on ice, cells were centrifuged at 13200 RPM for 20 minutes at 4°C to obtain proteins lysates that were transferred into fresh tubes. Concentration of isolated proteins was determined using a Bradford-based protein assay (Protein Assay Dye Reagent Concentrate, Bio Rad) and a standard curve made by serial dilution of known concentration of BSA. After quantification, protein samples were prepared with 30-40 µg of total extract up to a final volume of 20 µl with deionized water and 5X Leammli Sample Buffer (50 mM Tris–HCl pH 6.8, 2% SDS, 10% glycerol, 0.05% bromophenol blue and 125 mM beta-mercaptoethanol). Protein samples were then boiled at 95°C for 5 minutes and separated in a 4-20% polyacrylamide gel (Criterion™ Precast Gel TGX Stain-Free™, Bio Rad), which was plunged in running buffer 1 X (25 mM Tris, 192 mM glycine, 0.1% SDS in deionized water). Prestained protein SHARPMASS VI PLUS (10-250 KDa) was used as protein molecular weight marker. Proteins separated by their molecular weight were transferred to nitrocellulose membrane (Hybond™-ECL™, Amersham-Biosciences) at 600 mA for 1 hour in transfer buffer 1X (25 mM Tris, 0.2M glycine, 10% methanol in deionized water). Thereafter membrane was coloured with red Ponceau solution (0.1% Ponceau diluted in 5% acetic acid, Sigma-Aldrich) to ensure a good quality transfer. Finally, membrane was cut into horizontal strips to detect more proteins simultaneously differing from their molecular weight. The membrane was incubated with blocking buffer (5% non-fat dry milk diluted in Tris-Buffered Saline and 0.1% Tween-20 or Odyssey Blocking Buffer (LI-COR) commercial solution) for 1 hour at RT. Then membranes were incubated overnight at 4°C with appropriate primary antibodies diluted in Odyssey Blocking Buffer and TBS 0.1% Tween-20 (1:1). Membranes were washed three time in TBS 0.1% Tween-20 for 10 minutes and incubated for 1 hour at RT with secondary antibody IR-conjugated (Alexa Fluor 680, Invitrogen; IRDye 800, Rockland) for infrared detection (Odyssey Infrared Detection System, Li-Cor) or with horseradish peroxidase-conjugated secondary antibodies (GE Healthcare) for ECL detection (Clarity Western ECL Substrate, Bio-Rad). When re-blotting was needed, to remove primary and secondary antibodies, Re-blot Plus Strong Solution 10X (Merck Life Science) was used to strip the membranes.

Primary Antibodies	*Catalog Number*	*Vendor*	*Application and Dilution*
pRb (S780)	sc-12901	Santa Cruz Biotechnology	WB (1:1000)
Cyclin E	sc-28351	Santa Cruz Biotechnology	WB (1:200)
c-Myc	9402	Cell Signaling Technology	WB (1:1000)
Nf-kb	sc-8008	Santa Cruz Biotechnology	WB (1:200)
p27	610241	BD Transduction Laboratories	WB (1:700), IHC (1:50)
PR (Progesteron Receptor)	790-2223	Ventana	WB (1:1000), IHC (1:50)
ER (Estrogen Receptor)	790-4324	Ventana	WB (1:1000), IHC (1:50)
E-Cadherin	610181	BD Transduction Laboratories	WB (1:1000)
Vinculin	sc-73614	Santa Cruz Biotechnology	WB (1:1000)
CDK2	sc-6248	Santa Cruz Biotechnology	WB (1:700); IP (1:100)
Ki-67	#70-4286	Ventana	IHC (1:500)

***Table 1**: **Primary Antibodies**. The table summarizes the primary antibodies (catalog number and vendor) and the dilution used in the different experiments. WB: Western Blot, IP: immunoprecipitation and IHC: Immunohistochemistry.*

3.1.6 Kinase assay

Co-Immunoprecipitation (IP) experiments were performed incubating 0.3-0.4 mg of total lysate with anti-CDK2 and control antibody in HNTG buffer (20 mM HEPES, 150 mM NaCl, 10% Glycerol, 0.1% Triton X-100) supplemented with protease inhibitor cocktail (cOmplete^{TM} Protease Inhibitor Cocktail), dithiothreitol (1mM), sodium fluoride (50 mM) and sodium orthovanadate (1 mM) as phosphatase inhibitors, gently rocking overnight at 4 °C. A control sample (IgG) was prepared using a lysate incubated with a non-related antibody produced by the same animal species used for the assay. A mix of protein G Sepharose 4 Fast Flow (Amersham Biosciences) was added for the last 1 hour and 30 minutes of incubation. IPs were then washed 7 times in HNTG buffer and half part resuspended in 3× Laemmli Sample Buffer and loaded in gel to verify the IP. The other half part of the IP was resuspended in kinase buffer (20 mM TrisHCl pH 6.8,10 mM MgCl2). Then, a kinase reaction solution containing the sample plus 50 μM ATP, γ-P32 ATP (0.1uCi) and 2 μg of H1- Histone as substrate in buffered solution (20 mM TrisHCl pH 6.8, 10 mM MgCl2) was prepared. The reaction was carried out at 30°C for 30 min and then 5X Laemmli Sample Buffer was added. After denaturation at 95°C for 10 minutes, proteins were loaded on a 4-20% SDS-PAGE (Criterion Precast Gel, Biorad). The gel was dried at 80°C for 3 hours under

vacuum. Then gel was exposed on an autoradiographic film (GE, Amersham-Hyperfilm MP) at RT and developed at different time intervals.

3.1.7 Mammosphere assay

Mammosphere formation assay is commonly used to assess stem cell and self-renewal properties giving a measure of stem cell / early progenitor activity (Shaw et al. 2012) . Mammosphere assay was performed to test the stem-like properties of BPEC p27 KO clones and MCF-7 p27 clones upon treatment with Palbociclib (2.5 μM for 72 hours).

To establish primary mammospheres, cells were plated on poly-HEMA (Poly(2-hydroxyethyl methacrylate), Merck Life Science) coated dishes as single cell suspension ($1x10^4$ cells in 35 mm dishes or six-well plate) in the appropriate medium. MCF-7 cells were maintained in phenol red-free DMEM/F12 (Gibco) supplemented with B27 supplement (no vitamin A, 50X, Invitrogen), recombinant epidermal growth factor (hEGF, 20 ng/ml; PeproTech) and 1.5 % PS. BPEC clones were maintained in BMI-P (cholera toxin 100 ng/mL, 1% PS) supplemented with hEGF (20 ng/ml) or 2.5 % post-surgery wound fluids (WF).

After 10 days, primary mammospheres were counted. To establish secondary mammospheres, primary mammospheres were collected, resuspended in 0.5 % trypsin/0.2 % EDTA and disaggregate using 25-gauge needle fitted to a syringe. Cells were plated in the appropriate medium at the same seeding density that was used in the primary generation. After 10 days (MCF-7) or 30 days (BPEC), mammospheres numbers were counted and area was evaluated using *Volocity*® - PerkinElmer software.

3.1.8 Anchorage-independent growth

Anchorage-independent growth is the ability of transformed cells to grow independently of a solid surface and is a hallmark of carcinogenesis. Agar 0.6% (LowMelting Agarose, Merck Life Science) in DMEM 10% FBS was plated in six-well plate (2 ml / well) to constitute the bottom layer and placed at 4 °C to solidify. MCF-7 cells ($1x10^4$ cell/well) were re-suspended in 2 ml top agar medium (DMEM-10% FBS 0.4% Low Melting Agarose) and quickly overlaid on the previously gelified bottom agar medium. The plate was incubated at 37°C. Fresh medium was added to the wells twice a week as a feeder layer. After 2 weeks, the number and area were determined by shooting and counting at least 9 fields/well in duplicate at 10X magnification.

3.1.9 Three-dimensional cultures

Three-dimensional (3D) culture assay *in vitro* recapitulates the formation of mammary acini structures using a 3D matrix that mimics basement membrane functions (Hebner et al. 2008). MCF-7 cells (3000 cell/well) were embedded as single cells in Cultrex® Growth Factor Reduced Basement Membrane Extract (GFR-BME, 2%) (Trevigen), mixed with the appropriate medium and layered on the top of a bottom layer of polymerized matrix (GFR-BME, 8.5mg/ml) (Trevigen) in 12well glass chamber (50 µl/well) (Thermo Scientific™ Nunc™ Labtek™ II Chamber Slide™ System).
Embedded cells were incubated at 37°C for 10 days. At the end point, number of acini was counted and images were collected to calculate colonies areas, using the Volocity® (PerkinElmer) software.

3.2 *In vivo* experimentation

Animal experimentation was approved by the Italian Ministry of Health (#616/2015-PR) and by our Institutional Animal Care and Use Committee (OPBA) and conducted strictly complying with internationally accepted Institutional Animal Care and Use Committee guidelines (IACUC) for animal research and with the 3R principles. NOD.Cg-PrkdcSCID Il2rgtm1Wjl/SzJ (NSG) mice were purchased from Charles River and housed in CRO of Aviano animal facility, in ventilated biosafety cabinets under controlled temperature and humidity with a 12-hour dark/light cycle.
MCF-7 p27 KO or mutants clones were engrafted following the Mouse INtraductal (MIND) model essentially as described by Sflomos et al (Sflomos et al. 2016). In this model, Luminal tumor cells are injected directly into the mouse nipple, allowing them to reach and settle within the milk ducts. 5- to 6-week-old female mice were anesthetized and intraductally injected into the mammary glands with 4–10 µl of PBS containing 60000–150000 cells in at least 8 mammary glands/mouse.
3 mice were injected with MCF-7 control cells (WT#7 and Parental), 3 mice with MCF-7 p27 KO (clone #8 and #17), 2 mice with MCF-7 overexpressing p27 K134fs mutant (clone #244) and 2 mice with MCF-7 overexpressing p27 T171* mutant (clone #76). The onset of MIND-derived tumors was monitored by palpation once per week and once established, tumor growth was evaluated assigning to each tumor a score from 1 to 5. At least 8 tumors/mouse were recorded. After ~9 months from the injection, mice were sacrificed, engrafted mammary glands were collected, fixed in 4% paraformaldehyde for histology and IHC or snap-frozen for protein isolation. Distant organs such as lungs were collected to evaluate the presence of metastatic foci.

3.2.1 Protein extraction from tumor samples

Proteins extraction from MIND-derived tumors was performed using cold RIPA lysis buffer implemented with inhibitors (as described in detail in paragraph 3.1.5). Tumors homogenization was achieved by grinding the tissue using the gentle MACS^{TM} Octo Dissociator (MACS Miltenyi Biotec), following a incubation for 30 minutes on ice and a centrifugation at 13200 RPM for 20 minutes at 4°C. Protein lysates were then transferred into fresh tubes, processed and loaded in polyacrylamide gel as described in paragraph 3.1.5.

3.2.2 Histological analysis and immunohistochemistry of tumors samples

Mouse xenograft samples were fixed in formalin and processed for standard paraffin embedding. Histological sections (5 μm thick) were made from the paraffin blocks, deparaffinated with xylene, and stained with hematoxylin and eosin (H&E), according to standard procedures. For immunohistochemistry (IHC) analysis, routine deparaffinization of all sections mounted on positive charge slides was carried out according to standard procedures, followed by rehydration through serial ethanol treatments. Slides were immersed in citrate buffer [0.01 M sodium citrate (pH 6.0)] and heated in a microwave oven at 600W for 3 times, 5 min each, to enhance antigen retrieval. Endogenous peroxidase was blocked with 0.3% hydrogen peroxide in methanol for 30 min. Sections were immunostained with antibodies recognizing Ki-67, p27, PR and ER (Table 1) according to manufacturer's protocol and standardized procedures. Images were collected with Leica microscope at different magnifications.

3.3 Statistical analysis

All graphs and statistical analyses were performed using PRISM (version 6, GraphPad, Inc.). In all experiments, differences were considered significant when p was < 0.05. Statistical analyses including, Mann–Whitney test, Student's t-test and ANOVA test were used as appropriate and as specified in each figure.

4 RESULTS

4.1 Impact of $p27^{kip1}$ status in Luminal breast cancer cells

Several studies have highlighted that p27 downregulation/loss has prognostic and predictive potential, in various types of human tumors, particularly in Luminal breast cancer. CDKN1B gene, encoding for p27, displays an overall low but higher rate of mutation in LBC compared to other cancer types (Stephens et al. 2012; Ellis et al. 2012), as recently confirmed by our group in a large cohort of cancer patients, of which n. 396 solid biopsies were from LBC patients (Viotto, Russo et al. 2021). In line with previous findings, we observed that, of the 13 somatic mutations identified, four generated a stop codon and resulted in loss of p27 C-terminus. This observation supported the possibility that truncation of p27 C-terminus could contribute to onset and/or progression of LBC (Viotto, Russo et al. 2021). In order to investigate the role of p27 loss or C-terminal mutations, we employed the MCF-7 LBC cell line, genetically modified in our lab using Zinc-Finger technology (Berton et al. 2017), for the knock-out (KO) of CDKN1B gene. Then, using the MCF-7 KO cells, two different knock-in (KI, GPF-tagged) clones were generated, to express p27 truncated mutant form: the T171* (p27 T171*) and the K134 frameshift* (p27 K134fs), previously identified in LBC patients by the group of Ellis (Ellis et al. 2012). The T171* mutation generates a nonsense codon at position 171, resulting in loss of the last 28 amino acids, a region representing the so-called "intrinsically disordered region" of p27, known to be involved in protein-protein interactions and containing many phosphorylation sites (Cusan et al. 2018). The p27 K134fs mutation produces a frameshift at the lysine in position 134, which leads to a premature stop codon, loss of the intrinsically disordered region and, additionally, of the nuclear localization signal, located in amino acids 152–168. Together, we also generated p27 WT "rescue" clones, re-introducing untagged full length p27 in MCF-7 KO cells, in order to have control clones better comparable with mutant ones.

The results from the full characterization of the biological implications of p27 loss and expression of these mutants were already included in my graduation thesis and, in part, published in Viotto, Russo et al. 2021. Briefly, as expected, MCF-7 p27 KO cells displayed significant biological advantages compared to p27 WT clones and parental cells, while the p27 T171* and p27 K134fs KI clones showed intermediate phenotypes. This was true for proliferation in 2D, as well as for anchorage independence and growth in 3D-Matrigel, suggesting that the presence of the CDK-binding domain at the N-terminal portion of both mutants was able to restrain p27 KO phenotypes, but only in part (**figure 1A** and **C** showing growth curves and soft agar growth, as examples).

Starting from these observations, we next decided to verify whether and at what extent the two mutants were able to bind cyclins and CDKs, inhibit their kinase activities, and, eventually, control the cell cycle as the WT protein. During G1/S phase transition of the cell cycle, p27 principally interacts with and inhibits the activity of cyclin E-CDK2 complex, thereby blocking cell cycle progression. Co-immunoprecipitation assay of CDK2 with its binding partner cyclin E (CCNE1) showed that p27 mutants, T171* and K134fs, were part of the complex but at different extent compared to the WT (**figure 1B**). We next performed a kinase assay, looking at the phosphorylation of histone H1, as a substrate for CDK2 activity (**figure 1B**, top panel). While p27 WT bound cyclin E-CDK2 complex thereby inhibiting their phosphorylating activity on histone H1, p27 T171* and K134fs mutants, although still able to bind the complex, as expected by the fact that they retain the cyclin-CDK-binding domains, were less efficient in inhibiting its kinase activity and histone H1 phosphorylation level in MCF- 7 p27 T171* and p27 K134fs is at comparable level of that displayed by MCF-7 p27 KO. However, due to the lower stability of the K134fs p27 mutant protein, it remains to be established whether the lower inhibition could also be due to an overall lower binding to CDK2.

Together, these results indicated that, even if p27 mutants retain the ability to bind cyclin E-CDK2 complex, they partially lose the capability to inhibit it.

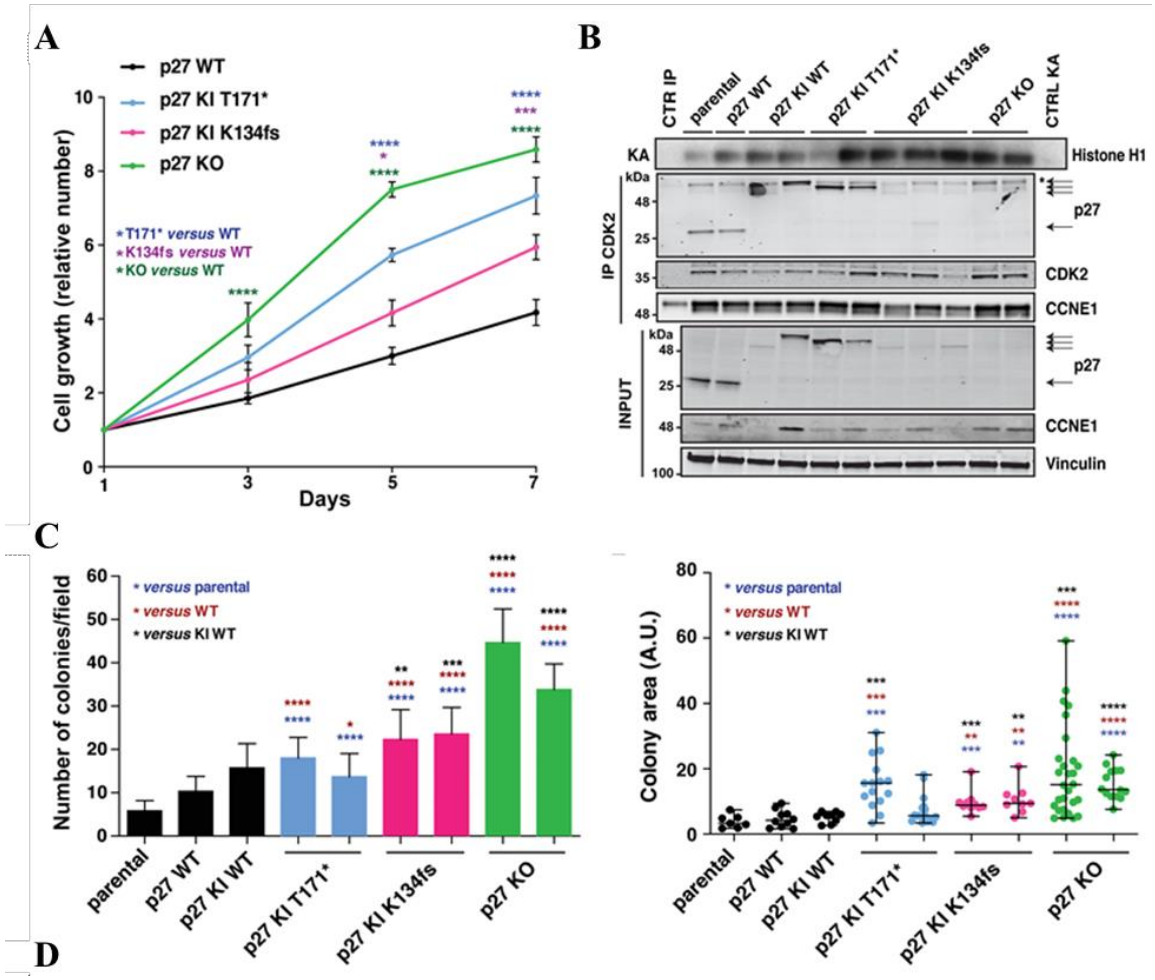

Figure 1. Characterization of p27 loss and expression of C-terminal deletion mutants in MCF-7 cell line*. **A)** Data from growth curve analysis of MCF-7 p27-modified cell clones. Data represents the mean (± SD) of clones for the different p27 status (MCF-7 p27 parental, KI untagged WT #139, WT #7; MCF-7 p27 KI GFP-T171* #33, #76; MCF-7 p27 KI GFP-K134fs #111, #234, #244; MCF-7 p27 KO #8, #17) performed in duplicate and expressed as fold-increase over the number cells plated on day 1. ANOVA test has been used for statistical analysis. **B)** Kinase assay and western blot analysis of co-immunoprecipitated cyclin E- CDK2 complex. Upper panel shows in vitro phosphorylation assay, using histone H1 as substrate. Arrows mark p27 at different molecular weights, from top: p27 KI WT, p27 T171*, p27 K134fs, and endogenous p27. Asterisk marks a non-specific band in the immunoprecipitated. Vinculin was used as loading control. **C)** Number of colonies (on the left) and area (on the right) of MCF-7 p27-modified clone grown in soft agar for 2 weeks. Data represents the mean (± SD) of experiment performed in duplicate. Colony size was measured using Image Lab™ software. Mann–Whitney test and Student's t-test have been used for statistical analysis, as more appropriate. Asterisks indicate significant differences, *p ≤ 0.05; **p ≤ 0.01; ***p ≤ 0.001;**** p ≤ 0.0001. Image adapted from Viotto, Russo et al. 2021.*

4.2 Impact of p27^{kip1} KO and mutations in tumor growth, *in vivo*

It is well known that the lack of p27 in conjunction with specific oncogenic stimuli increases malignancy and frequency of tumors, emphasizing that the presence of p27 is an important limiting factor for tumor progression (Belletti et al. 2005; Fero et al. 1998; Nakayama et al. 1996).

To establish whether the increased transformed potential of MCF-7 p27 KO, K134fs and T171* mutants that we observed *in vitro*, effectively resulted in increased growth *in vivo*, and, particularly, in the Luminal subtype of BC, we set up in our lab the Mouse INtraDuctal (MIND) model. The MIND model, recently described by the group of Dr Brisken (Sflomos et al. 2016), is a clinically relevant preclinical model to recapitulate the human Luminal mammary tumors. It consists in the injection of LBC cells directly into the ducts of the mammary gland, which are layered by the Luminal epithelium. This approach allows the LBC cells to properly grow in the ductal microenvironment, in the presence of the physiological hormone levels, maintaining the Luminal phenotype. This approach abolishes the need for exogenous estrogen supplementation, obviating to the deleterious effects of estradiol excess, such as urinary retention, cystitis, hydronephrosis and renal failure, which limit the utility of traditional xenografts (Gakhar et al. 2009; Pearse et al. 2009; Levin-Allerhand, Sokol, Smith et al 2003). Moreover, in commonly used orthotopic xenografts of BC the site of injection is in the mammary fat pad (MFP), in which LBC cells often switch to a more basal phenotype, *via* the induction of TGFβ/SLUG signaling (Sflomos et al. 2016) (**figure 2A**). This implies that MFP microenvironment may alter gene expression in LBC cells, making this model less appropriate to study LBC. Another advantage of the MIND model is that it offers the opportunity to study the transition from *in situ* to invasive disease, BC progression and the insurgence of spontaneous metastasis to distant sites.

We thus decided to employ the MIND approach to study the behavior of LBC cell lines modified for p27, in *in vivo* setting. To this aim, MCF-7 parental cells and two different clones of p27 KO, WT, or mutants have been introduced in the mouse mammary glands of 5-6 weeks NSG (NOD Scid Gamma) immunocompromised female mice, *via* nipple injection of at least eight mammary glands/mouse (**figure 2B**).

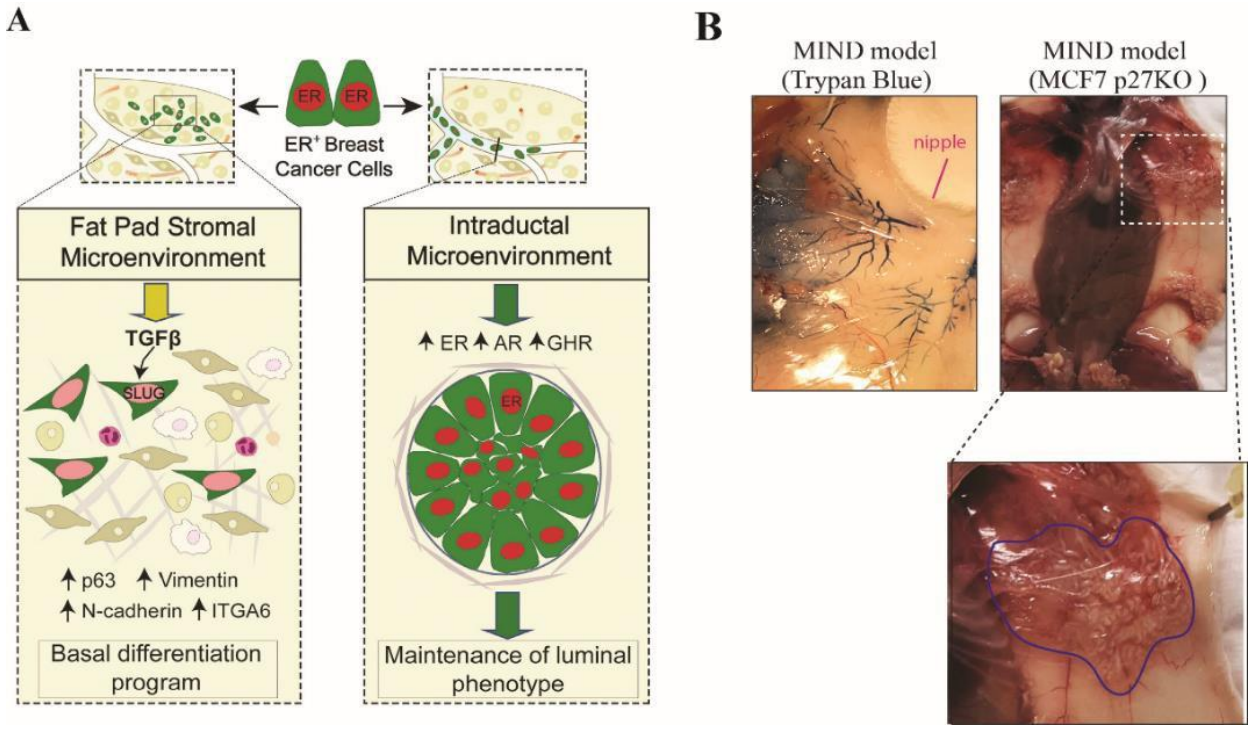

Figure 2. Mouse intraductal (MIND) model. A) *Scheme of the two xenograft approaches: tumor cells are injected either into the mammary fat pad (MFP) or intraductally, via the teat (MIND). Figure has been adapted from "A Preclinical Model for ERα-Positive Breast Cancer Points to the Epithelial Microenvironment as Determinant of Luminal Phenotype and Hormone Response" Sflomos et al. 2016.* ***B)*** *Pictures show the MIND model: on the left, mouse mammary glands after necroscopy of a mouse that was intraductally injected with Trypan Blue, is displayed. Pink line indicates the nipple, site of injection. On the right, the image of a mouse injected in all 10 mammary glands with MCF-7 p27KO cells, sacrificed 9 months after the injection. Below, outlined by the blue line, an enlargement of the 3rd left mouse mammary gland, to highlight the intraductal growth of the Luminal cancer cells is shown.*

Mice were weekly monitored by palpation to examine the insurgence of palpable tumors and followed-up for several months to evaluate the tumor growth. Intraductal engraftment was obtained in all cell clones and we could thus evaluate the timing of tumor onset in the different mouse groups (**figure 3A**). Absence of p27 in MCF-7 MIND induced a substantial, although not significant, anticipation of mammary tumor appearance, compared to p27 WT and mutant counterparts (20 weeks in p27 KO *versus* 25, 27 and 25 weeks in p27 WT, p27 T171*, and p27 K134fs, respectively).

The growth of tumors (**figure 3B**) was also affected by the absence of p27. p27 KO-derived MIND xenografts showed an increased growth compared to WT counterpart. Tumors derived from p27 T171* and p27 K134fs mutants displayed an intermediate phenotype, however more similar to the MCF-7 p27 WT than to the p27 KO clones.

Figure 3C reports some representative pictures of tumors collected during mouse necroscopy, performed 9-10 months from the injection. As clearly evident from the images, the ducts injected with p27 KO

clones were particularly engorged with tumor cells and tumors were bigger in size and denser than those from p27 WT cells. Again, p27 T171* and p27 K134fs -derived xenografts displayed an intermediate size and density, compared to p27 WT- and p27 KO-derived MIND tumors.

Next, we asked what could be, at molecular level, the cause of such different biological behaviors *in vivo*. To answer this question, MIND tumors, collected at necroscopy, were processed to allow the analysis of protein expression and histology. We lysed a fragment of the MIND tumors to extract proteins and performed a western blot to compare these lysates to those extracted from corresponding cellular clones, grown *in vitro* (**figure 3D**). First of all, we noticed that level of expression of p27 T171* and K134fs mutants had drastically decreased in tumors, indicating that, in this setting, cells were advantaged when p27 expression was maintained low. Moreover, E-cadherin, a cell adhesion molecule frequently downmodulated during EMT (Epithelial-to-Mesenchymal Transition), metastasis, chemoresistance and stemness (Alimperti et al. 2015), was greatly decreased in p27 KO tumors. Interestingly, we also observed that p27 KO, K134fs, and T171* tumors displayed a complete loss of the hormonal receptor PR and a consistent decrease of ER, which are very well expressed by the correspondent cells in culture. These results suggested that loss of p27 induced a transformation of the hormonal profile of these tumor cells, when challenged *in vivo*.

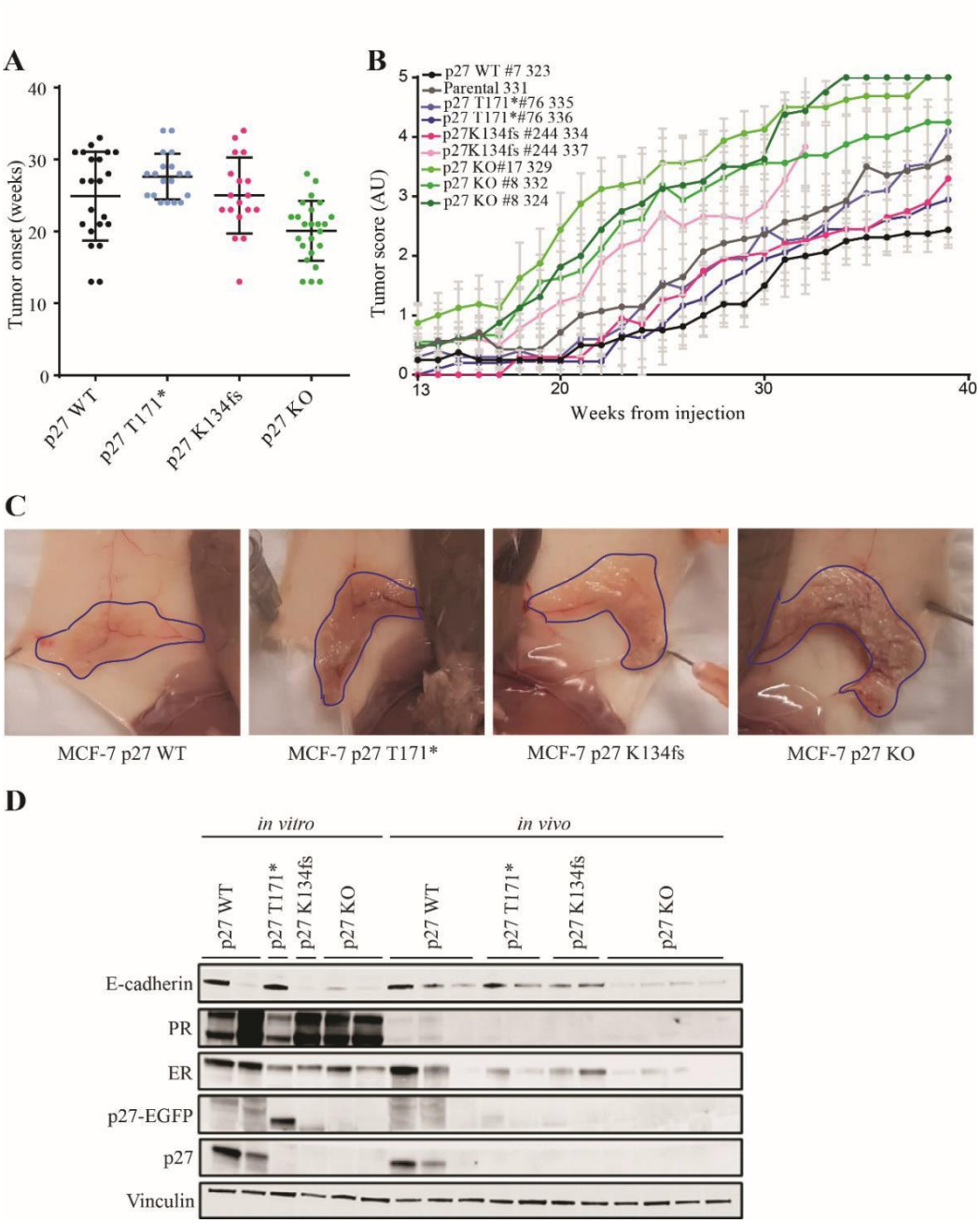

Figure 3. Onset, growth and molecular features of MIND tumors derived from MCF-7 modified clones. A) *Graph reports the onset of palpable tumors derived from the injection of MCF-7 p27 modified clones, as indicated. In the legend, p27 WT includes MCF-7 parental and WT#7 cells; p27 KO, MCF-7 p27 KO#8 and #17 clones. Each dot corresponds to a single tumor. No significant differences were detected.* ***B)*** *Graph shows the growth of MIND-tumors derived from the injection of different MCF-7 clones, as indicated. Tumors were weekly monitored by palpation and a score from 1 to 5 were assigned to each tumor to evaluate the tumor growth. The data represent the mean (± SD) of at least 8 MIND-tumors/mouse. The legend indicates the cell clone injected and the corresponding mouse ID.* ***C)*** *Representative pictures of the 4rd mouse mammary gland, outlined by blue line, inoculated through the MIND model with the MCF-7 cells reported below. Mice were sacrificed 9-10 months after the injection.* ***D)*** *Western blot analysis of the lysates obtained from the MIND tumors and the corresponding clones cultured in vitro. Vinculin was used as loading control.*

Tumor masses were collected to evaluate in detail the tumor histology and the expression of Luminal and proliferative markers. H&E-stained sections (**figure 4A**) highlighted that MIND tumors from p27 KO and, to a lesser extent, p27 mutants, were highly invasive. While p27 WT MCF-7 cells were grown within the ducts, p27 KO showed a clear expansion of the tumor cells outside the ducts and intravasation into blood vessels. We then performed the IHC analysis of Ki-67, ER, PR and p27 (**figure 4A** and **B**). As expected from the loss of p27 expression observed in p27 mutant tumors, the percentage of Ki-67 positive cells was similar in tumors from p27 KO and mutant clones, and much higher compared to the WT ones. Staining for the hormonal receptors ER and PR confirmed what already observed in western blot analysis (**figure 3D**), showing that lesions derived from WT cells preserved a good expression of ER and PR, confirming the Luminal phenotype of the MIND-derived tumors, while tumors from p27 KO and mutant clones were less positive for ER and almost negative for PR. IHC for p27 also confirmed results obtained by western blot (**figure 3D**), showing a substantial decrease of p27 protein expression in p27 K134fs and T171* tumors. These results suggest an interplay between p27 and PR/ER signaling pathway, not excluding a possible interplay between p27 loss and with environmental features, such as hypoxia, contact with activated fibroblasts, blood vessels, residual innate immune cells, that will be deeply analyzed in future studies.

Furthermore, we started the evaluation of the metastatic dissemination, by collecting, fixing and storing all distant organs typically metastasized in LBC, such as lungs, liver, brain and bones. Our preliminary analyses, still in progress, revealed the presence of distant dissemination to the lung tissue only when MCF-7 p27 KO cells were injected, as shown by the IHC analysis of panCK (pan C*ytokeratin)* human epithelial marker (**figure 4C**). These preliminary data indicate that the increased invasive phenotype observed in the primary MIND tumors from p27 KO MCF-7 cells was effectively coupled with an increased metastatic potential. More extensive analyses are currently in progress, to better characterized this phenotype and verify the presence of metastatic foci in the other distant organs collected.

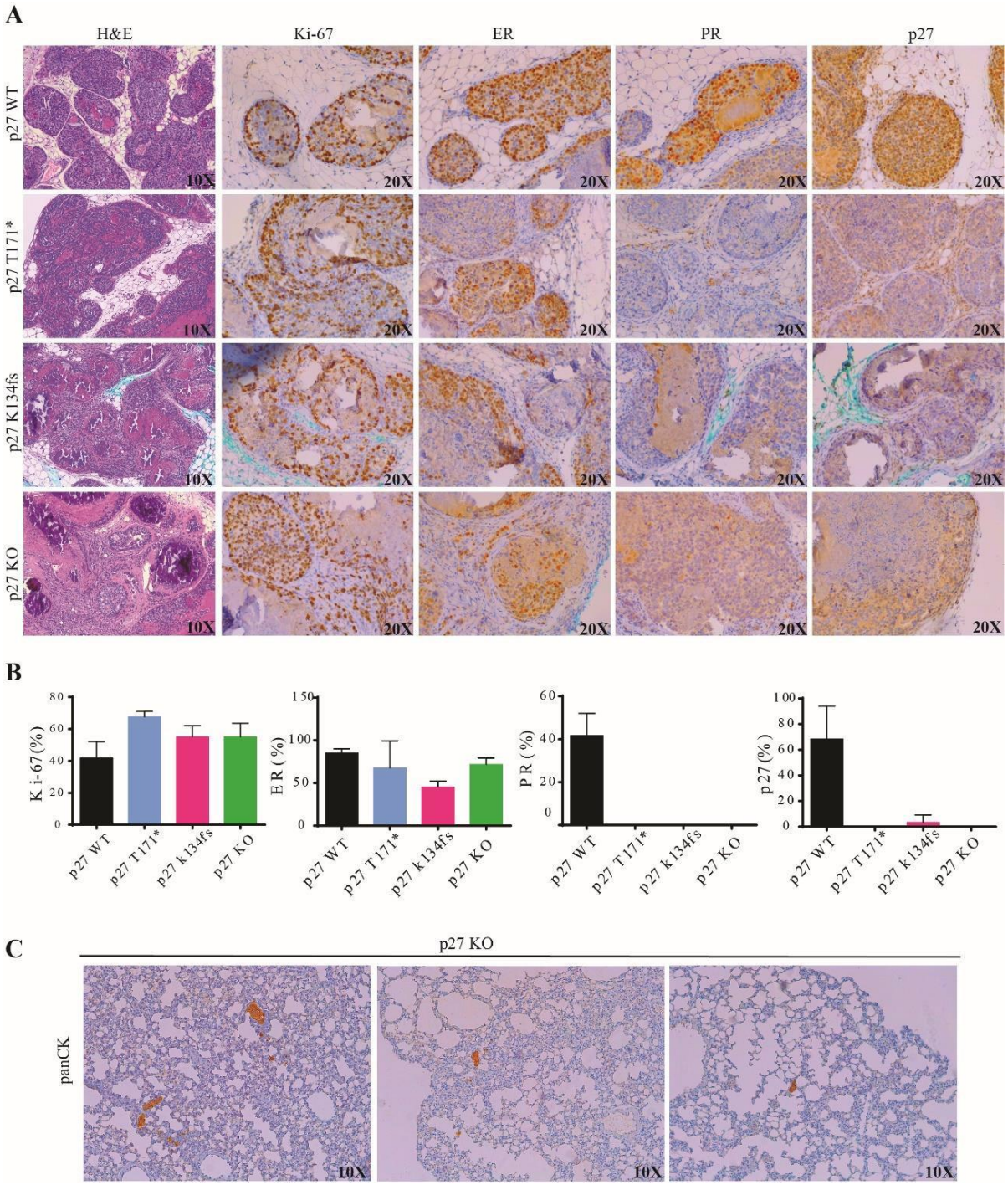

Figure 4. Histological analysis of MIND tumors derived from MCF-7 modified clones. ***A)*** *Representative images of H&E and IHC staining for Ki-67, ER, PR and p27 protein performed in the tumor sections, as indicated. The magnification is reported in each figure.* ***B)*** *Percentage of Ki-67, ER, PR and p27 positive cells obtained from the IHC analyses described in A. Data represent the mean (± SD) obtained from at least 3 slides evaluated in two different NSG mice.* ***C)*** *Representative pictures of lung sections collected from NSG mice injected with MCF-7 p27KO cells, stained for panCK marker and acquired at 10X magnification.*

4.3 Impact of $p27^{kip1}$ in drug response

4.3.1 Sensitivity to Palbociclib of MCF-7 $p27^{kip1}$ modified clones

Palbociclib is a target therapy recently introduced in the therapeutic portfolio of oncologists to treat, in combination with other antineoplastic agents, HER2-negative, HR-positive advanced or metastatic BC patients. Palbociclib is a CDK4/6 inhibitor (CDK4/6i) that acts by binding to the ATP pocket of the kinases (Wilson et al. 2017), that are involved, with their coregulatory partners cyclin Ds, in the G1-S transition of the cell cycle. Hence, inhibition of this step blocks cell cycle progression and prevents cell proliferation (Rocca et al. 2017). The use of CDK4/6i in cancer therapies is becoming more and more prominent; however, despite promising clinical outcomes, intrinsic or acquired resistance to CDK4/6i is limiting the success of these treatments, making the understanding of their actual mechanisms of action become quite urgent.

The expression of p27, functioning as a natural CDK4/6i, may modify the cellular sensitivity to CDK4/6i. For this reason, already during my graduation internship, we decided to test the efficacy of Palbociclib on MCF-7 p27 KO or mutants clones, to evaluate if p27 loss and its C-terminal mutations could affect drug response. **Figure 5A-C**, partially updated from my graduation thesis, show the kill curve using Palbociclib at different concentrations, in MCF-7 p27-modified clones. After 72 hours from treatment, viability and EC50 (half maximal effective concentration) were evaluated, using an MTS assay. These data highlighted that the lack of p27 or presence of the mutants slightly increased MCF-7 resistance to Palbociclib, even if the differences were not statistically significant. To validate these findings and, possibly, identify the mechanism underlying this increased resistance, we have then investigated the Palbociclib-dependent senescent phenotype.

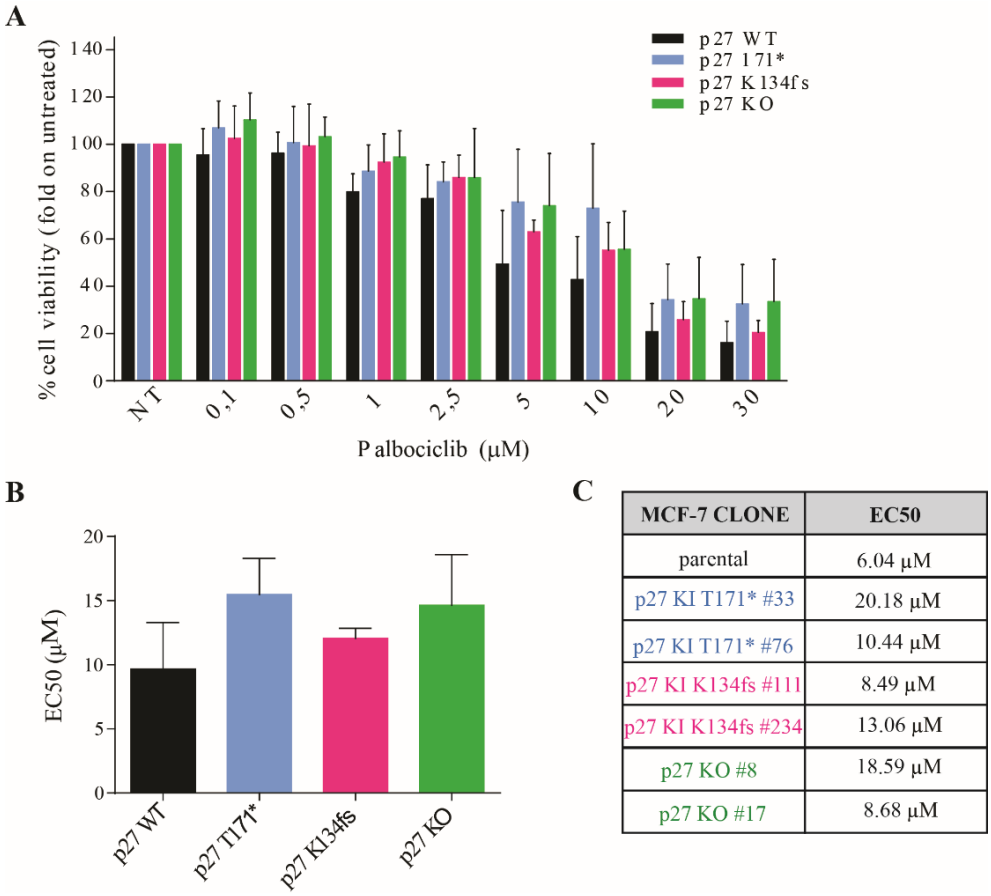

Figure 5. Palbociclib sensitivity of MCF-7 p27 KO and p27 mutants. ***A)*** *Dose response analysis of p27 KO, p27 T171*, p27 K134fs overexpressing clones or p27 WT MCF-7 cells, treated with increasing doses of Palbociclib for 72 hours. Cell viability was evaluated using a MTS assay. Data represents the mean (± SD) of two clones for each cell type (MCF-7 p27 KI WT #139, parental; MCF-7 p27 T171* #33, #76; MCF-7 p27 K134fs #111, #234; MCF-7 p27 KO #8, #17) performed in sextuplicate.* ***B)*** *Graph shows the Palbociclib EC50 in µM (mean ± SD) of MCF-7 clones obtained from experiment described in A.* ***C)*** *Table reports the EC50 of Palbociclib for each clone analyzed.*

4.3.2 Palbociclib-induced senescence in MCF-7 p27^{kip1} modified clones

According to literature data, one of the effects induced by Palbociclib in BC cells is the induction of cell senescence, which leads to cell cycle arrest (Thangavel et al. 2011; Kovatcheva et al. 2015; Michaud et al. 2010; Choi et al. 2012). To evaluate whether the increased resistance displayed by MCF-7 p27 KO cells was linked to the senescent phenotype, we performed the SA-β-Gal activity assay to highlight the senescent cells in our culture following treatment. To this aim, cells were treated with 0.1 µM of Palbociclib (as already tested by Thangavel et al. to evaluate senescence) for 24 hours, then washed, fixed and stained with β-galactosidase solution for 16 hours. Graph in **figure 6A** shows the results from counting β-Gal positive (blue) cells. All clones displayed a high "physiological" senescent background. After Palbociclib treatment, senescent cells increased particularly in MCF-7 p27KO and mutant clones

(although not significantly), but not in the WT. This result, taken individually, may indicate a greater efficacy of the drug on MCF-7 p27-modified clones, by inducing a stable cell cycle arrest. However, this increased senescence was not in line with the slightly higher resistance to Palbociclib displayed in kill curve analyses (**figure 5A**). To better clarify this apparent contradiction, we performed a growth curve experiment plating cell clones after being exposed to Palbociclib, using a higher dose of the drug, more in line with the EC50 of p27-modified clones. We thus treated cells with 2,5 µM of Palbociclib for 72 hours and evaluated their growth rate after 1, 3, 5, 7 and 9 days. Our results clearly showed that, following Palbociclib treatment, MCF-7 p27 WT cells were completely blocked in their proliferation, while the treatment was not able to arrest the growth of MCF-7 p27-modified clones (**figure 6B**), which maintained approximately the same growth rate of untreated clones, as shown in **figure 1A**. These results suggested that the senescent phenotype displayed by MCF-7 p27-modified clones was reversible and could lead to a transient dormancy, followed by cell reactivation when the drug was removed. To further test this possibility, we decided to better investigate the reversibility of Palbociclib-induced senescence in our context.

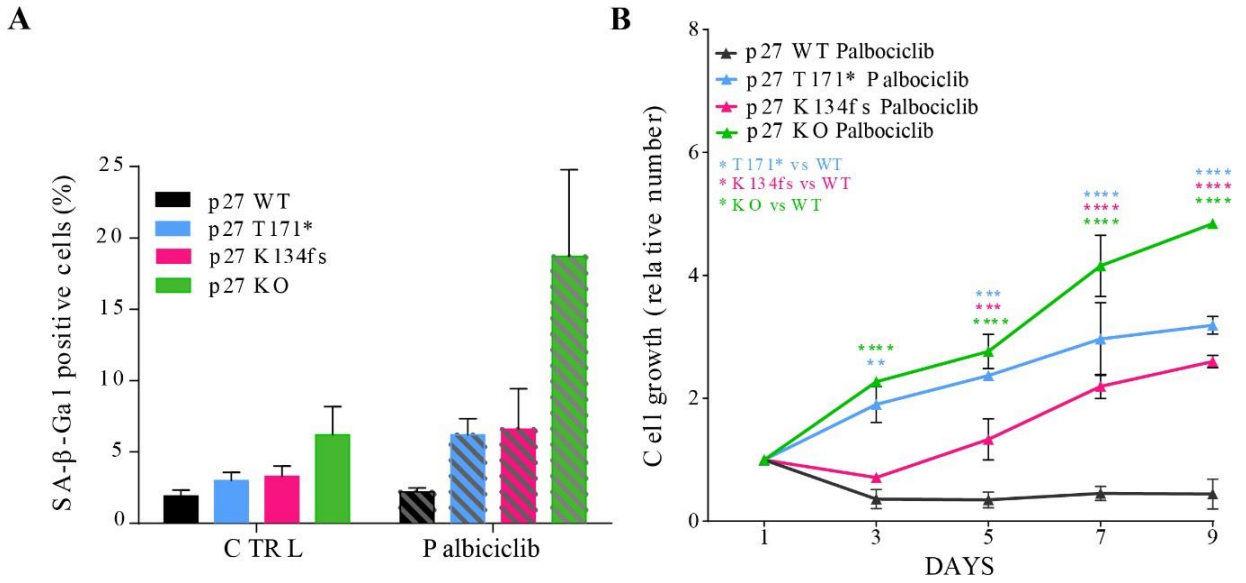

Figure 6. Palbociclib-induced senescence in MCF-7 p27 KO and mutants clones. **A)** *Percentage of SA-β-Gal positive cells in clones untreated (CTRL) or treated with Palbociclib at 0,1 µM for 24 hours. The experiment was performed in duplicate using MCF-7 p27 KI WT #139, MCF-7 p27 KI T171* #33, MCF-7 p27 KI K134fs #111 and MCF-7 p27 KO #8. No significant differences were detected.* ***B)*** *Growth curve of MCF-7 clones treated for 72 hours with Palbociclib at 2,5 µM for 72 hours and counted after 1,3,5,7 and 9 days of drug removal. Data represents the mean (± SD) of two clones for each cell type (MCF-7 p27 KI WT #7, parental; MCF-7 p27 KI T171* #33, #76; MCF-7 p27 KI K134fs #234, #244; MCF-7 p27 KO #8, #17) performed in duplicate and expressed as fold-increase over the number of cells plated on day 1. ANOVA test has been used for statistical analysis. Asterisks indicate significant differences, **P < 0.01; ***P < 0.001; ****P < 0.0001.*

4.3.3 Escape from Palbociclib-induced senescence in p27^{kip1}-modified MCF-7 clones

Literature data indicate that senescence induced by CDK4/6 inhibitors may be reversible and that the cells, once the drug is removed, may exit quiescence and resume proliferation. It is already known that chemotherapy-induced senescence may generate tumor cells that have an enhanced potential to drive tumor growth, if they exit senescence (Milanovic et al. 2018). To assess whether p27 could play a role in post-Palbociclib treatment phase, when cells "decide" whether to resume proliferation or remain senescent, we evaluated their long-term behavior after drug treatment. We treated cells with Palbociclib (2.5μM) for 72 hours and collected them after 1, 10 and 20 days from drug removal (**figure 7A**). Using the SA-β-Gal activity assay to evaluate senescence, we assessed that, even in this slightly different experimental setting, the number of senescent cells was significantly increased in p27 KO and mutant clones compared to the WT cells, especially after 20 days (**figure 7B**). Next, we investigated at molecular level the cell cycle status and the senescence, using the same timeline of the experiment described above (**figure 7C**). We analyzed the expression of cell cycle markers, such as the phosphorylation of Rb (pRb) and cyclin E, proliferation marker, such as c-Myc, and senescence-associated cytokine response marker, such as NF-kB (Jing et al. 2014). In accord with our hypothesis, compared to WT cells p27 KO and mutant clones showed an increase of the senescent response, underlined by augmented NF-kB, coupled with a significant increase of Rb phosphorylation (pRB) and cyclin E, suggesting that a reactivation of the cell cycle was operating in these cells. Also, c-Myc increased after Palbociclib treatment in p27 modified clones, especially in the p27 KO cells. The c-Myc protein is a transcription factor of great importance in the control of cell growth and survival (Dhanasekaran et al. 2022) and plays also a fundamental role in the induction of stem-like features (Yoshida et al. 2018). To deepen the investigation of this re-awakening from a dormant status of our MCF-7 p27 modified clones, we next focused on stem cell and on early progenitor activity of our clones.

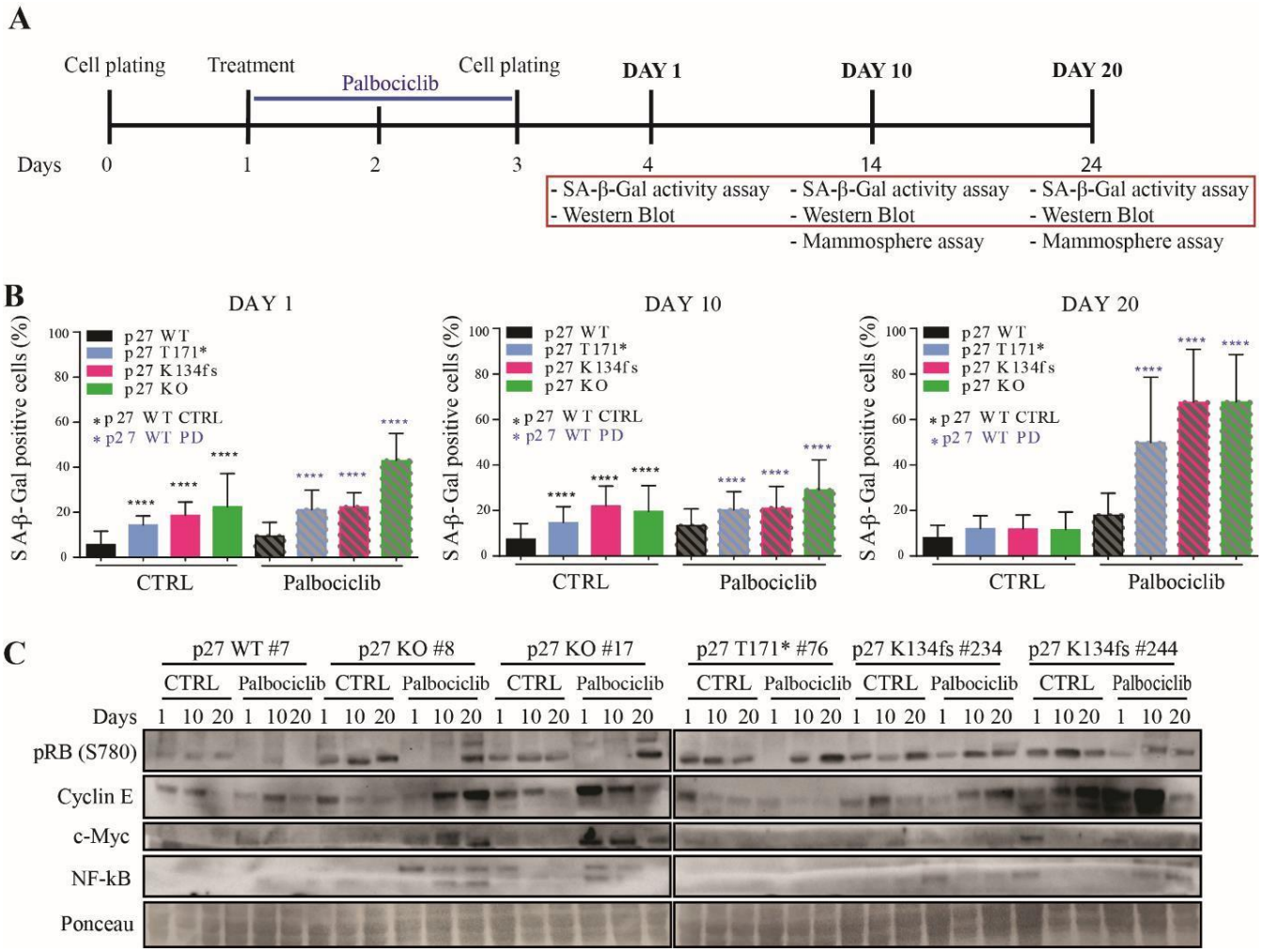

Figure 7. Escape from Palbociclib-induced senescence in MCF-7 p27 KO and p27 mutants. A) *Schematic representation of the experimental workflow used to analyze MCF-7 modified clones in response to Palbociclib.* ***B)*** *Percentage of SA-β-Gal positive cells in untreated (CTRL) or treated (Palbociclib) clones evaluated after 1, 10 and 20 days after Palbociclib washout. Data represents the mean (± SD) of two clones for each cell type (MCF-7 p27 KI WT #7, parental; MCF-7 p27 KI T171* #33, #76; MCF-7 p27 KI K134fs #234, #244; MCF-7 p27 KO #8, #17) performed in duplicate. Mann–Whitney test has been used for statistical analysis. Asterisks indicate significant differences ****P < 0.0001.* ***C)*** *Western blot analysis of the MCF- 7 clones treated for 72h with Palbociclib (2,5μM) and collected after 1, 10, and 20 days, as indicated.*

4.3.4 Escape from Palbociclib-induced senescence in MCF-7 p27^{kip1} modified clones boosts tumor aggressiveness

Milanovic and colleagues observed that cellular signaling pathways activated during chemotherapy-induced senescence are similar to the gene-expression patterns observed in stem cells (Milanovic et al. 2018). Moreover, it is well known that senescence, and in particular the Senescence-Associated Secretory Phenotype (SASP), can promote stemness, both in autocrine and paracrine manner (Haas et al. 2018). An active role of p27 in the differentiation process has been mainly deduced by the evidence that its

expression increases in most terminally differentiated cells (Baldassarre et al. 1999). It has been shown that overexpression of p27 in mouse induced Pluripotent Stem Cells (iPSCs) preserves their pluripotency characteristics but induces the loss of the stemness-state earlier than in normal mouse iPSCs (Matsu-ura et al. 2016). There is also a connection between p27 and Sox2, one of the so called "Yamanaka factors" (Takahashi et al. 2006). Interestingly, cells and tissues from p27 null mice, including brain, lung, and retina, present an elevated basal expression of Sox2, suggesting that p27 could actively contribute to the repression of Sox2 (Li et al. 2012). All these data highlighted the potential implication of p27 in the stemness phenotype.

To investigate the possibility that after Palbociclib treatment p27 KO cells could escape from senescence thanks to the acquisition of stem-like features, we used the same timeline of experiment described above, and, following the 72 hours of Palbociclib treatment, we plated cells to form mammospheres. This assay is based on sphere-forming capability of cells, allowing to investigate stem cell or early progenitor activity (Shaw et al. 2012). The cells are plated in non-adherent plates in presence of 20ng/ml EGF (Epidermal Growth Factor), the usual growth factor that is used to stimulate mammary epithelial cells in this assay. After 10 days, mammospheres were counted and their area evaluated. Our results clearly indicated that expression of p27 T171* and K134fs mutants and especially the KO of p27, significantly increased MCF-7 cells ability to form primary mammospheres, compared to p27 WT, both under untreated conditions and following Palbociclib treatment, evaluated both as size and number of primary mammospheres (**figure 8B**). Then, first generation mammospheres was collected, disaggregated and plated in suspension to generate a second generation of mammosheres, to better investigate the stem-like properties of the clones. In accord with what observed in first generation, mammospheres number and area were highly stimulated in absence of p27 or in presence of mutant forms, in both untreated and Palbociclib-treated conditions (**figure 8C**). Interesting to note, Palbociclib seems not to affect the MCF-7 p27 KO, T171* and K134fs mutant ability to grow as mammospheres.

Together, our data suggested that the Palbociclib-induced senescent phenotype that we observe in p27 KO and in C-terminus mutants clones could represent a transient state. Following drug wash-out and FBS stimulation, p27 KO and mutant clones, unlike the WT cells, are able to exit from senescence and reactivate cell growth and upregulate their stem-like features and self-renewal abilities.

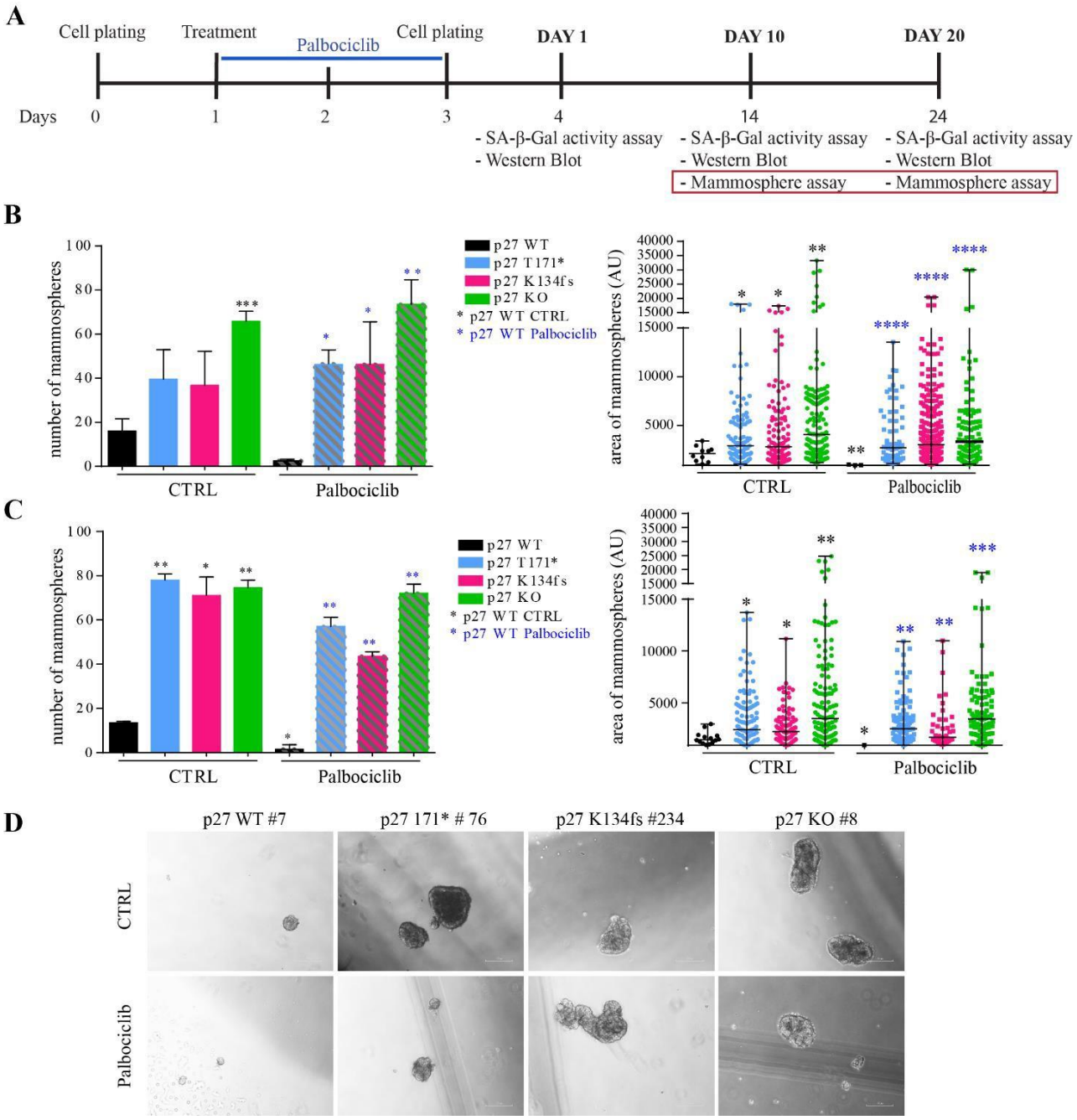

Figure 8. Stem cell-like properties of MCF-7 p27 KO and p27 mutants after Palbociclib treatment. ***A)*** *Schematic representation of the experimental workflow used to analyze MCF-7 modified clones in response to Palbociclib.* ***B)*** *Graphs show the number (on the left) and area (on the right) of primary generation mammospheres in untreated (CTRL) and treated (Palbociclib) condition, plated after 72 hours of Palbociclib treatment (2,5 μM) and evaluated after 10 days.* ***C)*** *Same as in B, but regarding the secondary generation of mammospheres. Data in B and C represent respectively the mean (± SD) and median (+ range) of two clones for each cell type (MCF-7 p27 KI WT #7, parental; MCF-7 p27 KI T171* #33, #76; MCF-7 p27 KI K134fs #234, #244; MCF-7 p27 KO #8, #17) performed in duplicate. Spheres size was measured using Image Lab™ software. Mann–Whitney test (mammospheres number) and Student's t-test (mammospheres area) have been used for statistical analysis.* ***D)*** *Representative images of the mammospheres generated from the experiment described in C. 10× magnification is shown. Asterisks indicate significant differences *P < 0.05; **P < 0.01; ***P < 0.001; ****P < 0.0001.*

4.4 Implication of $p27^{kip1}$ in cell transformation and tumor initiation

4.4.1 Generation of $p27^{kip1}$ KO, $p27^{kip1}$ mutants in normal human mammary epithelial cell line.

In the previous paragraphs, we have investigated the role of p27 in Luminal BC, demonstrating the involvement of p27 in many aspects linked to tumor aggressiveness, such as proliferation, survival, transition from Luminal to basal subtype and drug response.

However, our model could not allow the evaluation of the role of p27 during the early steps of mammary epithelial cell transformation, since MCF-7 cells display an overt transformed phenotype. To better mimic what in facts happens in patients, during the early steps of BC formation, we decided to generate p27 KO, p27 T171* and p27 K134fs clones also in a normal human mammary Luminal epithelial cell line, using the CRISPR-Cas9 technology.

We chose the Breast Primary Epithelial Cells (BPEC) that are human immortalized normal mammary epithelial cells of the Luminal subtype, generated in 2007 by the group of Weinberg (Ince et al. 2007). Differently from other cellular models, such as HMEC (Human Mammary Epithelia Cells), these cells express and maintain the expression of hormonal receptors, ER and PR, if cultured in appropriate medium and plated on specific modified plastic surface.

Using GenomeCRISPR tool online (http://genomecrispr.dkfz.de) we custom designed different guides RNA (gRNA) to edit the genome at the CDKN1B gene level. In particular, to generate p27 KO clones, we designed two guides (gRNA 18 and gRNA 20, hereafter 18 and 20) positioned within the initial 100 nucleotides from the ATG codon, in order to totally abolish the gene transcription and protein expression; to generate a mutant similar as much as possible to the K134fs mutant, we designed a guide to target the 10-20 nucleotides around the K134, at the end of the first exon; to generate a mutant similar as much as possible to the T171*, we designed a guide to target 6 nucleotides close to T170, in the second exon of CDKN1B.

To get more chances to succeed in this very hard to transfect cell line, we have undertaken different approaches, using different vectors and different ways of transfection/transduction.

Eventually, the winning strategy, depicted in **figure 9A**, has been to generate first stable pools of Cas9-overexpressing BPEC, using Cas-9 lentiviral particles (**figure 9B**), then, after Blasticidin selection, transfect this pool with the different guides, by an electroporation approach.

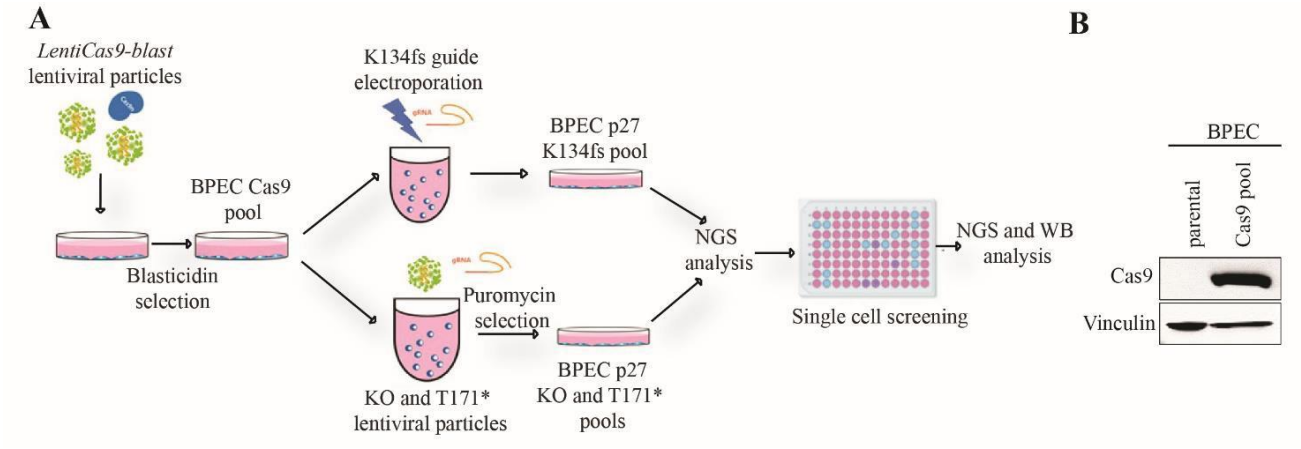

Figure 9. Generation of BPEC p27 KO and T171* and K134f overexpressing cells. A) *Schematic representation of the experimental workflow used to generate BPEC p27KO and mutant clones.* ***B)*** *Western blot analysis of Cas9 expression of BPEC Cas9 pool. Vinculin was used as loading control.*

First, we used a phU6-gRNA vector, encoding for each of the desired guide, to electroporate the Cas9 BPEC pool. When, after cell recovering, we analyzed the corresponding DNA extract by Next Generation Sequencing (NGS) to evaluate the efficiency of the cut, we were able to identify only a p27 K134fs pool, which resulted already 50% deleted/mutated at the desired site (**figure 10C**).

After many unsuccessful attempts of obtaining p27 KO and p27 T171* pools with the same strategy, we have used lentiviral particles (instead of the phU6-gRNA vector) encoding for each of the desired guides to transduce the BPEC Cas9 pool, and, after puromycin selection, we finally obtained mutated/deleted pools: p27 KO 18, 80% of deletions/mutations; p27 KO 20, 60% of deletions/mutations (**figure 10A**); and p27 T171*, 60% deletions/mutations (**figure 10B**).

At this point, to obtain clones that were 100% carrying the same alteration, we have single-cell cloned each pool (0.7 cell/well of 96-well plates). Once recovered and expanded, clones have been collected, their DNA extracted and analyzed by NGS to find the desired deletion/mutation at 100%. At this point, clone was further expanded to collect proteins to evaluate, by western blot, the actual loss of p27 protein or the expression of its deleted forms. At this moment, while the generation of T171* and K134fs single-cell clones is still ongoing, we have been able to generate and start the characterization of BPEC p27 KO clones.

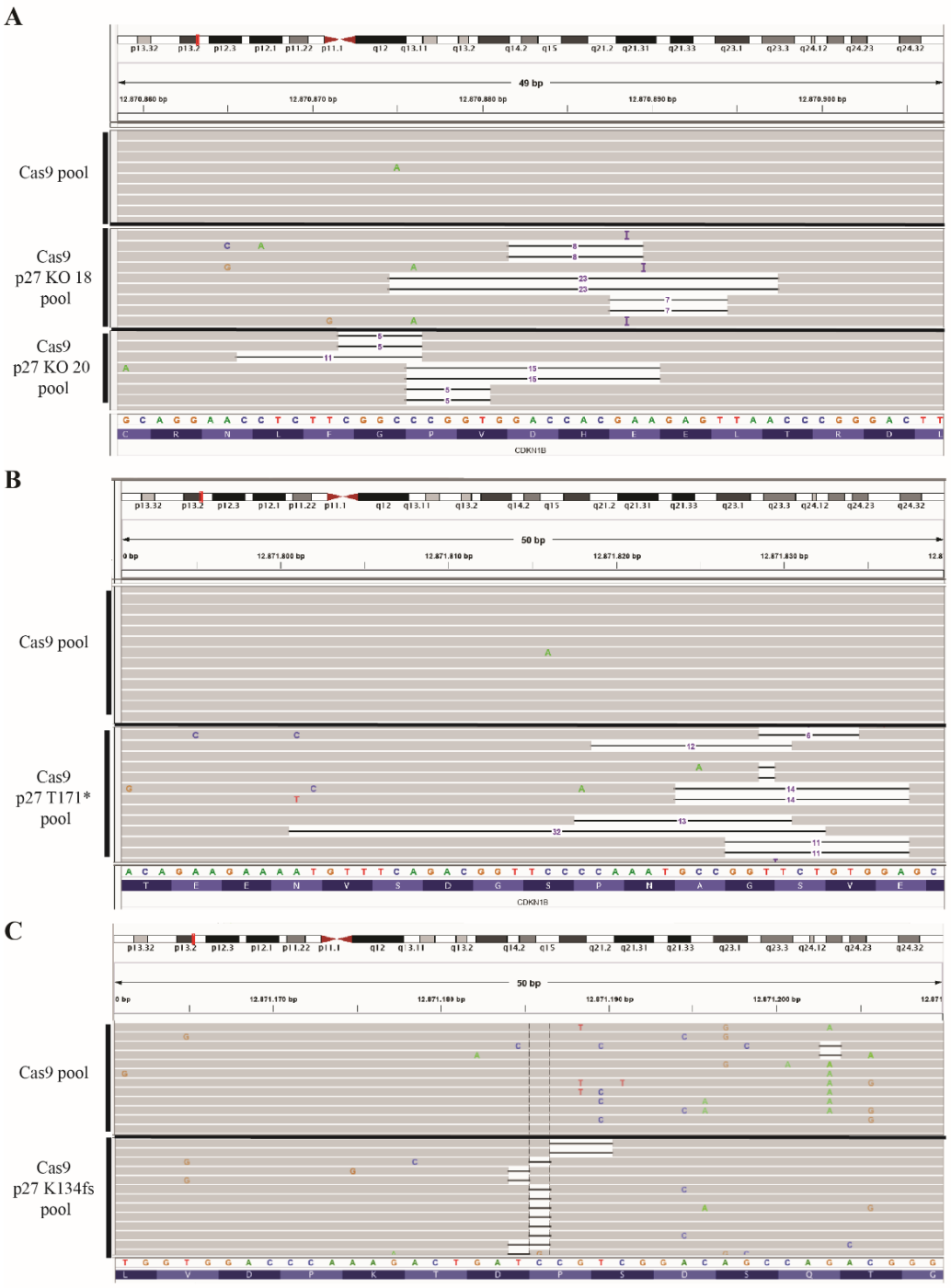

Figure 10. BPEC Cas9 p27 modified pools analysis in NGS. *Representative images of the CDKN1B DNA sequence, obtain from IGV software representing p27 KO 18 and KO 20 pools (**A**), p27 T171* (**B**) and p27 K134fs pool (**C**)..*

4.4.2 Impact of $p27^{kip1}$ KO in biological phenotypes of normal human mammary epithelial cell line

After single-cell plating of two p27 KO pools (from guides 18 and 20), we have confirmed the 100% deletion/insertion in different clones by NGS (**figure 11A**) and by western blot (**figure 11B**) showing the complete loss of p27 expression. As experimental controls, we have selected two different clones that remained totally WT during the entire process of transduction, electroporation and clonal selection. The clones that we have collected, characterized, and stored are:

- BPEC p27 WT #12
- BPEC p27 WT #19
- BPEC p27 KO 18 #2
- BPEC p27 KO 18 #9
- BPEC p27 KO 18 #14
- BPEC p27 KO 20 #3
- BPEC p27 KO 20 #8
- BPEC p27 KO 20 #10

First, we have investigated the impact of p27 loss in the proliferation rate of these otherwise normal mammary epithelial cells, and set up a growth curve to evaluate p27 KO cells compared to the WT counterparts. The effect of loss of p27 in the cell cycle of BPEC was very strong, significantly increasing proliferation compared to parental cells and clones expressing the WT protein, indicating that expression of p27 was critical for the regulation of the normal cell cycle of BPEC cells, under normal culture conditions (**figure 11C**).

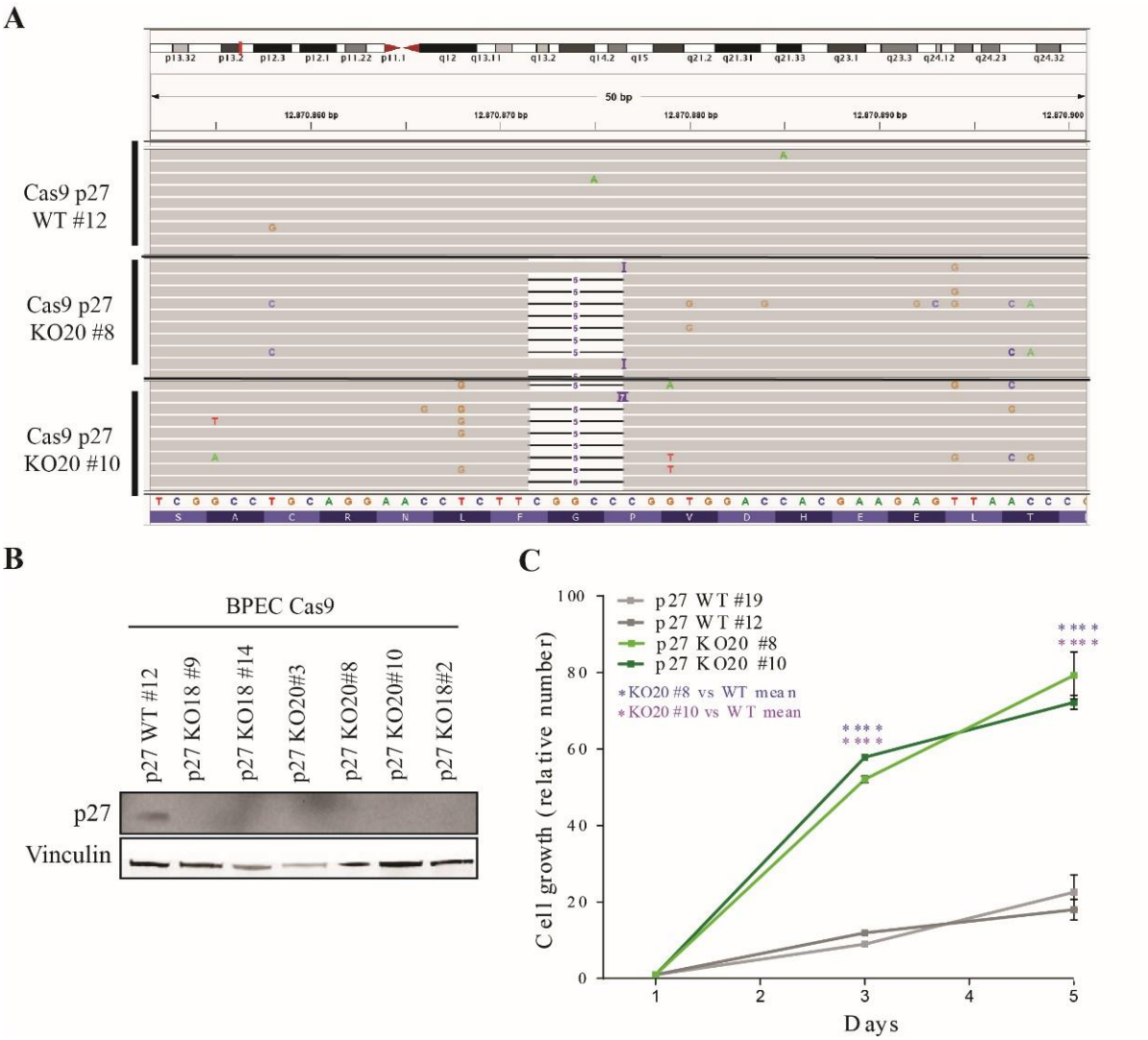

Figure 11. BPEC p27 KO clones screening and characterization. A) *Representative images of the CDKN1B DNA sequence, evaluated by NGS analysis, showing the WT form and the mutated/deleted sequences in p27 KO 20 #8 and #10 clones. Image was obtained from IGV software.* ***B)*** *Western blot analysis of BPEC clones found to be p27 KO in NGS analysis. Vinculin was used as loading control.* ***C)*** *Growth curve analysis of BPEC p27 KO and WT clones. Data represents the mean (± SD) expressed as fold-increase over the number of cells plated on day 1. ANOVA test has been used for statistical analysis. Asterisks indicate significant differences ****P < 0.0001.*

We previously showed that p27 was implicated self-renewal of MCF-7. To understand if p27 loss could confer stem-like properties to BPECs, we have analyzed the ability of these new p27 KO clones to grow and survive as mammospheres. BPEC clones were plated in non-adherent plates in two different conditions: in presence of EGF (20ng/ml) or in presence of post-surgery wound fluids (WF, at 2.5%), drained from breast cancer patients. WF is rich in cytokines and growth factors, able to stimulate growth and also stem-like properties of mammary cells (Belletti et al. 2008, Segatto et al. 2014). After 10 days,

spheres were counted and their area was evaluated. Our experiments with EGF indicated that loss of p27 slightly increase the ability to form primary mammospheres, especially affecting their size, compared to control WT. This result became even more evident in the presence of WF in the BPEC medium, showing p27 KO clones formed much larger mammospheres then WT counterpart.

First generation mammospheres were collected, disaggregated, and plated in suspension to generate a second generation, in order to better investigate the stem-like properties of the cells. Surprisingly, only the p27 KO clones plated in WF have grown in second generation mammospheres. Representative pictures second generation mammospheres are reported in **figure 12D**. This result indicated that the absence of p27, combined with some of the factors contained in the WF, but not EGF, were able to stimulate BPEC stem-like features, such as self-renewal.

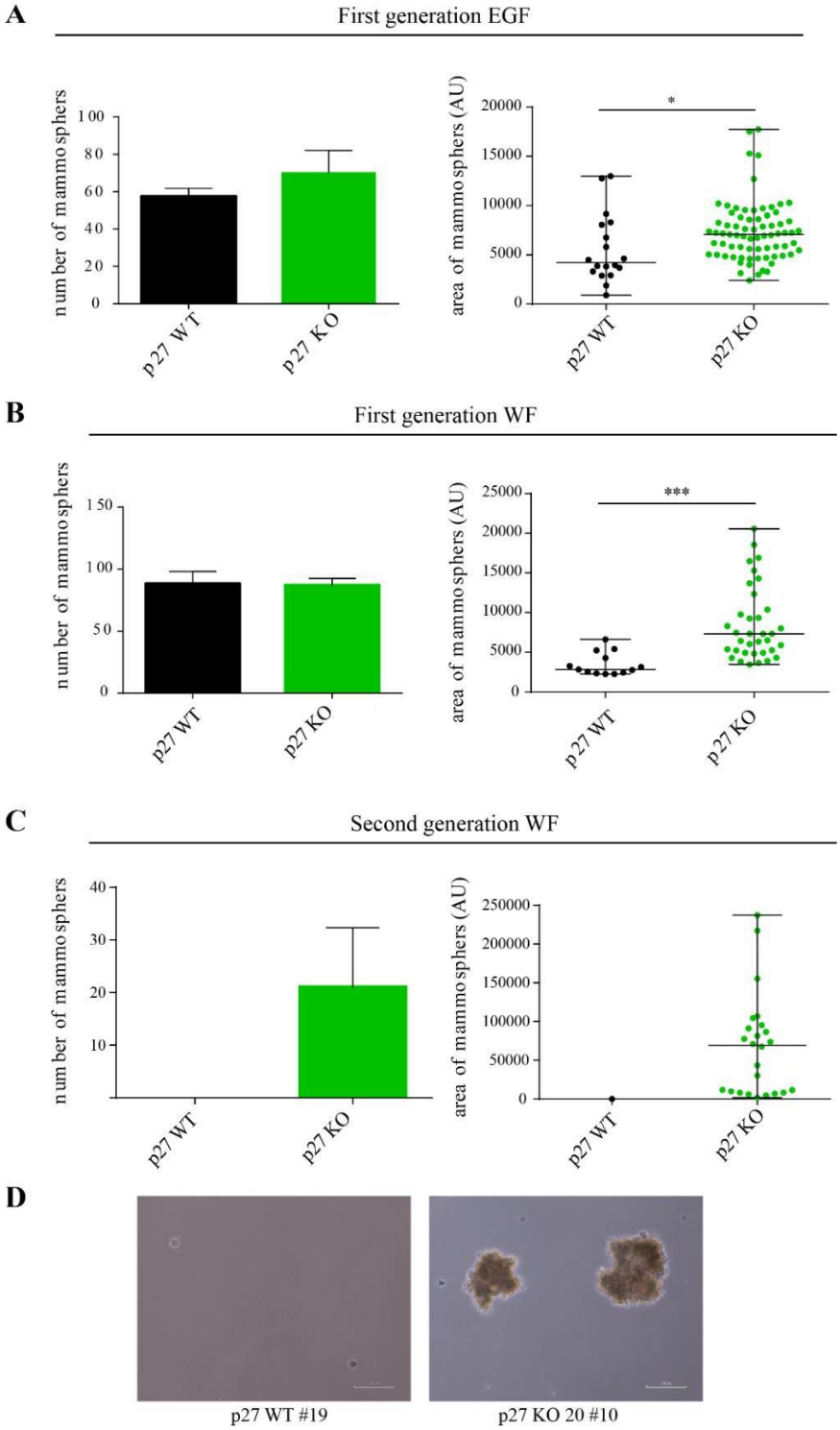

Figure 12. Stem cell-like properties of BPEC p27 KO cells. A) *Number (on the left) and area (on the right) of first generation mammospheres plated in presence of EGF.* ***B)*** *Same as in A, but plating cells in presence of WF 2.5%.* ***C)*** *Same as in B, but showing the second generation of mammospheres. Data in A, B and C represent the mean (± SD) and median (+ range) of p27 BPEC p27 KO 20 #10 and BPEC p27 WT #19 performed in duplicate. Mammospheres size was measured using Image Lab™ software. Mann–Whitney test and Student's t-test have been used for statistical analysis as more appropriate.* ***D)*** *Representative images of mammospheres from the experiment described in C. 20× magnification is shown. Asterisks indicate significant differences *P < 0.05; ***P < 0.001; ****P < 0.0001.*

The evidence described above highlight that loss of p27 increase the ability of cells to survive and grow in different conditions. We next decided to explore their ability to grow in 3D-culture by embedding cells in Matrigel. Matrigel is a gelatinous protein mixture, mainly composed by laminins, that well mimics the composition and function of the basal membrane of the mammary gland. To evaluate the impact of p27 KO in this context, BPEC clones were embedded in Matrigel and, after 10 days of culture, number and size of the mammary acini formed in 3D were determined.

In accord with what already seen in MCF-7, BPEC p27 KO clones show a significant increase in colony size compared to BPEC p27 WT clones, while the colony number was only slightly increased in BPEC p27 KO, but not significantly (**figure 13A**). Representative pictures are reported in **figure 13B**.

These data confirms that p27 loss can affect the growth of BPECs in different conditions leading them toward a more aggressive phenotype.

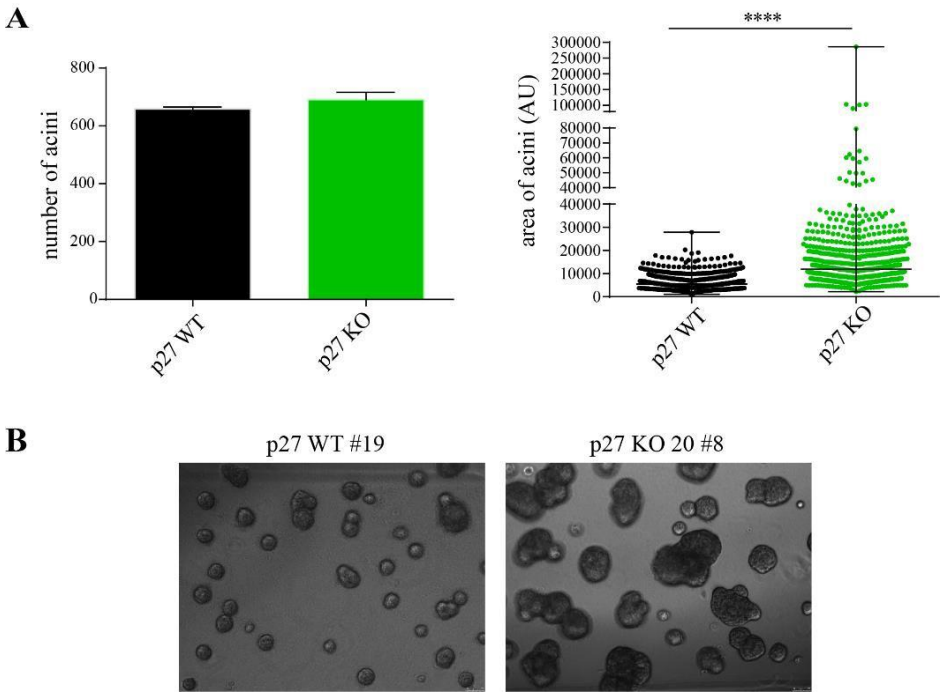

Figure 13. 3D-growth in matrigel of BPEC p27 KO cells. A) *Graphs report the number (on the left) and area (on the right) of BPEC WT and p27 KO colonies grown in 3D-Matrigel. Data represent respectively the mean (± SD) and median (+ range) of p27 KO 20 #8 and WT #19 performed in duplicate. Colony size was measured using Image Lab™ software. Mann–Whitney test and Student's t-test have been used for statistical analysis as more appropriate.* ***B)*** *Representative images of acini generated from the experiment describe in A. Asterisks indicate significant differences ****P < 0.0001.*

4.4.3 Evaluation of $p27^{kip1}$ role in BPEC in response to Palbociclib treatment

Finally, we tested whether p27 expression was able to alter the response to Palbociclib, also in normal human mammary epithelial cells, as showed previously in MCF-7. The BPEC p27 KO clones were treated with different drug doses of Palbociclib: 0.1, 0.5, 1.0, 2.5, 5, 10, 20 μM and after 72 hours, the cell viability was calculated. The results of this kill curve analysis clearly showed that p27 KO in this cell line had a greater impact in terms of Palbociclib resistance, showing that, at the higher drug concentrations, vital cells decreased substantially among the WT cells, while p27 KO ones still displayed almost 50% of cell viability (**figure 14A**).

Next, we evaluated the expression of cell cycle modulators during the BPEC response to Palbociclib. Cells were treated with Palbociclib at a sub-lethal dose (1.5μM) extrapolated from the kill curve, collected 24, 48 and 72 hours after treatment and analyzed by western blot analysis (**figure 14B**). Evaluation of phosphorylated RB protein (pRB) revealed that p27 KO clones displayed very high levels of pRB under normal culture conditions, explaining the very high growth rate of these clones (**figure 11C**). Surprisingly, the reduction of pRB under treatment with Palbociclib was more marked in the absence of p27. Interestingly, the level of oncosuppressor p53 decrease in KO clones, especially in Palbociclib treated cells and Cyclin D1 seems to be less expressed than in WT clones, but after treatment with Palbociclib its levels are restored. These data will be better dissected in future experiments and a more detailed molecular characterization will be needed to understand some unexpected results and, eventually, provide a molecular mechanism explaining, at least in part, the resistance to Palbociclib displayed by p27 KO BPEC clones.

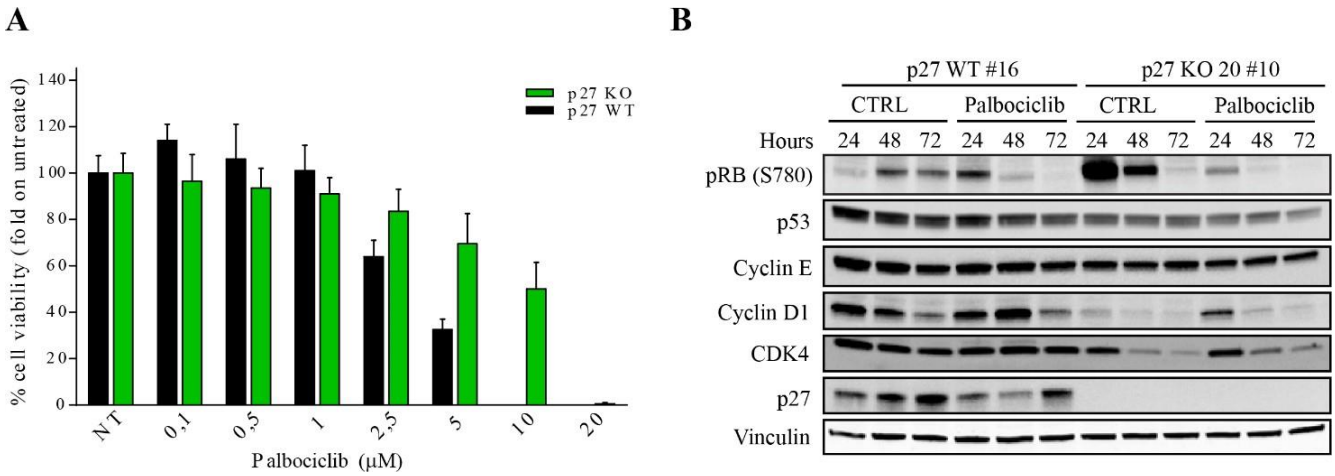

Figure 14. Response to Palbociclib treatment of BPEC p27 KO cells. A) *Dose response analysis of BPEC p27 KO and WT clones, treated with increasing doses of Palbociclib for 72 hours. Cell viability was evaluated using a MTS assay. Data represent the mean (± SD) of two clones for each cell type (BPEC p27 WT #16, parental; BPEC p27 KO 20 #10, KO 20 #8) performed in sextuplicate.* ***B)*** *Western blot analysis of BPEC p27 WT #16 and p27 KO 20 #10 clones collected after 24, 48, and 72 hours from the treatment with Palbociclib 1.5μM, as indicated.*

5 CONCLUSIONS

The cell cycle inhibitor p27 is a tumor suppressor mainly acting as negative regulator of cell proliferation. Through distinct domains, p27 has been also involved in the control of other cellular processes, such as migration, differentiation and cytoskeleton dynamics. p27 is frequently inactivated at protein level in human cancers and its subcellular localization (nuclear versus cytoplasmic) can be prognostic in some tumors, such as breast, colon, prostate, lung, esophageal, and gastric cancers (Ananthanarayanan et al. 2011; Wen et al. 2012).

CDKN1B gene, encoding for p27, has been identified as one of the most frequently (although still rare) mutated genes in Luminal breast cancer (Stephens et al. 2012; Ellis et al. 2012; Belletti, Baldassarre et al 2012; Viotto, Russo et al. 2021) and the analysis of copy number variation further showed that a fraction of LBC displayed loss or gain of CDKN1B copy number (Viotto, Russo et al. 2021), reinforcing the idea that p27 plays important functions in LBC.

Since some of the identified somatic mutations were located in the C-terminal domain, resulting in protein truncation or loss, we focused our studies on the effect of p27 absence and C-terminal mutations (p27 K134fs and T171*, truncated proteins) in tumor transformation, progression and response to therapies.

To understand the impact of p27 in tumor progression, we used p27 KO, p27 KI WT, p27 KI T171* and p27 KI K134fs MCF-7 clones, generated and partially characterized in our laboratory already during my graduation thesis. We have explored the molecular features of these mutants and the biological phenotypes of these genetically modified cells, both *in vitro* and *in vivo.*

First, both p27 mutants maintained the ability to bind the cyclin E - CDK2 complex but they lost the capacity to inhibit it, thus resulting in a final CDK2 kinase activity that was similar to the one observed in p27 KO cells. This is the first evidence indicating that beyond the loss of the C-terminal domains and their relative functions, these truncated proteins also loose the functions linked to the N-terminal domains, where the cyclin- and CDK-binding domains are located. This finding may explain why, although overall quite rare, mutations of CDKN1B gene occur with quite high incidence in the C-terminal (Ellis et al., 2012; Stephens et al., 2012; Viotto, Russo et al. 2021). Accordingly, p27 K134fs and T171* mutants failed to rescue most of the phenotypes induced by CDKN1B gene KO (p27 KO), further indicating that the functions retained by this portion of the protein are critical for p27 role as oncosuppressor (Viotto, Russo et al. 2021).

In line with this observation, we have observed that loss or mutated p27 induced a significant increase of the growth ability of cell clones, particularly evident when cells were cultured in "challenging" conditions, such as in anchorage independence.

Next, we asked whether the increased transformed potential of MCF-7 p27 KO and mutants, observed *in vitro*, effectively resulted in increased growth *in vivo*. To test this possibility, we have set up the mouse intraductal (MIND) model of mammary tumorigenesis, that is currently considered the most faithful in recapitulating the typical features of Luminal BC occurring in patients. MCF-7 modified clones were injected into the mouse nipple to reach and settle into the milk duct system, without supplying exogenous hormones. The results obtained in this model were very clear and showed that MIND tumors from p27 KO displayed a marked anticipation of tumor onset and an increase in tumor growth rate, leading to the formation of bigger and denser tumors compared to p27 WT. Tumors arising from p27 mutants, if and when mutant protein expression was maintained, appeared to slow down tumor growth at similar rate of the endogenous p27. This may be due to the fact that they conserved the cyclin-CDK binding domains at the N-terminal and, thus, some cell cycle inhibitory activity.

We also took advantage of the MIND model to investigate the transition from *in situ* to invasive disease and spontaneous metastasis formation to relevant sites. Our preliminary analyses that will be further expanded indicated that p27 KO clones were highly invasive, showing intravasation of tumor cells and, also, metastatic foci to the lungs.

We next explored the effect of p27 loss or its mutations on the response of LBC cells to current therapeutic strategies, evaluating in particular the response to Palbociclib.

Palbociclib is a small molecule CDK4/6 inhibitor that leads the induction of cell cycle arrest and senescence in breast cancer cells (Kovatcheva et al. 2015). Palbociclib has been recently approved for the treatment of advanced LBC patients in combination with endocrine therapy. Despite very promising initial clinical outcomes, intrinsic or acquired resistance to CDK4/6 inhibitors has limited the success of these drugs. The mechanisms of *de novo* and acquired Palbociclib resistance are not fully understood and an approach to overcome them is urgently needed. Interestingly, lack of p27 or presence of the mutant forms slightly increased cell resistance to Palbociclib. This result was even more evident when p27 KO was performed on a normal mammary epithelial cell line, the BPEC, treated with Palbociclib, although the augmented resistance did not match with an increased level of RB phosphorylation, leaving the door open for more in-depth future studies. The assessment of Palbociclib-induced senescence in these clones revealed that MCF-7 p27 T171*, p27 K134fs and p27 KO cells displayed an already high "physiological" senescent level in culture, which seemed to contrast with the growth capacity of these clones. This could be interesting evidence, to investigate about the possible links between p27 and senescence. Following drug treatment, in p27 KO, T171* and K134fs clones, the number of senescent cells significantly increased compared to WT clones and compared to their basal level. Deepening our studies, it emerged that the senescent phenotype that we observed in p27 KO and p27 mutant clones could represents a transient state. Following inhibition of CDK4/6, in presence of serum stimulation, our p27 modified clones, unlike the WT cells, slowly acquired ability to exit from senescence and reactivate cell growth, highlighting the possibility to giving rise to recurrence and metastasis in a p27 KO and mutant context in LBC.

Given the results obtained with MCF-7 LBC cells which highlighted the impactful role of p27 in tumor progression, we investigated the effects of p27 loss or mutations during the early steps of mammary epithelial cell transformation. The generation of BPEC p27 K134fs and p27 T171* clones is currently in progress while BPEC p27 KO clones are already available and have been partially characterized during my PhD. In line with the results obtained in MCF-7 cells, BPEC p27 KO cells display a significantly higher proliferation rate compared to WT clones and an increased ability to form mammospheres, indicating that cells with stem or early progenitor activity were stimulated to self-renew, when p27 was ablated. Interestingly, p27 loss also increased BPEC ability to grow in 3D-Matrigel, a condition in which crucial microenvironmental cues are restored (Yamada e Cukierman 2007).

Taken together, our *in vitro* and *in vivo* approaches, robustly show how p27 plays a critical role in

restraining many of the hallmarks of LBC. Our work establishes a role for p27 in the tumor progression and transformation of LBC and also highlights the relevance of its C-terminus in the control of BC cell growth and drug response, suggesting that its evaluation could be of value to predict the efficacy of anti-cancer therapies.

Many insights and future perspectives stem from the results collected so far, using these unique *in vitro* and *in vivo* models. We are currently better investigating the possible mechanisms of Palbociclib resistance elicited by absence of p27 in LBC cells, focusing on the multiple pathways involved in cellular senescence, underlying the transition from sustained to reversible senescence. One important aspect of the senescent phenotype, is the senescence-associated secretory phenotype (SASP), which is known to profoundly affect both cancer cells and their microenvironment, making it more permissive to engraftment. Accordingly, the cytokines and factors secreted by senescent cells can be associated with local and distant promotion of tumor growth, angiogenesis, metastasis, and immunosuppression (Coppé et al. 2010) and these aspects are being thoroughly dissected the lab.

Once all BPEC p27 K134fs and T171* clones will be obtained, they will be characterized for their molecular and biological behavior, as previously done with MCF-7. Then, these cells will be precious to clarify how and at which extent these genetic alterations might induce full/partial transformation of a "normal" mammary Luminal epithelial cells. In this context, we plan to test p27-modified BPEC clones in the MIND model and, hopefully, will offer an opportunity to better study Luminal mammary cell transformation and cancer initiation, *in vivo*. Finally, thanks to the availability of a very large cohort of LBC specimens collected over the years in collaboration with the Pathology Unit, we will have the opportunity to assess whether our results have a positive correlation in patients. The possibility, for instance, to use the expression level of p27 as biomarker of response to Palbociclib will be evaluated, using retrospective cohorts of patients who have been treated with Palbociclib at progression, for which we have a complete follow up information.

Our efforts will further establish whether p27 loss or mutations could represent a prognostic and/or predictive marker that could be used to better stratify Luminal breast cancer patients, eventually improving their survival and quality of life.

6 REFERENCES

Acosta J. C., A. Banito, T. Wuestefeld, A. Georgilis, P. Janich, J.P. Morton, D. Athineos, et al. 2013. «A Complex Secretory Program Orchestrated by the Inflammasome Controls Paracrine Senescence». *Nature Cell Biology* 15 (8): 978–90. https://doi.org/10.1038/ncb2784.

Acosta J.C., A. O'Loghlen, A. Banito, S. Raguz, j. Gil. 2008. «Control of Senescence by CXCR2 and Its Ligands». *Cell Cycle (Georgetown, Tex.)* 7 (19): 2956–59. https://doi.org/10.4161/cc.7.19.6780.

Ades F., D. Zardavas, I. Bozovic-Spasojevic, L.Pugliano, D. Fumagalli, E. De Azambuja, G.Viale, C. Sotiriou, e M. Piccart. 2014. «elyLuminal B Breast Cancer: Molecular Characterization, Clinical Management, and Future Perspectives». *Journal of Clinical Oncology* 32 (25): 2794–2803. https://doi.org/10.1200/JCO.2013.54.1870.

Alimperti S., S.T. Andreadis. 2015. «CDH2 and CDH11 as Regulators of Stem Cell Fate Decisions». *Stem cell research* 14 (3): 270–82. https://doi.org/10.1016/j.scr.2015.02.002.

Allred D.C. 2010. «Ductal Carcinoma In Situ: Terminology, Classification, and Natural History». *JNCI Monographs* 2010 (41): 134–38. https://doi.org/10.1093/jncimonographs/lgq035.

Althubiti M., L. Lezina, S. Carrera, R. Jukes-Jones, S. M. Giblett, A. Antonov, N. Barlev, et al. 2014. «Characterization of Novel Markers of Senescence and Their Prognostic Potential in Cancer». *Cell Death & Disease* 5 (novembre): e1528. https://doi.org/10.1038/cddis.2014.489.

American Cancer Society. Breast Cancer Facts & Figures 2017-2018. Breast Cancer Facts Fig. 2017-2018.

Ananthanarayanan V., R.J. Deaton, A. Amatya, V. Macias, E. Luther, A. Kajdacsy-Balla, e P. H. Gann. 2011. «Subcellular Localization of p27 and Prostate Cancer Recurrence: Automated Digital Microscopy Analysis of Tissue Microarrays». *Human pathology* 42 (6): 873–81. https://doi.org/10.1016/j.humpath.2010.10.006.

Arpino G., G.M. Clark, S. Mohsin, V.J. Bardou, e R.M. Elledge. 2002. «Adenoid Cystic Carcinoma of the Breast: Molecular Markers, Treatment, and Clinical Outcome». *Cancer* 94 (8): 2119–27. https://doi.org/10.1002/cncr.10455.

Ayrapetov M.K., O. Gursoy-Yuzugullu, C. Xu, Y. Xu, B. D. Price. 2014. «DNA Double-Strand Breaks Promote Methylation of Histone H3 on Lysine 9 and Transient Formation of Repressive Chromatin». *Proceedings of the National Academy of Sciences of the United States of America* 111 (25): 9169–74. https://doi.org/10.1073/pnas.1403565111.

Bagnardi V., M. Rota, E. Botteri, I. Tramacere, F. Islami, V. Fedirko, L. Scotti, et al. 2015. «Alcohol Consumption and Site-Specific Cancer Risk: A Comprehensive Dose-Response Meta-Analysis». *British Journal of Cancer* 112 (3): 580–93. https://doi.org/10.1038/bjc.2014.579.

Baldassarre G., M. V. Barone, B. Belletti, C. Sandomenico, P. Bruni, S. Spiezia, A. Boccia, et al. 1999. «Key Role of the Cyclin-Dependent Kinase Inhibitor P27kip1 for Embryonal Carcinoma Cell Survival and Differentiation». *Oncogene* 18 (46): 6241–51. https://doi.org/10.1038/sj.onc.1203031.

Barbieri C. E., S.C. Baca, M.S. Lawrence, F. Demichelis, M. Blattner, J.P Theurillat, T.A. White, et al. 2012. «Exome Sequencing Identifies Recurrent SPOP, FOXA1 and MED12 Mutations in Prostate Cancer». *Nature Genetics* 44 (6): 685–89. https://doi.org/10.1038/ng.2279.

Barnes A., S. E. Pinder, J. A. Bell, E. C. Paish, P. M. Wencyk, J. F. R. Robertson, C. W. Elston, e I. O. Ellis. 2003. «Expression of P27kip1 in Breast Cancer and Its Prognostic Significance». *The Journal of Pathology* 201 (3): 451–59. https://doi.org/10.1002/path.1464.

Baughn L.B., M. Di Liberto, Kaida Wu, P.L. Toogood, T. Louie, R. Gottschalk, R. Niesvizky, et al. 2006. «A Novel Orally Active Small Molecule Potently Induces G1 Arrest in Primary Myeloma Cells and Prevents Tumor Growth by Specific Inhibition of Cyclin-Dependent Kinase 4/6». *Cancer Research* 66 (15): 7661–67. https://doi.org/10.1158/0008-5472.CAN-06-1098.

Belletti B., M. S. Nicoloso, M. Schiappacassi, E. Chimienti, S. Berton, F. Lovat, A. Colombatti, e G. Baldassarre. 2005. «P27(Kip1) Functional Regulation in Human Cancer: A Potential Target for Therapeutic Designs». *Current Medicinal Chemistry* 12 (14): 1589–1605. https://doi.org/10.2174/0929867054367149.

Belletti B., Jayant S. Vaidya, S. D'Andrea, F. Entschladen, M. Roncadin, F. Lovat, S. Berton, et al. 2008. «Targeted Intraoperative Radiotherapy Impairs the Stimulation of Breast Cancer Cell Proliferation and Invasion Caused by Surgical Wounding». *Clinical Cancer Research* 14 (5): 1325–32. https://doi.org/10.1158/1078-0432.CCR-07-4453.

Belletti B., G.Baldassarre. 2012. 'New Light on P27(Kip1) in Breast Cancer'. *Cell Cycle (Georgetown, Tex.)* 11 (19): 3701–2. https://doi.org/10.4161/cc.21573.

Ben-Porath I., R. A. Weinberg. 2005. «The Signals and Pathways Activating Cellular Senescence». *The International Journal of Biochemistry & Cell Biology* 37 (5): 961–76. https://doi.org/10.1016/j.biocel.2004.10.013.

Berton S, M.Cusan, I. Segatto, F. Citron, S. D'Andrea, S. Benevol, M. Avanzo, et al. 2017. «Loss of P27kip1 Increases Genomic Instability and Induces Radio-Resistance in Luminal Breast Cancer Cells». *Scientific Reports* 7 (1): 595. https://doi.org/10.1038/s41598-017-00734-3.

Besson A., M. Gurian-West, X. Chen, K. S. Kelly-Spratt, C. J. Kemp, J. M. Roberts. 2006. «A Pathway in Quiescent Cells That Controls P27Kip1 Stability, Subcellular Localization, and Tumor Suppression». *Genes & Development* 20 (1): 47–64. https://doi.org/10.1101/gad.1384406.

Boehm M., T. Yoshimoto, M. F. Crook, S. Nallamshetty, A. True, G. J. Nabel, e E. G. Nabel. 2002. «A Growth Factor-Dependent Nuclear Kinase Phosphorylates P27(Kip1) and Regulates Cell Cycle Progression». *The EMBO Journal* 21 (13): 3390–3401. https://doi.org/10.1093/emboj/cdf343.

Brooks A. N., E. Kilgour, P.D. Smith. 2012. «Molecular Pathways: Fibroblast Growth Factor Signaling: A New Therapeutic Opportunity in Cancer». *Clinical Cancer Research: An Official Journal of the American Association for Cancer Research* 18 (7): 1855–62. https://doi.org/10.1158/1078-0432.CCR-11-0699.

Cassimere E. K., C. Mauvais, C. Denicourt. 2016. «P27Kip1 Is Required to Mediate a G1 Cell Cycle Arrest Downstream of ATM Following Genotoxic Stress». *PloS One* 11 (9): e0162806. https://doi.org/10.1371/journal.pone.0162806.

Celeste A., S. Petersen, P. J. Romanienko, O. Fernandez-Capetillo, H.T. Chen, O. A. Sedelnikova, B. Reina-San-Martin, et al. 2002. «Genomic Instability in Mice Lacking Histone H2AX». *Science (New York, N.Y.)* 296 (5569): 922–27. https://doi.org/10.1126/science.1069398.

Cen B. L. Carlson, M. A. Schroeder, J. L. Ostrem, G. J. Kitange, A. C. Mladek, S. R. Fink, et al. 2012. «P16-Cdk4-Rb Axis Controls Sensitivity to a Cyclin-Dependent Kinase Inhibitor PD0332991 in Glioblastoma Xenograft Cells». *Neuro-Oncology* 14 (7): 870–81. https://doi.org/10.1093/neuonc/nos114.

Choi J., X. Li, P. Hydbring, T. Sanda, J. Stefano, A.L. Christie, S. Signoretti, et al. 2012. «The Requirement for Cyclin D Function in Tumor Maintenance». *Cancer Cell* 22 (4): 438–51. https://doi.org/10.1016/j.ccr.2012.09.015.

Chu I., J. Sun, A. Arnaout, H. Kahn, W. Hanna, S. Narod, P. Sun, C. Tan, L. Hengst, J. Slingerland. 2007. «P27 Phosphorylation by Src Regulates Inhibition of Cyclin E-Cdk2». *Cell* 128 (2): 281–94. https://doi.org/10.1016/j.cell.2006.11.049.

Coats, S., W. M. Flanagan, J. Nourse, e J. M. Roberts. 1996. «Requirement of P27Kip1 for Restriction Point Control of the Fibroblast Cell Cycle». *Science (New York, N.Y.)* 272 (5263): 877–80. https://doi.org/10.1126/science.272.5263.877.

Coppé J. P., P. Y. Desprez, A. Krtolica, J. Campisi. 2010. «The Senescence-Associated Secretory Phenotype: The Dark Side of Tumor Suppression». *Annual Review of Pathology* 5: 99–118. https://doi.org/10.1146/annurev-pathol-121808-102144.

Corrao G., A. Zambon, V. Conti, F. Nicotra, C. La Vecchia, C. Fornari, G. Cesana, et al. 2008. «Menopause Hormone Replacement Therapy and Cancer Risk: An Italian Record Linkage Investigation». *Annals of Oncology* 19 (1): 150–55. https://doi.org/10.1093/annonc/mdm404.

Creighton C. J. 2012. «The Molecular Profile of Luminal B Breast Cancer». *Biologics: Targets and Therapy* 6 (agosto): 289–97. https://doi.org/10.2147/BTT.S29923.

Cserni G. 2020. «Histological Type and Typing of Breast Carcinomas and the WHO Classification Changes over Time». *Pathologica - Journal of the Italian Society of Anatomic Pathology and Diagnostic Cytopathology* 112 (1): 25–41. https://doi.org/10.32074/1591-951X-1-20.

Cusan M., G. Mungo, M. De Marco Zompit, I. Segatto, B. Belletti, G. Baldassarre. 2018. «Landscape of CDKN1B Mutations in Luminal Breast Cancer and Other Hormone-Driven Human Tumors». *Frontiers in Endocrinology* 9: 393. https://doi.org/10.3389/fendo.2018.00393.

Dean, J. L., C. Thangavel, A. K. McClendon, C. A. Reed, e E. S. Knudsen. 2010. «Therapeutic CDK4/6 Inhibition in Breast Cancer: Key Mechanisms of Response and Failure». *Oncogene* 29 (28): 4018–32. https://doi.org/10.1038/onc.2010.154.

Desmedt C., B. Haibe-Kains, P. Wirapati, M. Buyse, D. Larsimont, G. Bontempi, M. Delorenzi, M. Piccart, C. Sotiriou. 2008. «Biological Processes Associated with Breast Cancer Clinical Outcome Depend on the Molecular Subtypes». *Clinical Cancer Research: An Official Journal of the American Association for Cancer Research* 14 (16): 5158–65. https://doi.org/10.1158/1078-0432.CCR-07-4756.

Dhanasekaran R, A. Deutzmann, W. D. Mahauad-Fernandez, A. S. Hansen, A. M. Gouw, D. W. Felsher. 2022. «The MYC Oncogene - the Grand Orchestrator of Cancer Growth and Immune Evasion». *Nature Reviews. Clinical Oncology* 19 (1): 23–36. https://doi.org/10.1038/s41571-021-00549-2.

Dimri G. P., X. Lee, G. Basile, M. Acosta, G. Scott, C. Roskelley, E. E. Medrano, M. Linskens, I. Rubelj, e O. Pereira-Smith. 1995. «A Biomarker That Identifies Senescent Human Cells in Culture and in Aging Skin in Vivo». *Proceedings of the National Academy of Sciences of the United States of America* 92 (20): 9363–67. https://doi.org/10.1073/pnas.92.20.9363.

Ding L., L. B. Shunkwiler, N. W. Harper, Y. Zhao, K. Hinohara, S. Huh, M.B. Ekram, et al. 2019. «Deletion of Cdkn1b in ACI Rats Leads to Increased Proliferation and Pregnancy-Associated Changes in the Mammary Gland Due to Perturbed Systemic Endocrine Environment». *PLoS Genetics* 15 (3): e1008002. https://doi.org/10.1371/journal.pgen.1008002.

Dossus L., M.C. Boutron-Ruault, R. Kaaks, I. T. Gram, A. Vilier, B. Fervers, J. Manjer, et al. 2014. «Active and Passive Cigarette Smoking and Breast Cancer Risk: Results from the EPIC Cohort». *International Journal of Cancer* 134 (8): 1871–88. https://doi.org/10.1002/ijc.28508.

Eisen M. B., P. T. Spellman, P. O. Brown, e D. Botstein. 1998. «Cluster Analysis and Display of Genome-Wide Expression Patterns». *Proceedings of the National Academy of Sciences of the United States of America* 95 (25): 14863–68. https://doi.org/10.1073/pnas.95.25.14863.

Elbauomy E. S., A. R. Green, M. K. Lambros, N. C. Turner, M. J. Grainge, D. Powe, I. O. Ellis, J. S. Reis-Filho. 2007. «FGFR1 Amplification in Breast Carcinomas: A Chromogenic in Situ Hybridisation Analysis». *Breast Cancer Research: BCR* 9 (2): R23. https://doi.org/10.1186/bcr1665.

Eliyatkın N., E. Yalçın, B. Zengel, S. Aktaş, E. Vardar. 2015. «Molecular Classification of Breast Carcinoma: From Traditional, Old-Fashioned Way to A New Age, and A New Way». *The Journal of Breast Health* 11 (2): 59–66. https://doi.org/10.5152/tjbh.2015.1669.

Ellis M. J., L. Ding, D. Shen, J. Luo, V. J. Suman, J. W. Wallis, B. A. V. Tine, et al. 2012. «Whole-Genome Analysis Informs Breast Cancer Response to Aromatase Inhibition». *Nature* 486 (7403): 353–60. https://doi.org/10.1038/nature11143.

Ellis M. J., C. M. Perou. 2013. «The Genomic Landscape of Breast Cancer as a Therapeutic Roadmap». *Cancer Discovery* 3 (1): 27–34. https://doi.org/10.1158/2159-8290.CD-12-0462.

Fero M. L., E. Randel, K. E. Gurley, J. M. Roberts, e C. J. Kemp. 1998. «The Murine Gene P27Kip1 Is Haplo-Insufficient for Tumour Suppression». *Nature* 396 (6707): 177–80. https://doi.org/10.1038/24179.

Finn R. S., Y. Liu, Z. Zhu, M. l Martin, H. S. Rugo, V. Diéras, S. Im, et al. 2020. «Biomarker Analyses of Response to Cyclin-Dependent Kinase 4/6 Inhibition and Endocrine Therapy in Women with Treatment-Naïve Metastatic Breast Cancer». *Clinical Cancer Research: An Official Journal of the American Association for Cancer Research* 26 (1): 110–21. https://doi.org/10.1158/1078-0432.CCR-19-0751.

Finn R. S., J. Dering, D. Conklin, O. Kalous, D. J. Cohen, A. J. Desai, C. Ginther, et al. 2009. «PD 0332991, a Selective Cyclin D Kinase 4/6 Inhibitor, Preferentially Inhibits Proliferation of Luminal Estrogen Receptor-Positive Human Breast Cancer Cell Lines in Vitro». *Breast Cancer Research: BCR* 11 (5): R77. https://doi.org/10.1186/bcr2419.

Finn R. S., M. Martin, H. S. Rugo, S. Jones, S. Im, K. Gelmon, N. Harbeck, et al. 2016. «Palbociclib and Letrozole in Advanced Breast Cancer». *The New England Journal of Medicine* 375 (20): 1925–36. https://doi.org/10.1056/NEJMoa1607303.

Fisusi, Funmilola A., e Emmanuel O. Akala. s.d. «Drug Combinations in Breast Cancer Therapy». *Pharmaceutical Nanotechnology* 7 (1): 3–23.

Francis J. M., A. Kiezun, A. H. Ramos, S. Serra, C. S. Pedamallu, Z. R. Qian, M. S. Banck, et al. 2013. «Somatic Mutation of CDKN1B in Small Intestine Neuroendocrine Tumors». *Nature Genetics* 45 (12): 1483–86. https://doi.org/10.1038/ng.2821.

Fujita N., S. Sato, K. Katayama, T. Tsuruo. 2002. «Akt-Dependent Phosphorylation of P27Kip1 Promotes Binding to 14-3-3 and Cytoplasmic Localization». *The Journal of Biological Chemistry* 277 (32): 28706–13. https://doi.org/10.1074/jbc.M203668200.

Fumagalli D., T. R. Wilson, R. Salgado, X. Lu, J. Yu, C. O'Brien, K. Walter, et al. 2016. «Somatic Mutation, Copy Number and Transcriptomic Profiles of Primary and Matched Metastatic Estrogen Receptor-Positive Breast Cancers». *Annals of Onclogy: Official Journal of the European Society for Medical Oncology* 27 (10): 1860–66. https://doi.org/10.1093/annonc/mdw286.

Giltnane J. M., K. E. Hutchinson, T. P. Stricker, L. Formisano, C. D. Young, Monica V. Estrada, Mellissa J. Nixon, et al. 2017. «Genomic Profiling of ER+ Breast Cancers after Short-Term Estrogen Suppression Reveals Alterations Associated with Endocrine Resistance». *Science Translational Medicine* 9 (402): eaai7993. https://doi.org/10.1126/scitranslmed.aai7993.

Goldhirsch A., W. C. Wood, A. S. Coates, R. D. Gelber, B. Thürlimann, e H. -J. Senn. 2011. «Strategies for Subtypes Dealing with the Diversity of Breast Cancer: Highlights of the St Gallen International Expert Consensus on the Primary Therapy of Early Breast Cancer 2011». *Annals of Oncology*, In this issue: EU recognition for Medical Oncology Focus on translational research, 22 (8): 1736–47. https://doi.org/10.1093/annonc/mdr304.

González-Gualda E., A. G. Baker, L. Fruk, D. Muñoz-Espín. 2021. «A Guide to Assessing Cellular Senescence in Vitro and in Vivo». *The FEBS Journal* 288 (1): 56–80. https://doi.org/10.1111/febs.15570.

Grimmler M., Y. Wang, T. Mund, Z. Cilensek, E. M. Keidel, M. B. Waddell, H. Jäkel, M. Kullmann, Ri. W. Kriwacki, e Ludger Hengst. 2007. «Cdk-Inhibitory Activity and Stability of P27Kip1 Are Directly Regulated by Oncogenic Tyrosine Kinases». *Cell* 128 (2): 269–80. https://doi.org/10.1016/j.cell.2006.11.047.

Guan X., Y. Wang, R. Xie, L. Chen, J. Bai, J. Lu, M. T. Kuo. 2010. «P27(Kip1) as a Prognostic Factor in Breast Cancer: A Systematic Review and Meta-Analysis». *Journal of Cellular and Molecular Medicine* 14 (4): 944–53. https://doi.org/10.1111/j.1582-4934.2009.00730.x.

Haas S., A. Trumpp, M. D. Milsom. 2018. «Causes and Consequences of Hematopoietic Stem Cell Heterogeneity». *Cell Stem Cell* 22 (5): 627–38. https://doi.org/10.1016/j.stem.2018.04.003.

Hauck L., C. Harms, J. An, J. Rohne, K. Gertz, R. Dietz, M. Endres, R. Von Harsdorf. 2008. «Protein Kinase CK2 Links Extracellular Growth Factor Signaling with the Control of P27(Kip1) Stability in the Heart». *Nature Medicine* 14 (3): 315–24. https://doi.org/10.1038/nm1729.

Hara, T., T. Kamura, K. Nakayama, K. Oshikawa, S. Hatakeyama, e K. Nakayama. 2001. «Degradation of P27(Kip1) at the G(0)-G(1) Transition Mediated by a Skp2-Independent Ubiquitination Pathway». *The Journal of Biological Chemistry* 276 (52): 48937–43. https://doi.org/10.1074/jbc.M107274200.

Harbour, J. W., R. X. Luo, A. Dei Santi, A. A. Postigo, e D. C. Dean. 1999. «Cdk Phosphorylation Triggers Sequential Intramolecular Interactions That Progressively Block Rb Functions as Cells Move through G1». *Cell* 98 (6): 859–69. https://doi.org/10.1016/s0092-8674(00)81519-6

Hebner C., V. M. Weaver, J. Debnath. 2008. «Modeling Morphogenesis and Oncogenesis in Three-Dimensional Breast Epithelial Cultures». *Annual Review of Pathology* 3: 313–39. https://doi.org/10.1146/annurev.pathmechdis.3.121806.151526.

Herbig U., M. Ferreira, L. Condel, D. Carey, J. M. Sedivy. 2006. «Cellular Senescence in Aging Primates». *Science (New York, N.Y.)* 311 (5765): 1257. https://doi.org/10.1126/science.1122446.

Hernandez-Segura A., J. Nehme, M. Demaria. 2018. «Hallmarks of Cellular Senescence». *Trends in Cell Biology* 28 (6): 436–53. https://doi.org/10.1016/j.tcb.2018.02.001.

Herrera-Abreu M. T., M. Palafox, U. Asghar, M.A. Rivas, R. J. Cutts, I. Garcia-Murillas, A. Pearson, et al. 2016. «Early Adaptation and Acquired Resistance to CDK4/6 Inhibition in Estrogen Receptor-Positive Breast Cancer». *Cancer Research* 76 (8): 2301–13. https://doi.org/10.1158/0008-5472.CAN-15-0728.

Ignatiadis M., C. Sotiriou. 2013. «Luminal Breast Cancer: From Biology to Treatment». *Nature Reviews. Clinical Oncology* 10 (9): 494–506. https://doi.org/10.1038/nrclinonc.2013.124.

Iwanaga R., C. Wang, D.S. Micalizzi, J. C. Harrell, P. Jedlicka, C. A. Sartorius, P. Kabos, S. M. Farabaugh, A.P. Bradford, H. L. Ford. 2012. «Expression of Six1 in Luminal Breast Cancers Predicts Poor Prognosis and Promotes Increases in Tumor Initiating Cells by Activation of Extracellular Signal-Regulated Kinase and Transforming Growth Factor-Beta Signaling Pathways». *Breast Cancer Research: BCR* 14 (4): R100. https://doi.org/10.1186/bcr3219.

James M. K., A. Ray, D. Leznova, S. W. Blain. 2008. «Differential Modification of P27Kip1 Controls Its Cyclin D-Cdk4 Inhibitory Activity». *Molecular and Cellular Biology* 28 (1): 498–510. https://doi.org/10.1128/MCB.02171-06.

Jansen V. M., N. E. Bhola, J. A. Bauer, L. Formisano, K. Lee, K. E. Hutchinson, A. K. Witkiewicz, et al. 2017. «Kinome-Wide RNA Interference Screen Reveals a Role for PDK1 in Acquired Resistance to CDK4/6 Inhibition in ER-Positive Breast Cancer». *Cancer Research* 77 (9): 2488–99. https://doi.org/10.1158/0008-5472.CAN-16-2653

Jiang Y., K. Yu, W. Zuo, W. Peng, e Z. Shao. 2014. «GATA3 Mutations Define a Unique Subtype of Luminal-like Breast Cancer with Improved Survival». *Cancer* 120 (9): 1329–37. https://doi.org/10.1002/cncr.28566.

Jing H., S. Lee. 2014. «NF-κB in Cellular Senescence and Cancer Treatment». *Molecules and Cells* 37 (3): 189–95. https://doi.org/10.14348/molcells.2014.2353.

Kamura T., T. Hara, M. Matsumoto, N. Ishida, F. Okumura, S. Hatakeyama, M. Yoshida, K. Nakayama, K. I. Nakayama. 2004. «Cytoplasmic Ubiquitin Ligase KPC Regulates Proteolysis of P27(Kip1) at G1 Phase». *Nature Cell Biology* 6 (12): 1229–35. https://doi.org/10.1038/ncb1194.

Koboldt, Daniel C., Robert S. Fulton, Michael D. McLellan, Heather Schmidt, Joelle Kalicki-Veizer, Joshua F. McMichael, Lucinda L. Fulton, et al. 2012. «Comprehensive Molecular Portraits of Human Breast Tumours». *Nature* 490 (7418): 61–70. https://doi.org/10.1038/nature11412.

Konecny G. E., B. Winterhoff, T. Kolarova, J. Qi, K. Manivong, J. Dering, G. Yang, et al. 2011. «Expression of P16 and Retinoblastoma Determines Response to CDK4/6 Inhibition in Ovarian Cancer». *Clinical Cancer Research: An Official Journal of the American Association for Cancer Research* 17 (6): 1591–1602. https://doi.org/10.1158/1078-0432.CCR-10-2307.

Kotoshiba S., T. Kamura, T. Hara, N. Ishida, K. I. Nakayama. 2005. «Molecular Dissection of the Interaction between P27 and Kip1 Ubiquitylation-Promoting Complex, the Ubiquitin Ligase That Regulates Proteolysis of P27 in G1 Phase». *The Journal of Biological Chemistry* 280 (18): 17694–700. https://doi.org/10.1074/jbc.M500866200.

Kovatcheva M., D. D. Liu, M. A. Dickson, M. E. Klein, R. O'Connor, F. O. Wilder, N. D. Socci, et al. 2015. «MDM2 Turnover and Expression of ATRX Determine the Choice between Quiescence and Senescence in Response to CDK4 Inhibition». *Oncotarget* 6 (10): 8226–43. https://doi.org/10.18632/oncotarget.3364.

Kumari R., P. Jat. 2021. «Mechanisms of Cellular Senescence: Cell Cycle Arrest and Senescence Associated Secretory Phenotype». *Frontiers in Cell and Developmental Biology* 9 (marzo): 645593. https://doi.org/10.3389/fcell.2021.645593.

Lai A. C., C. M. Crews. 2017. «Induced Protein Degradation: An Emerging Drug Discovery Paradigm». *Nature Reviews Drug Discovery* 16 (2): 101–14. https://doi.org/10.1038/nrd.2016.211.

Langlands F.E., K. Horgan, D.D. Dodwell, L. Smith. 2013. «Breast cancer subtypes: response to radiotherapy and potential radiosensitisation». *The British Journal of Radiology* 86 (1023): 20120601. https://doi.org/10.1259/bjr.20120601.

Larrea M. D., J. Liang, T. Da Silva, F. Hong, S. H. Shao, K. Han, D. Dumont, J. M. Slingerland. 2008. «Phosphorylation of P27Kip1 Regulates Assembly and Activation of Cyclin D1-Cdk4». *Molecular and Cellular Biology* 28 (20): 6462–72. https://doi.org/10.1128/MCB.02300-07.

Lee M., N. S. Pellegata. 2013. «Multiple Endocrine Neoplasia Type 4». *Frontiers of Hormone Research* 41: 63–78. https://doi.org/10.1159/000345670.

Li H., M. Collado, A. Villasante, A. Matheu, C. J. Lynch, M. Cañamero, K. Rizzoti, et al. 2012. «P27(Kip1) Directly Represses Sox2 during Embryonic Stem Cell Differentiation». *Cell Stem Cell* 11 (6): 845–52. https://doi.org/10.1016/j.stem.2012.09.014.

Liang J., J. Zubovitz, T. Petrocelli, R. Kotchetkov, M. K. Connor, K. Han, J.H. Lee, et al. 2002. «PKB/Akt Phosphorylates P27, Impairs Nuclear Import of P27 and Opposes P27-Mediated G1 Arrest». *Nature Medicine* 8 (10): 1153–60. https://doi.org/10.1038/nm761.

Lynce F., A. N. Shajahan-Haq, S. M. Swain. 2018. «CDK4/6 Inhibitors in Breast Cancer Therapy: Current Practice and Future Opportunities». *Pharmacology & Therapeutics* 191 (novembre): 65–73. https://doi.org/10.1016/j.pharmthera.2018.06.008.

Loi S., B. Haibe-Kains, S. Majjaj, F. Lallemand, V. Durbecq, D. Larsimont, A. M. Gonzalez-Angulo, et al. 2010. «PIK3CA Mutations Associated with Gene Signature of Low MTORC1 Signaling and Better Outcomes in Estrogen Receptor–Positive Breast Cancer». *Proceedings of the National Academy of Sciences* 107 (22): 10208–13. https://doi.org/10.1073/pnas.0907011107.

Marcotte R., A. Sayad, K. R. Brown, F. Sanchez-Garcia, J. Reimand, M. Haider, C. Virtanen, et al. 2016. «Functional Genomic Landscape of Human Breast Cancer Drivers, Vulnerabilities, and Resistance». *Cell* 164 (1–2): 293–309. https://doi.org/10.1016/j.cell.2015.11.062.

Matsu-ura T., H. Sasaki, M. Okada, K. Mikoshiba, M. Ashraf. 2016. «Attenuation of Teratoma Formation by P27 Overexpression in Induced Pluripotent Stem Cells». *Stem Cell Research & Therapy* 7 (febbraio): 30. https://doi.org/10.1186/s13287-016-0286-3.

Michaud K., D. A. Solomon, E. Oermann, J. Kim, W. Zhong, M. D. Prados, T. Ozawa, C. James, T. Waldman. 2010. «Pharmacologic Inhibition of Cyclin-Dependent Kinases 4 and 6 Arrests the Growth of Glioblastoma Multiforme Intracranial Xenografts». *Cancer Research* 70 (8): 3228–38. https://doi.org/10.1158/0008-5472.CAN-09-4559

Milanovic M., D. N. Y. Fan, D. Belenki, J. H. M. Däbritz, Z. Zhao, Y. Yu, J. R. Dörr, et al. 2018. «Senescence-Associated Reprogramming Promotes Cancer Stemness». *Nature* 553 (7686): 96–100. https://doi.org/10.1038/nature25167.

Miller E, H. J. Lee, A. Lulla, L. Hernandez, P. Gokare, B. Lim. 2014. «Current Treatment of Early Breast Cancer: Adjuvant and Neoadjuvant Therapy». 3:198. F1000Research. https://doi.org/10.12688/f1000research.4340.1.

Miller T. W., J. M. Balko, C. L. Arteaga. 2011. «Phosphatidylinositol 3-Kinase and Antiestrogen Resistance in Breast Cancer». *Journal of Clinical Oncology: Official Journal of the American Society of Clinical Oncology* 29 (33): 4452–61. https://doi.org/10.1200/JCO.2010.34.4879.

Muñoz-Espín D., M. Cañamero, A. Maraver, G. Gómez-López, J. Contreras, S. Murillo-Cuesta, A. Rodríguez-Baeza, et al. 2013. «Programmed Cell Senescence during Mammalian Embryonic Development». *Cell* 155 (5): 1104–18. https://doi.org/10.1016/j.cell.2013.10.019.

Nag S., J. Qin, K. S. Srivenugopal, M Wang, R. Zhang. 2013. «The MDM2-p53 pathway revisited». *Journal of Biomedical Research* 27 (4): 254–71. https://doi.org/10.7555/JBR.27.20130030.

Nahta R., T. Takahashi, N. T. Ueno, M. Hung, F. J. Esteva. 2004. «P27(Kip1) down-Regulation Is Associated with Trastuzumab Resistance in Breast Cancer Cells». *Cancer Research* 64 (11): 3981–86. https://doi.org/10.1158/0008-5472.CAN-03-3900.

Nakayama K., H. Nagahama, Y. A. Minamishima, S. Miyake, N. Ishida, S. Hatakeyama, M. Kitagawa, Shun-ichiro Iemura, T. Natsume, K. I. Nakayama. 2004. «Skp2-Mediated Degradation of P27 Regulates Progression into Mitosis». *Developmental Cell* 6 (5): 661–72. https://doi.org/10.1016/s1534-5807(04)00131-5.

Nakayama K., H. Nagahama, Y. A. Minamishima, S. Miyake, N. Ishida, S. Hatakeyama, M. Kitagawa, S. Iemura, T. Natsume, I. Nakayama. 2004. «Skp2-Mediated Degradation of P27 Regulates Progression into Mitosis». *Developmental Cell* 6 (5): 661–72. https://doi.org/10.1016/s1534-5807(04)00131-5.

Neurohr G. E., R. L. Terry, J. Lengefeld, M. Bonney, G. P. Brittingham, F. Moretto, T. P. Miettinen, et al. 2019. «Excessive Cell Growth Causes Cytoplasm Dilution And Contributes to Senescence». *Cell* 176 (5): 1083-1097.e18. https://doi.org/10.1016/j.cell.2019.01.018.

Newman L., W. Xia, H. Y. Yang, A. Sahin, M. Bondy, F. Lukmanji, M. C. Hung, e M. H. Lee. 2001. «Correlation of P27 Protein Expression with HER-2/Neu Expression in Breast Cancer». *Molecular Carcinogenesis* 30 (3): 169–75. https://doi.org/10.1002/mc.1025.

Nielsen F. C., T. van Overeem Hansen, C. Storgaard Sørensen. 2016. «Hereditary Breast and Ovarian Cancer: New Genes in Confined Pathways». *Nature Reviews. Cancer* 16 (9): 599–612. https://doi.org/10.1038/nrc.2016.72.

Ohtani N., A. Takahashi, D. J. Mann, E. Hara. 2012. «Cellular Senescence: A Double-Edged Sword in the Fight against Cancer». *Experimental Dermatology* 21 Suppl 1 (luglio): 1–4. https://doi.org/10.1111/j.1600-0625.2012.01493.x.

Olanich M. E., W. Sun, S. M. Hewitt, Z. Abdullaev, S. D. Pack, G. Barr. 2015. «CDK4 Amplification Reduces Sensitivity to CDK4/6 Inhibition in Fusion-Positive Rhabdomyosarcoma». *Clinical Cancer Research: An Official Journal of the American Association for Cancer Research* 21 (21): 4947–59. https://doi.org/10.1158/1078-0432.CCR-14-2955.

O'Leary B., R. S. Finn, N. C. Turner. 2016. «Treating Cancer with Selective CDK4/6 Inhibitors». *Nature Reviews. Clinical Oncology* 13 (7): 417–30. https://doi.org/10.1038/nrclinonc.2016.26.

Pandey K., H. An, S. Ki Kim, S. Ah Lee, S. Kim, S. Min Lim, G. Min Kim, J. Sohn, Y. Wha Moon. 2019. «Molecular mechanisms of resistance to CDK4/6 inhibitors in breast cancer: A review». *International Journal of Cancer* 145 (5): 1179–88. https://doi.org/10.1002/ijc.32020.

Payne S. R., S. Zhang, K. Tsuchiya, R. Moser, K. E. Gurley, G. Longton, J. de Boer, J. Kemp. 2008. «P27kip1 Deficiency Impairs G2/M Arrest in Response to DNA Damage, Leading to an Increase in Genetic Instability». *Molecular and Cellular Biology* 28 (1): 258–68. https://doi.org/10.1128/MCB.01536-07.

Pearse G., J. Frith, K. J. Randall, T. Klinowska. 2009. «Urinary Retention and Cystitis Associated with Subcutaneous Estradiol Pellets in Female Nude Mice». *Toxicologic Pathology* 37 (2): 227–34. https://doi.org/10.1177/0192623308329281.

Philipp-Staheli, J., S. R. Payne, e C. J. Kemp. 2001. «P27(Kip1): Regulation and Function of a Haploinsufficient Tumor Suppressor and Its Misregulation in Cancer». *Experimental Cell Research* 264 (1): 148–68. https://doi.org/10.1006/excr.2000.5143.

Picon-Ruiz M., C. Morata-Tarifa, J. J. Valle-Goffin, E. R. Friedman, J. M. Slingerland. 2017. «Obesity and Adverse Breast Cancer Risk and Outcome: Mechanistic Insights and Strategies for Intervention». *CA: A Cancer Journal for Clinicians* 67 (5): 378–97. https://doi.org/10.3322/caac.21405.

Pohl G., M. Rudas, O. Dietze, S. Lax, E. Markis, R. Pirker, C. C. Zielinski, et al. 2003. «High P27Kip1 Expression Predicts Superior Relapse-Free and Overall Survival for Premenopausal Women with Early-Stage Breast Cancer Receiving Adjuvant Treatment with Tamoxifen plus Goserelin». *Journal of Clinical Oncology: Official Journal of the American Society of Clinical Oncology* 21 (19): 3594–3600. https://doi.org/10.1200/JCO.2003.02.021.

Polyak K., J. Y. Kato, M. J. Solomon, C. J. Sherr, J. Massague, J. M. Roberts, e A. Koff. 1994. «P27Kip1, a Cyclin-Cdk Inhibitor, Links Transforming Growth Factor-Beta and Contact Inhibition to Cell Cycle Arrest». *Genes & Development* 8 (1): 9–22. https://doi.org/10.1101/gad.8.1.9.

Porter P.L., W. E. Barlow, I.-Tien Yeh, M. G. Lin, X. P. Yuan, E. Donato, G. W. Sledge, et al. 2006. «P27(Kip1) and Cyclin E Expression and Breast Cancer Survival after Treatment with Adjuvant Chemotherapy». *Journal of the National Cancer Institute* 98 (23): 1723–31. https://doi.org/10.1093/jnci/djj467.

Rampioni Vinciguerra G. L., M. Sonego, I. Segatto, A. Dall'Acqua, A. Vecchione, G. Baldassarre, B. Belletti. 2022. «CDK4/6 Inhibitors in Combination Therapies: Better in Company Than Alone: A Mini Review». *Frontiers in Oncology* 12. https://www.frontiersin.org/article/10.3389/fonc.2022.891580.

Rampioni Vinciguerra G.L., F.Citron, I. Segatto, B. Belletti, A.Vecchione, G. Baldassarre. 2019. «P27kip1 at the Crossroad between Actin and Microtubule Dynamics». *Cell Division* 14: 2. https://doi.org/10.1186/s13008-019-0045-9

Ratre P., K. Mishra, A. Dubey, A. Vyas, A. Jain, S. Thareja. 2020. «Aromatase Inhibitors for the Treatment of Breast Cancer: A Journey from the Scratch». *Anti-Cancer Agents in Medicinal Chemistry* 20 (17): 1994–2004. https://doi.org/10.2174/1871520620666200627204105.

Reis-Filho J. S., P. T. Simpson, N. C. Turner, M. B. Lambros, C. Jones, A. Mackay, A. Grigoriadis, et al. 2006. «FGFR1 Emerges as a Potential Therapeutic Target for Lobular Breast Carcinomas». *Clinical Cancer Research: An Official Journal of the American Association for Cancer Research* 12 (22): 6652–62. https://doi.org/10.1158/1078-0432.CCR-06-1164.

Ritschka B., M. Storer, A. Mas, F. Heinzmann, M. C. Ortells, J. P. Morton, O. J. Sansom, L. Zender, W. M. Keyes. 2017. «The Senescence-Associated Secretory Phenotype Induces Cellular Plasticity and Tissue Regeneration». *Genes & Development* 31 (2): 172–83. https://doi.org/10.1101/gad.290635.116.

Rocca A., A. Schirone, R. Maltoni, S. Bravaccini, L. Cecconetto, A. Farolfi, G. Bronte, D. Andreis. 2017. «Progress with Palbociclib in Breast Cancer: Latest Evidence and Clinical Considerations». *Therapeutic Advances in Medical Oncology* 9 (2): 83–105. https://doi.org/10.1177/1758834016677961.

Rodier F., J. Campisi. 2011. «Four Faces of Cellular Senescence». *The Journal of Cell Biology* 192 (4): 547–56. https://doi.org/10.1083/jcb.201009094.

Rodon J., R. Dienstmann, V. Serra, J. Tabernero. 2013. «Development of PI3K Inhibitors: Lessons Learned from Early Clinical Trials». *Nature Reviews. Clinical Oncology* 10 (3): 143–53. https://doi.org/10.1038/nrclinonc.2013.10.

Rojas K., A. Stuckey. 2016. «Breast Cancer Epidemiology and Risk Factors». *Clinical Obstetrics and Gynecology* 59 (4): 651–72. https://doi.org/10.1097/GRF.0000000000000239.

Schiappacassi M., S. Lovisa, F. Lovat, L. Fabris, A. Colombatti, B. Belletti, G. Baldassarre. 2011. «Role of T198 Modification in the Regulation of P27(Kip1) Protein Stability and Function». *PloS One* 6 (3): e17673. https://doi.org/10.1371/journal.pone.0017673.

Serres M. P., U. Kossatz, Y. Chi, J. M. Roberts, N. P. Malek, A. Besson. 2012. «P27(Kip1) Controls Cytokinesis via the Regulation of Citron Kinase Activation». *The Journal of Clinical Investigation* 122 (3): 844–58. https://doi.org/10.1172/JCI60376.

Sflomos G., V. Dormoy, T. Metsalu, R. Jeitziner, L. Battista, V. Scabia, W. Raffoul, et al. 2016. «A Preclinical Model for ERα-Positive Breast Cancer Points to the Epithelial Microenvironment as Determinant of Luminal Phenotype and Hormone Response». *Cancer Cell* 29 (3): 407–22. https://doi.org/10.1016/j.ccell.2016.02.002.

Sharma, S. S., L. Ma, T. K. Bagui, K. D. Forinash, e W. J. Pledger. 2012. «A P27Kip1 Mutant That Does Not Inhibit CDK Activity Promotes Centrosome Amplification and Micronucleation». *Oncogene* 31 (35): 3989–98. https://doi.org/10.1038/onc.2011.550.

Shaw F. L., H. Harrison, K. Spence, M. P. Ablett, B. M. Simões, G. Farnie, R. B. Clarke. 2012. «A Detailed Mammosphere Assay Protocol for the Quantification of Breast Stem Cell Activity». *Journal of Mammary Gland Biology and Neoplasia* 17 (2): 111–17. https://doi.org/10.1007/s10911-012-9255-3.

Sheaff R. J., M. Groudine, M. Gordon, J. M. Roberts, e B. E. Clurman. 1997. «Cyclin E-CDK2 Is a Regulator of P27Kip1». *Genes & Development* 11 (11): 1464–78. https://doi.org/10.1101/gad.11.11.1464.

Sherr C. J., J. M. Roberts. 1999. «CDK Inhibitors: Positive and Negative Regulators of G1-Phase Progression». *Genes & Development* 13 (12): 1501–12. https://doi.org/10.1101/gad.13.12.1501.

Shin, F. M. Yakes, F. Rojo, N. Shin, A. V. Bakin, J. Baselga, C. L. Arteaga. 2002. «PKB/Akt Mediates Cell-Cycle Progression by Phosphorylation of P27(Kip1) at Threonine 157 and Modulation of Its Cellular Localization». *Nature Medicine* 8 (10): 1145–52. https://doi.org/10.1038/nm759.

Spataro V. J., H. Litman, G. Viale, F. Maffini, M. Masullo, R. Golouh, F. J. Martinez-Tello, et al. 2003. «Decreased Immunoreactivity for P27 Protein in Patients with Early-Stage Breast Carcinoma Is Correlated with HER-2/Neu Overexpression and with Benefit from One Course of Perioperative Chemotherapy in Patients with Negative Lymph Node Status: Results from International Breast Cancer Study Group Trial V». *Cancer* 97 (7): 1591–1600. https://doi.org/10.1002/cncr.11224.

Stendahl M., S. Nilsson, C. Wigerup, K. Jirström, P. Jönsson, O. Stål, G. Landberg. 2010. «P27Kip1 Is a Predictive Factor for Tamoxifen Treatment Response but Not a Prognostic Marker in Premenopausal Breast Cancer Patients». *International Journal of Cancer* 127 (12): 2851–58. https://doi.org/10.1002/ijc.25297.

Stephens P. J., P. S. Tarpey, H. Davies, P. Van Loo, C. Greenman, D. C. Wedge, S. Nik-Zainal, et al. 2012. «The Landscape of Cancer Genes and Mutational Processes in Breast Cancer». *Nature* 486 (7403): 400–404. https://doi.org/10.1038/nature11017.

Storer M., A. Mas, A. Robert-Moreno, M. Pecoraro, M. C. Ortells, V. Di Giacomo, R. Yosef, et al. 2013. «Senescence Is a Developmental Mechanism That Contributes to Embryonic Growth and Patterning». *Cell* 155 (5): 1119–30. https://doi.org/10.1016/j.cell.2013.10.041.

Susaki E., K. I. Nakayama. 2007. «Multiple Mechanisms for P27(Kip1) Translocation and Degradation». *Cell Cycle (Georgetown, Tex.)* 6 (24): 3015–20. https://doi.org/10.4161/cc.6.24.5087.

Taherian-Fard A., S. Srihari, M. A. Ragan. 2015. «Breast Cancer Classification: Linking Molecular Mechanisms to Disease Prognosis». *Briefings in Bioinformatics* 16 (3): 461–74. https://doi.org/10.1093/bib/bbu020.

Thangavel C., J. L. Dean, A. Ertel, K. E. Knudsen, C. M. Aldaz, A. K. Witkiewicz, R. Clarke, E. S. Knudsen. 2011. «Therapeutically Activating RB: Reestablishing Cell Cycle Control in Endocrine Therapy-Resistant Breast Cancer». *Endocrine-Related Cancer* 18 (3): 333–45. https://doi.org/10.1530/ERC-10-0262.

Takahashi K., S. Yamanaka. 2006. «Induction of Pluripotent Stem Cells from Mouse Embryonic and Adult Fibroblast Cultures by Defined Factors». *Cell* 126 (4): 663–76. https://doi.org/10.1016/j.cell.2006.07.024.

Tapia J. C., V. M. Bolanos-Garcia, M. Sayed, C. C. Allende, J. E. Allende. 2004. «Cell Cycle Regulatory Protein P27KIP1 Is a Substrate and Interacts with the Protein Kinase CK2». *Journal of Cellular Biochemistry* 91 (5): 865–79. https://doi.org/10.1002/jcb.20027

Taylor-Harding B., P. Aspuria, H. Agadjanian, D. Cheon, T. Mizuno, D. Greenberg, J. R. Allen, et al. 2015. «Cyclin E1 and RTK/RAS Signaling Drive CDK Inhibitor Resistance via Activation of E2F and ETS». *Oncotarget* 6 (2): 696–714. https://doi.org/10.18632/oncotarget.2673.

Tavani A., C. Braga, C. La Vecchia, E. Negri, A. Russo, S. Franceschi. 1997. «Attributable Risks for Breast Cancer in Italy: Education, Family History and Reproductive and Hormonal Factors». *International Journal of Cancer* 70 (2): 159–63. https://doi.org/10.1002/(sici)1097-0215(19970117)70:2<159::aid-ijc4>3.0.co;2-w.

Toyoshima H., T. Hunter. 1994. «P27, a Novel Inhibitor of G1 Cyclin-Cdk Protein Kinase Activity, Is Related to P21». *Cell* 78 (1): 67–74. https://doi.org/10.1016/0092-8674(94)90573-8.

Tripathy D., S. Im, M. Colleoni, F. Franke, A. Bardia, N. Harbeck, S. A. Hurvitz, et al. 2018. «Ribociclib plus Endocrine Therapy for Premenopausal Women with Hormone-Receptor-Positive, Advanced Breast Cancer (MONALEESA-7): A Randomised Phase 3 Trial». *The Lancet. Oncology* 19 (7): 904–15. https://doi.org/10.1016/S1470-2045(18)30292-4.

Turenne G. A., P. Paul, L. Laflair, B. D. Price. 2001. «Activation of P53 Transcriptional Activity Requires ATM's Kinase Domain and Multiple N-Terminal Serine Residues of P53». *Oncogene* 20 (37): 5100–5110. https://doi.org/10.1038/sj.onc.1204665.

Turner N., R. Grose. 2010. «Fibroblast Growth Factor Signalling: From Development to Cancer». *Nature Reviews Cancer* 10 (2): 116–29. https://doi.org/10.1038/nrc2780.

Turner N., A. Pearson, R. Sharpe, M. Lambros, F. Geyer, M. A. Lopez-Garcia, R. Natrajan, et al. 2010. «FGFR1 Amplification Drives Endocrine Therapy Resistance and Is a Therapeutic Target in Breast Cancer». *Cancer Research* 70 (5): 2085–94. https://doi.org/10.1158/0008-5472.CAN-09-3746.

Ustun I., K. Beksac, O. Kandemir, U. Berberoglu. 2019. «Location and Frequency of Residual Breast Tissue after Mastectomy». *Breast Care* 14 (4): 212–15. https://doi.org/10.1159/000494765.

Victora C. G., R. Bahl, A. J. D. Barros, G. V. A. França, S. Horton, J. Krasevec, S. Murch, et al. 2016. «Breastfeeding in the 21st Century: Epidemiology, Mechanisms, and Lifelong Effect». *Lancet (London, England)* 387 (10017): 475–90. https://doi.org/10.1016/S0140-6736(15)01024-7.

Victorelli S., J. F. Passos. 2019. «Reactive Oxygen Species Detection in Senescent Cells». *Methods in Molecular Biology (Clifton, N.J.)* 1896: 21–29. https://doi.org/10.1007/978-1-4939-8931-7_3.

Viotto D., F. Russo, I. Anania, I. Segatto, G. L. Rampioni Vinciguerra, A. Dall'Acqua, R. Bomben, et al. 2021. «CDKN1B mutation and copy number variation are associated with tumor aggressiveness in Luminal breast cancer». *The Journal of Pathology* 253 (2): 234–45. https://doi.org/10.1002/path.5584.

Vlach J., S. Hennecke, K. Alevizopoulos, D. Conti, e B. Amati. 1996. «Growth Arrest by the Cyclin-Dependent Kinase Inhibitor P27Kip1 Is Abrogated by c-Myc». *The EMBO Journal* 15 (23): 6595–6604.

Weinberg R. A. 1995. «The Retinoblastoma Protein and Cell Cycle Control». *Cell* 81 (3): 323–30. https://doi.org/10.1016/0092-8674(95)90385-2.c

Wen H. Y., E. Brogi. 2018. «Lobular Carcinoma In Situ». *Surgical Pathology Clinics* 11 (1): 123–45. https://doi.org/10.1016/j.path.2017.09.009.

Wen, S., Y. So, K. Singh, J. M. Slingerland, M. B. Resnick, S. Zhang, V. Ruiz, e S. F. Moss. 2012. «Promotion of Cytoplasmic Mislocalization of P27 by Helicobacter Pylori in Gastric Cancer». *Oncogene* 31 (14): 1771–80. https://doi.org/10.1038/onc.2011.362.

Wilson F. R., A. Varu, D. Mitra, C. Cameron, S. Iyer. 2017. «Systematic Review and Network Meta-Analysis Comparing Palbociclib with Chemotherapy Agents for the Treatment of Postmenopausal Women with HR-Positive and HER2-Negative Advanced/Metastatic Breast Cancer». *Breast Cancer Research and Treatment* 166 (1): 167–77. https://doi.org/10.1007/s10549-017-4404-4.

Wu A., B.Wu, J. Guo, W. Luo, D. Wu, H. Yang, Y. Zhen, et al. 2011. «Elevated Expression of CDK4 in Lung Cancer». *Journal of Translational Medicine* 9 (aprile): 38. https://doi.org/10.1186/1479-5876-9-38.

Xue W., L. Zender, C. Miething, R. A. Dickins, E. Hernando, V. Krizhanovsky, C. Cordon-Cardo, S. W. Lowe. 2007. «Senescence and Tumour Clearance Is Triggered by P53 Restoration in Murine Liver Carcinomas». *Nature* 445 (7128): 656–60. https://doi.org/10.1038/nature05529.

Yamada K. M., E. Cukierman. 2007. «Modeling Tissue Morphogenesis and Cancer in 3D». *Cell* 130 (4): 601–10. https://doi.org/10.1016/j.cell.2007.08.006.

Yang C., Z. Li, T. Bhatt, M. Dickler, D. Giri, M. Scaltriti, J. Baselga, N. Rosen, e S. Chandarlapaty. 2017. «Acquired CDK6 Amplification Promotes Breast Cancer Resistance to CDK4/6 Inhibitors and Loss of ER Signaling and Dependence». *Oncogene* 36 (16): 2255–64. https://doi.org/10.1038/onc.2016.379.

Yang Y., J. Luo, X. Chen, Z. Yang, X. Mei, J. Ma, Z. Zhang, X. Guo, X. Yu. 2020. «CDK4/6 Inhibitors: A Novel Strategy for Tumor Radiosensitization». *Journal of Experimental & Clinical Cancer Research: CR* 39 (1): 188. https://doi.org/10.1186/s13046-020-01693-w.

Yoon, Nam K., Erin L. Maresh, Dejun Shen, Yahya Elshimali, Sophia Apple, Steve Horvath, Vei Mah, et al. 2010. «Higher Levels of GATA3 Predict Better Survival in Women with Breast Cancer». *Human Pathology* 41 (12): 1794–1801. https://doi.org/10.1016/j.humpath.2010.06.010.

Yosef R., N. Pilpel, R. Tokarsky-Amiel, A. Biran, Y. Ovadya, S. Cohen, E. Vadai, et al. 2016. «Directed Elimination of Senescent Cells by Inhibition of BCL-W and BCL-XL». *Nature Communications* 7 (aprile): 11190. https://doi.org/10.1038/ncomms11190.

Yoshida G. J. 2018. «Emerging Roles of Myc in Stem Cell Biology and Novel Tumor Therapies». *Journal of Experimental & Clinical Cancer Research: CR* 37 (1): 173. https://doi.org/10.1186/s13046-018-0835-y.

Zardavas D., J. Baselga, M. Piccart. 2013. «Emerging Targeted Agents in Metastatic Breast Cancer». *Nature Reviews. Clinical Oncology* 10 (4): 191–210. https://doi.org/10.1038/nrclinonc.2013.29.

Zhao H., C. M. Faltermeier, L. Mendelsohn, P. L. Porter, B. E. Clurman, J. M. Roberts. 2014. «Mislocalization of P27 to the Cytoplasm of Breast Cancer Cells Confers Resistance to Anti-HER2 Targeted Therapy». *Oncotarget* 5 (24): 12704–14. https://doi.org/10.18632/oncotarget.2871

Zoncu R., A. Efeyan, D.M. Sabatini. 2011. «MTOR: From Growth Signal Integration to Cancer, Diabetes and Ageing». *Nature Reviews. Molecular Cell Biology* 12 (1): 21–35. https://doi.org/10.1038/nrm3025.

«2020-Numeri-Cancro » https://www.aiom.it

Jun J., Lester F. Lau. 2010. «The Matricellular Protein CCN1 Induces Fibroblast Senescence and Restricts Fibrosis in Cutaneous Wound Healing». *Nature Cell Biology* 12 (7): 676–85. https://doi.org/10.1038/ncb2070.

Lovisa S., S. Citro, M. Sonego, A. Dall'Acqua, V. Ranzuglia, S. Berton, A. Colombatti, et al. 2016. «SUMOylation Regulates P27Kip1 Stability and Localization in Response to TGFβ». *Journal of Molecular Cell Biology* 8 (1): 17–30. https://doi.org/10.1093/jmcb/mjv056.

ACKNOWLEDGEMENTS

This work was performed in the division of Molecular Oncology at National Cancer Institute (CRO) of Aviano, directed by Dr. Gustavo Baldassarre.

I like to thank Dr. Barbara Belletti, Dr. Gustavo Baldassarre and Dr. Ilenia Segatto for accepting me in the lab and for giving me the opportunity to carry out my PhD project, helping and supporting me in any occasions, in joy and in difficult moments.

I am really grateful to all the other members of SCICC group. You have enriched my research project but also my life inside and outside the laboratory. Each one of you contributed to my PhD project and period.

I like also to thank Prof. Cristina Marchini that welcome me in laboratory "Biologia Applicata" for my time spent in UNICAM. You have been my safe harbor.